SOILS AND GEOMORPHOLOGY OF THE UPPER-AGUÁN VALLEY, HONDURAS

BY

FERNANDO J. CABRERA-MARTINEZ

A DISSERTATION PRESENTED TO THE GRADUATE SCHOOL
OF THE UNIVERSITY OF FLORIDA IN PARTIAL FULFILLMENT
OF THE REQUIREMENTS FOR THE DEGREE OF
DOCTOR OF PHILOSOPHY

UNIVERSITY OF FLORIDA

1993

ACKNOWLEDGMENTS

I would like to express my sincere gratitude to my major professor Dr. Mary E. Collins, first, for offering the opportunity to continue graduate studies and more importantly for her support, guidance and motivation during my doctoral studies at the University of Florida. I am indebted to the members of my committee, Dr. Willie G. Harris, Dr. Randall B. Brown, Dr. Guerry H. McClellan, and Dr. Joann Mossa for their patience, time, and encouragement throughout my research.

I extend recognition to Larry Schwandes and Keith Hollien for their assistance in the Environmental Pedology and Land Use laboratory. Special recognition goes to: Dr. Onesimo Medina, Dr. Jorge Gonzales and the Standard Fruit Company of Honduras for the financial support and the opportunity to conduct my research in the Aguán Valley, Honduras. A very special thanks goes to Irma L. Smith and Helen Huseman for help and advice in the preparation of this manuscript. Thanks to Dr. Laura Newman for her spiritual guidance.

Former fellow graduate student and my best American friend, Stanley Horn Crownover, deserves my deep and sincere gratitude for his encouragement, wisdom and counseling

throughout the graduate school years and his fine sense of humor during the difficult times.

A very special thanks and love to my mother Caridad Martinez who is truthfully responsible for my education. Finally, my lovely family deserves the utmost recognition. My friend and wife Sonia Diaz for her dedication to my success and great patience and each one of my four children, Fernando, Isis, Carmela, and Luis Rafael for their love and exemplary behavior.

TABLE OF CONTENTS

Page

Page

LIST OF TABLES

Page

LIST OF FIGURES

Page

Page

Abstract of Dissertation Presented to the Graduate School of the University of Florida in Partial Fulfillment of the Requirements for the degree of Doctor of Philosophy

SOILS AND GEOMORPHOLOGY OF THE UPPER-AGUÁN VALLEY, HONDURAS

By

Fernando J. Cabrera-Martinez

August 1993

Chair: Mary Elizabeth Collins
Major Department: Soil and Water Science

The Aguán Valley, Honduras, is controlled by a strike-slip fault, which is a prolongation of fault systems located in northwestern Honduras and eastern Guatemala. These systems constitute the inland northern boundary between the Caribbean Tectonic Plate and the North American Plate. The fault system continues seaward as the Cayman Trough.

Aguán Fault controls the northern margin of the valley whereas La Esperanza Fault dominates the southern margin. Saba Fault separates the Aguán Fault into two parts of different tectonic activity. La Esperanza and La Ceiba Faults present similar tectonic activity greater than that of the Aguán Fault.

Coeval coalescing alluvial fans occur on both sides of the valley. The Aguán River flows along the junction that merges the piedmonts of both sides of the valley in its

first reaches. From this point, the river downcuts and widens the valley floor, building a floodplain. A section of the upper valley encompassing the alluvial-fan piedmonts and the floodplain was investigated.

Fluvial geomorphic processes control the landforms and associated soils in the floodplain. The river's regime is characterized by moderate and frequent and larger and less frequent flood events.

1. A floodplain basin deposited by vertical accretion dominates the floodplain.
2. A narrower meander belt along the river channel is generated by lateral accretion.
3. A still narrower landform found at the base of the alluvial scarp consists of fine colluvium eroded from the scarp.

Soils of the floodplain present negligible development in an environment characterized by frequent sediment deposition.

Three geomorphic surfaces were separated on the alluvial-fan piedmonts and resulting soils. The surfaces are level with no incised distributary drainage pattern, and have weakly developed soils with cambic and stage I calcic horizons. Rates of uplift in the mountain-piedmont junction dominate over river downcutting and piedmont aggradation, maintaining relatively young piedmont surfaces and associated soils.

The Trojas paleosol located in the southern alluvial scarp represents a considerable period of equilibrium in the area. It has calcic horizons and a well developed natric horizon, which suggests that its genesis is related to dryer than present conditions during latest Pleistocene times (Younger Dryas).

CHAPTER I
INTRODUCTION AND DESCRIPTION OF STUDY AREA

Introduction

The alluvial landscapes of north and northwestern Honduras, encompassed mainly by the Ulua and the Aguán Valleys, are the richest agricultural areas in this country. The banana agroindustry of Honduras has been established in these valleys for more than a century.

The Aguán Valley, Honduras, is located in northern Central America (Fig. 1-1) along the northwestern margin of the Caribbean Tectonic Plate. This area is considered a tectonically active zone (Molnar and Sykes, 1969; Kesel, 1985; Gardner, 1987). The longitudinal Aguán and La Ceiba Faults, are regarded as the western prolongation of the Polochic-Motagua and Jocotan-Chamelecon Fault systems, located on southeast Guatemala and northwestern Honduras separated from La Ceiba and Aguán Faults by the Ulua graben (Fig. 1-2).

The Motagua Fault system, in eastern Guatemala, separates the Maya and Chortis blocks of Nuclear Central America (Dengo and Bohnenberger, 1969) and forms the northwestern boundary of the relatively small Caribbean Plate with the larger North American Plate (Molnar and

Figure 1-1. Location of the Aguán River watershed in Honduras, Central America. The map of Central America in the inset, shows the Cayman Trough and its westward inland continuation as the major fault system of eastern Guatemala.

AY = Aguán and Yaguala Rivers confluence.

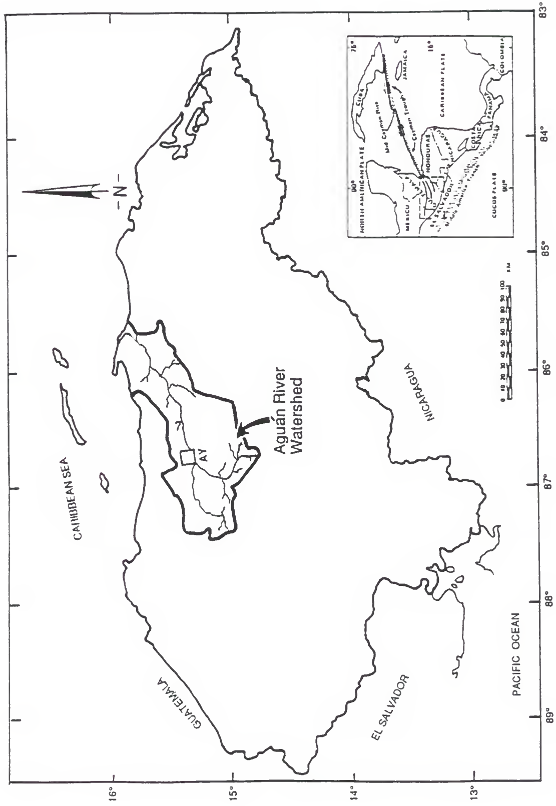

N
CARIBBEAN SEA
GUATEMALA
EL SALVADOR
NICARAGUA
PACIFIC OCEAN
Aguán River
Watershed
AY
0 10 20 30 40 50 60 70 80 90 100 KM
83°
84°
85°
86°
87°
88°
89°
16°
15°
14°
13°
NORTH AMERICAN PLATE
CUBA
JAMAICA
CARIBBEAN PLATE
COCOS PLATE
MEXICO
HONDURAS
NICARAGUA
EL SALVADOR
COSTA RICA
PANAMA
COLOMBIA
Cayman Trough

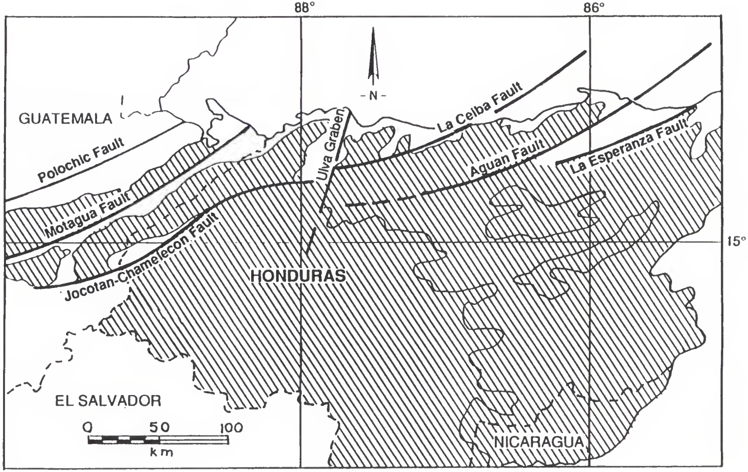

Figure 1-2. Map of Honduras and eastern Guatemala showing the major fault systems of the area (Modified after Horne et al., 1976).

Sykes, 1969; Weyl, 1980). This boundary extends seaward to the east as an elongate deep basin, the Cayman Trough, which begins north of the Bay Island (Honduras) and ends on the east in the Windward Passage between Hispaniola and Cuba (Pinet, 1975; Rosencrantz and Sclater, 1986).

The geomorphology of the Upper-Aguán Valley, which runs along the major Aguán Fault, consists of coalescing alluvial fans which form two alluvial piedmonts flanking both sides of the valley, within the Cordillera Nombre de Dios. At the beginning of the valley, the Aguán River is essentially entrenched between the piedmonts until its junction with its first important tributary, the Yaguala River. Below its confluence with the Yaguala River, the resulting, more powerful Aguán River, has formed a relatively wide floodplain separated, in both margins, from the piedmonts by an abrupt alluvial scarp. The piedmonts remain as a system of paired terraces along both sides of the floodplain.

Despite the economic, tectonic, and geomorphologic relevance of the Aguán Valley, few studies have been performed to characterize and interpret its geomorphic history. Most studies have been carried out along the Central America boundary between the Caribbean and the North American Plate and have focused on the Motagua and Polochic Faults in Guatemala (Schwartz, 1976; Schwartz et al., 1979). A few studies refer to the Aguán Valley and surrounding

areas, though most of these studies only make general remarks about the Aguán Valley. The one exception to this is the study of Manton (1987).

Tectonics and climate both seem to play an important role on the geomorphic processes that have shaped the Upper-Aguán Valley. Any intent to weigh the relative importance of each of these independent variables will help to clarify and decipher the geomorphic history of the valley itself and, perhaps, to bring more detail and insight about the interaction of the above mentioned interacting tectonic plates during the Quaternary.

Mountain ranges and alluvial landscapes historically have been extremely useful to geologists, geomorphologists, pedologists, and other earth scientists who try to understand and decipher the origin of different characteristics on the earth's surface (Bull, 1984). The study area, in addition to its important location and semiarid climate, offers very interesting surface features which include fault-bounded mountain fronts, alluvial fan piedmonts, alluvial scarps, alluvial terraces, and an active floodplain.

The landscapes and landforms displayed in the study area enable the use of soil genesis, stratigraphy, fluvial geomorphology, and morphotectonic concepts and techniques, to be applied to study and interpret the history of landscape evolution. These geomorphic surfaces constitute

reference features useful in deducing the geomorphological evolution of the area and may help to infer relative uplifting and/or river downcutting, using absolute or relative dating techniques (Knuepfer, 1988).

Soils have proven to be important stratigraphic markers and have been increasingly useful to estimate relative and absolute ages of geomorphic surfaces. Conversely, the comprehension of landscapes can be used to explain the relative development of soils there. Pedology is founded mainly on working models that seek to resolve the relationships between sets of soil properties and associated landscapes (Arnold and Gilbert, 1979). In this regard, the soil characteristics and the relative development of the soils on the two piedmonts of the Upper-Aguán Valley may help to explain the evolution of these piedmonts, as well as the relative tectonic activity of the flanking mountain fronts.

Fluvial geomorphologists attempt to decipher the usually complex fluvial stratigraphy created by most rivers. It is important to comprehend several aspects of river evolution, including the geomorphic variables that dominate such evolution. Channel patterns and morphology are controlled mainly by stream power which is associated with the slope and stream discharge available to carry suspended and bedload sediments (Schumm, 1977). Sudden changes of slope along a river channel, due to uplifting or subsidence,

influence stream power, and consequently, channel patterns and floodplain morphology.

Changes in climate through time translate not only into changes in stream discharges but also in changes of sediment yields (Knox, 1984). Tectonics and climate are, in this regard, external independent variables that relate to river pattern and floodplain morphology.

The relationship between landforms and geological structures have been used largely to understand processes in tectonically active areas. Recently, the study of neotectonics has included other morphotectonic approaches such as the study of drainage systems, slopes, and landform history in recent active tectonic areas (Doornkamp, 1986). Morphometric analyses of mountain fronts consist of recognition of geomorphic features and measurement of parameters on aerial photographs, topographic maps, and satellite images (e.g., mountain-front sinuosity, longitudinal stream profiles). These parameters are useful to correlate fluvial systems and mountain-piedmont junction adjustments to grades of Quaternary uplift (Bull, 1977; Bull and McFadden, 1977; Bull, 1978; Menges et al., 1987).

The broad aim of this research is to utilize a combined approach of field, cartographic, and laboratory investigations to examine the different geomorphic surfaces, landforms, and soils in order to illuminate the history and evolution of the Upper-Aguán Valley in Honduras. Further,

more detailed and quantitative studies in other reaches of the Aguán Valley, and other regional fluvial systems will be necessary to better understand the geomorphic history of this tectonically active area.

Description of Study Area

Location

The study area encompasses the Aguán Valley in northwestern Honduras, Central America. The Aguán Valley covers an area of 2,100 km^2, and is located between 85°-25′ and 87°-00′ west longitude, and between 15°-20′ and 16°-00′ north latitude (Fig. 1-1). The width of the valley ranges from 8-15 km and it is approximately 160 km long. It extends toward the northeast from the small town of San Lorenzo to the Caribbean Sea.

A specific study area was selected from the valley to investigate the first reaches of the Aguán River floodplain and the soils of both the floodplain and adjacent alluvial-fan piedmonts. It is located in the upper part of the valley and extends from about 3 km before the confluence of the Yaguala River with the Aguán River to about 5 km downstream from the confluence of the Agaltecas River with the Aguán River (See Chapter III). Most of this area is

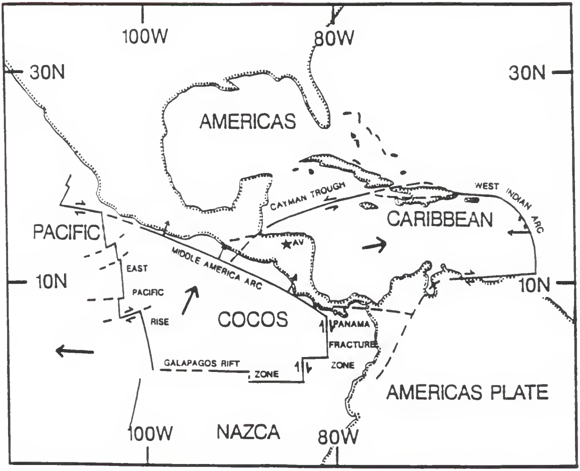

Figure 1-3. Tectonic plates of Central America. Large arrows indicate the motion direction of the plates relative to America's Plate. Small arrows show relative motion at plate boundaries (after Molnar and Sykes, 1969). AV = Aguán Valley

currently occupied by a banana plantation known as "Coyoles" owned by the Standard Fruit Company of Honduras.

<u>Climate</u>

Information about the climate of the valley is incomplete due to the absence of long-term climatic records and insufficient weather stations along the valley. The valley is located in a subtropical zone. According to Bull's (1991) climatic classification, the climate of the valley can be classified as semiarid in the west, subhumid in the center, and humid in the east. The precipitation is strongly seasonal. In regard to temperature, the whole valley regime is hyperthermic and is weakly seasonal. The soils have an isohyperthermic soil temperature regime and a soil moisture regime that ranges from ustic in the west to udic in the east of the valley (Soil Survey Staff, 1992).

As stated before, long-term climatic records are not available in the valley. A 15-year record at Coyoles farms, in the west-central part of the valley, indicates an average annual rainfall of 900 mm and an annual air temperature average of 27° C.

The region is characterized by two marked seasons, a dry season which extends from January to July, and a wet season from August to December. There is an east-west precipitation gradient along the valley. This gradient ranges from approximately 800 mm of rainfall in the western

part of the valley to more that 2,000 mm in the eastern domain. In the western part of the valley, potential evapotranspiration exceeds precipitation during the whole year. In the east, during the rainy season, rarely does potential evapotranspiration exceed precipitation.

Maximum monthly temperature is 35°C from April to June, and minimum average monthly temperature of 18°C occurs from December to March. The three hottest months average 28°C while the three coldest months average 24°C.

Paleoclimate

Paleoclimatic studies have not been performed in Honduras, but several have been performed around the Caribbean basin. These investigations have identified similar climatic trends during late Pleistocene-Holocene Ages that could be reasonably extrapolated to north Honduras.

Paleoclimatic reconstruction of the tropics based on atmospheric general circulation models (Gates, 1976; Manabe and Hahn, 1977; Kutzbach and Street-Perot, 1985) have postdicted aridic conditions during the late-Pleistocene period and more humid conditions during the early-Holocene period. A few geomorphic studies (Garner, 1959), and many paleolimnologic studies (Bradbury et al., 1981; Bindford, 1982; Leyden, 1984; 1985; Markgraf, 1989; Piperno et al., 1990; Curtis, 1992) in the lowland of the tropics have been

used to decipher the principal climatic tendencies during late-Pleistocene and Holocene periods around the circum-Caribbean region.

Markgraf (1989), in his paleoclimatic synthesis, concluded that during glacial and post-glacial times, temperatures in Central and South America were 4-5°C cooler than present, but found distinctive humidity patterns throughout the region.

The Younger Dryas, a climatic event initially documented in Europe and the North Atlantic and recently confirmed in tropical areas of Africa and the Americas, affected the circum-Caribbean area. It is characterized by a relative short period of returning cooler temperatures during the transition of the last glacial age to the present interglacial age. More specifically, the Younger Dryas has been identified between 11 and 10 ka.

Discussing the paleoclimate of the tropical and subtropical lowlands in Central and South America at 3.0 ky intervals, Markgraf (1989) concluded that for the lowland of the neotropics no inference can be made prior to 13 ka, at the present time, due to the lack of records. By 12 ka the climate was cool and dry and by 9.0 ka, moisture conditions reach unsurpassed levels with temperatures remaining lower than today. From 8.5 ka, moisture conditions steadily decreased reaching a minimum at 6.0 ka. Finally, by 3.0 ka

moisture increased to levels higher than present, but lower than during the early-Holocene age.

In Central America and the Caribbean, pollen, isotopic and trace element analyses, and lake level records indicated arid conditions during the late-Pleistocene period and humid conditions in the early-Holocene period (Bindford, 1982; Deevey et al., 1983; Leyden, 1984; 1985; Curtis, 1992). Leyden (1984) considered this dry-latest-Pleistocene/humid-early-Holocene period transition to be pantropical in the lowlands. She also concluded that arid conditions predominated during the middle- and late-Holocene Age except for the period between 5.2 and 2.2 ka.

Curtis (1992), using high resolution climate reconstruction, based on the isotopic, trace element, and pollen results in a lake of Haiti, illustrated the climate during the last 10.5 ka in the Caribbean. He concluded that cool and dry conditions prevailed from 10.5 to 10 ka in the Caribbean, coinciding with the latter part of the Younger Dryas. From 10 to 7.0 ka, both temperature and moisture increased significantly. Maximum moisture levels, inferred from decreasing salinity in the lake, were reached between 7.0 to 3.5 ka. During the period between 3.5 to 2.5 ka dry conditions returned as inferred from lake level declination and increased salinity levels. A severe dry period marked the 2.5 to 1.0 ka interval. Apparently, by 1.0 ka, wet conditions resumed for a short period of time.

The last 1.0 ka period is characterized by an increase in arid conditions that also have been documented by the desiccation of other lakes in the Caribbean. However, the desiccation of those lakes also has been attributed to human influence.

Both geophysical modelling and proxy data in the lowlands of the Caribbean indicate alternation of humid and arid conditions during the last 11.0 ka to 12.0 ka. During the last part of this period, the climatic conditions alternated from arid to semiarid. Some of the climatic changes have lasted long enough to effectively influence the environment. On occasions the climatic changes have not persisted long enough to create significant vegetation changes and/or direct impact on the landscapes, i.e. the wet conditions claimed by Curtis (1992) during a short period of the late-Holocene Age.

Drainage

Surface drainage dominates the landscapes in the Aguán Valley. On both sides of the valley, the surrounding mountains display a dendritic to subparallel drainage pattern. Within the specific study area two major tributaries, the Yaguala River from the south and the Agaltecas River from the north, converge with the Aguán River. Several smaller--mostly permanent and some ephemeral--streams also drain into the Aguán River within

this section of the valley. These smaller tributaries, like the Calpules and Nombre de Jesus Rivers, are responsible for the formation of the alluvial fans that constitute the piedmonts flanking both sides of the floodplain.

Upon entering into the valley, the Yaguala River is slightly entrenched into the mountain front and piedmont, and has built a relatively narrow floodplain before merging with the Aguán River. Along its relatively short course within the valley, the Yaguala River flows in a meandric pattern. The other smaller streams are braided at the beginning, as they enter the valley from the mountains and flow on the fan heads, then they become slightly entrenched until reaching the main stream. On the southern margin of the valley, the tributaries enter the main stream at almost right angles, whereas, in the northern margin, the joining occurs at very low angles.

Floods originated by tropical storms and hurricanes, are considered high magnitude, low frequency events in northwestern Honduras (Schramm, 1981). The last of such events occurred in 1974, during hurricane Fifi. In the absence of river discharge records, Schramm (1981), based upon long rainfall records obtained from Tela R.R. Company in La Lima and El Progreso (northwestern Honduras), calculated a 50-year recurrence period for a precipitation event of Fifi magnitude. Flooding events, not so extreme as Fifi but still considered of high magnitude, have a shorter

recurrence interval of 10 to 12 years. Unfortunately, the lack of river discharge records in the area prevents the estimation of important parameters such as the frequency of river bankfull stage.

Physiography and Geology

Physiographically, the northern part of Nuclear Central America embodies two large morphotectonic blocks, the Maya block in the northwest and the Chortis block in the southeast (Dengo and Bohnenberger, 1969). The boundary of these two blocks is traversed longitudinally by three principal east- to northeast-trending fault zones, the Polochic Fault in the northwest, the Motagua Fault in the center, and the Jocotan-Chamelecon Fault in the southeast (Fig. 1-2).

The Motagua Fault is considered to be the eastward inland extension of the Cayman Trough and the border between the crustal Maya Block on the north belonging to the North American Plate and the Chortis Block on the south pertaining to the Caribbean plate. Horne et al. (1976) regarded the Aguán Fault as an eastward prolongation of the eastern Guatemala and western Honduras fault systems. The north trending Ulua graben lies between both fault zones.

The Aguán Fault, on its western extreme, runs along the Cordillera Nombre de Dios, further to the northeast within the Aguán Valley. The fault separates the Cordillera

Nombre de Dios on the north from the Montana de Botaderos, and Sierra de La Esperanza on the south (Mills et al., 1967). Northward of the Aguán Valley, along the Cordillera Nombre de Dios, two blocks are displayed, the Cangrejal and Trujillo horsts. They are bounded on the north by the La Ceiba Fault and on the south by the Pueblo Viejo Fault. These more recently uplifted blocks are separated on the east-west direction by the Saba Fault (Manton, 1987).

Geologic History

Horne et al. (1976) proposed the following chronology of events for the geology of northwestern Honduras. A pre-Pennsylvanian metamorphism of pre-Cambrian or Paleozoic deposited sediments was followed by plutonic intrusion. This sequence was then overlain by thick pelitic strata weakly metamorphosed in the pre-Jurassic and later intruded by nonmetamorphosed plutons. They proposed that this basement complex was covered during the early-Cretaceous period by sublittoral carbonate deposits which were eroded and deposited to the south as conglomerates in the late-Cretaceous time. Widespread granitic plutonism during late-Cretaceous or early-Tertiary times on western Honduras was responsible for the uplift of the Sierra de Omoa and Cordillera Nombre de Dios. The Ulua graben was developed by a northerly trend faulting during the late-Tertiary period.

During the late-Pliocene and Quaternary, early subsidence of the Nuclear Foreland of Honduras continued, forming a closed trough which divided the Bay Island from the Northern Cordilleras of Honduras. The trough consisted of the Tela and Aguán basins which received clastic alluvial deposits from the Cordilleras, except for the time(s) when two marine transgressions occupied part of these basins (Mills et al., 1967).

Gose (1985), based on the works of Dengo and Bohnenberger (1969), Bonis et al. (1970), and Weyl (1980), summarized the geologic history of Honduras as occurring in three predominant episodes. A metamorphic basement called the Cacaguapa Schist of Paleozoic Age; a Mesozoic, mainly Cretaceous, sedimentary sequence consisting of clastic and carbonaceous rocks; and a volcanic sequence containing mainly ignimbrites deposited during the Tertiary period.

Bedrock Geology and Lithology

The lack of accessibility, the robust vegetation covering the rocks, and the scarp topography have contributed to the poor understanding of Honduran geology (Kozuch, 1991). The surrounding mountains of the Aguán Valley display several geomorphic features and geologic units as well as areas of unknown geology in the stratigraphic column of western and central Honduras

(Fig. 1-4). The main geologic units (Fig. 1-5) are the Cacaguapa Schist (Pzm), Valle de Angeles group (Kva), Aguán formation (Kag), Nondifferentiated Tertiary volcanic rocks (Tv), intrusive rocks of Cretaceous age (Ki) and Cretaceous-Tertiary age (Kti) (Kozuch, 1991). The stratigraphic column showing the associated epochs of these units are presented in Figure 1-5.

The Cacaguapa Schist (Pzm) is the complex basement and is made up of sericitic and graphitic schists, phyllites, gneisses, quartzite, marble, and thick quartz veins and lenses (Horne et al., 1976). Kozuch (1991) cited Fakundiny (1970) describes this formation as consisting of two members: a lower member, Humuya, with metamorphic and mylotinized rocks with plutonic intrusions, and an upper member, Las Marias, consisting of pelitic strata with marble and quartzite. The exact age of this formation is unknown, but it is estimated to be Paleozoic or pre-Jurassic.

The Valle de Angeles group (Kva) basically consists of a suite of clastic red beds, lithologically heterogeneous (Finch, 1981). These beds contain mudstones, shales, sandstones, limestones, and conglomerates of various colors. The conglomerates consist of schist, phyllite, quartz, limestones clasts and volcanic rock fragments. The red beds of the Valle de Angeles group are divided into a lower member and an upper member with two distinct formations in

Figure 1-4. Geological map of Central Honduras. From the Geologic map of Honduras compiled by Kozuch (1991).

——— — — — Formation contact (dashed where covered or inferred).

——— — — — Fault (dashed where covered or inferred).

Qal Recent continental and marine sediments including talus deposits, gravel terraces, flood plain deposits, and alluvium.

Qv Silts and flows of volcanic basalt, olivine series andesite, and pyroclastic deposits.

Tv Nondifferentiated volcanic rocks of unknown age: generally tuffs, andesites, and pyroclastic rocks.

Pzm Cacaguapa Schists metamorphic basement complex made up of sericitic and graphitic schists, phyllites, gneisses, quartzite, marble, and thick quartz veins and lenses.

Ti)
KTi) Intrusive rocks: granites, granodiorites, diorites, and tonalites of
Ki) various ages.

Kag Aguán Formation: fine-grained siliceous sediments, limestone, and volcanic ashes of late Cretaceous age.

Kva Valle de Angeles: Suite of clastic red-beds, mainly mudstones, shales, sandstones, limestones, and conglomerates.

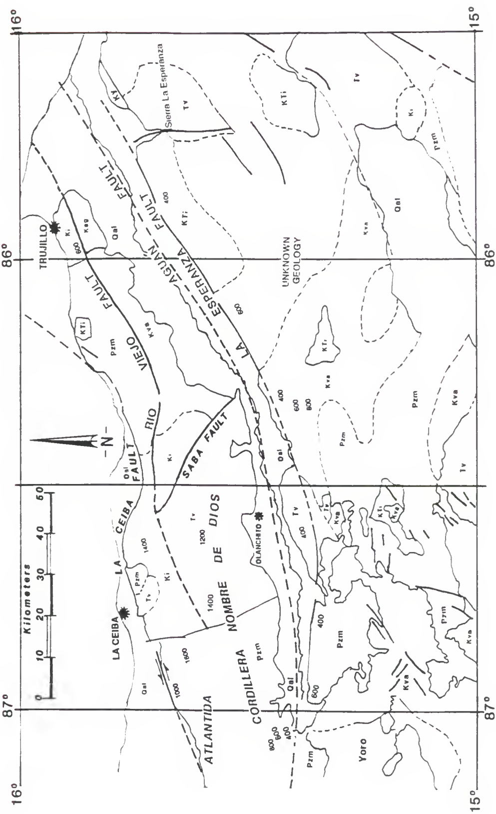
16°
86°
87°
15°
Kilometers
0
10
20
30
40
50
-N-
TRUJILLO
LA CEIBA
OLANCHITO
Sierra La Esperanza
RIO VIEJO FAULT
AGUAN FAULT
LA ESPERANZA FAULT
SABA FAULT
LA CEIBA FAULT
CORDILLERA NOMBRE DE DIOS
ATLANTIDA
Yoro
UNKNOWN GEOLOGY
Qal
Pzm
Kva
KTi
Tv
Ki

Figure 1-5. Geological stratigraphic column of Western Honduras (after Kozuch, 1991).

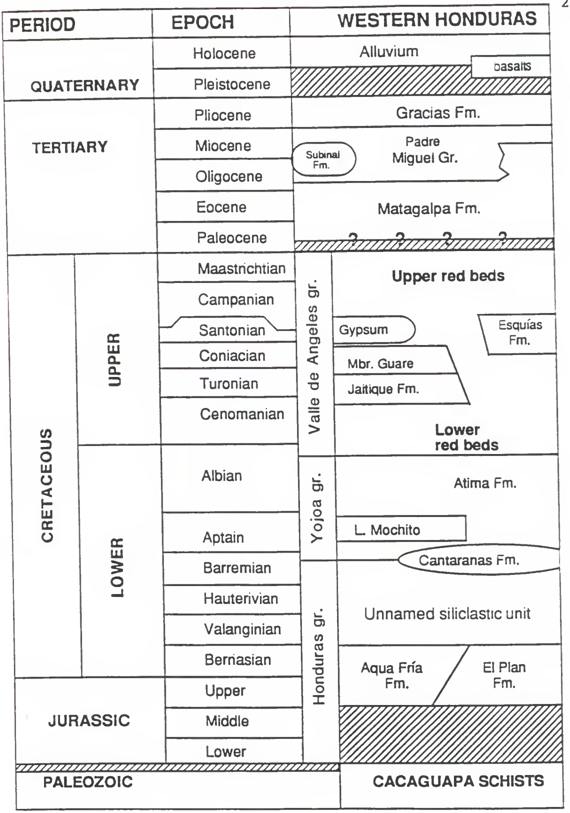
PERIOD
EPOCH
WESTERN HONDURAS
Holocene
Alluvium
basalts
QUATERNARY
Pleistocene
Pliocene
Gracias Fm.
TERTIARY
Miocene
Subinal Fm.
Padre Miguel Gr.
Oligocene
Eocene
Matagalpa Fm.
Paleocene
? ? ? ?
Maastrichtian
Upper red beds
Campanian
Santonian
Gypsum
Esquías Fm.
UPPER
Coniacian
Mbr. Guare
Turonian
Jaitique Fm.
Cenomanian
Valle de Angeles gr.
Lower red beds
CRETACEOUS
Albian
Atima Fm.
Yojoa gr.
Aptain
L. Mochito
LOWER
Barremian
Cantaranas Fm.
Hauterivian
Unnamed siliclastic unit
Valanginian
Honduras gr.
Berriasian
Aqua Fría Fm.
El Plan Fm.
Upper
JURASSIC
Middle
Lower
PALEOZOIC
CACAGUAPA SCHISTS

between, the Esquias and the Jaitique formations. The Esquias formation is a bluish-gray massive limestone unit. The Jaitique formation comprises two members, an unnamed lower member consisting of thick-bedded fossiliferous, micritic shallow-marine limestone; and an upper member (Guare Member) consisting of thin-bedded dark-gray to black microcrystalline limestone. The age of the Valle de Angeles group ranges from late-Cretaceous to early-Tertiary (Finch, 1981).

The geologic unit of "Nondifferentiated Volcanic Rocks of Unknown Age" (Tv) that cannot be classified within the other well-known volcanic formations in Honduras, the Matagalpa and Padre Miguel Formations, are also exposed in the study area. Throughout Honduras they generally consist of tuffs, andesites, and pyroclastic flows (Kozuch, 1991).

Intrusive rocks consisting of granites, granodiorites, diorites, and tonalites occurring in small dikes and extensive bodies also occur in the area. Their distribution and age vary over the country. In the area large bodies of Cretaceous (Ki) and Tertiary (Kti) ages occur.

Finally, a relatively small unit called the Aguán Formation (Kag) is exposed in the northeastern section of the valley, nearby Trujillo. This formation, described by Manton (1987), consists of fine-grained siliceous sediments, limestones, and interstratified volcanic ashes of late-Cretaceous age.

As stated before, the Cacaguapa Schist Formation (Pzm) is the basement rock of Nuclear Central America. Along the valley it is mainly exposed on both sides at the very beginning of the valley, where it extends northward to the La Ceiba Fault. It also occurs on the eastern part along the littoral where it is separated from the Valle de Angeles group geologic unit by the Rio Viejo Fault (Fig. 1-5). The Valle de Angeles Group rises in the central part of the south margin and in the eastern part, on the north margin of the valley.

The Nondifferentiated Volcanic Rocks of the Tertiary (Tv) occur mainly on the west-central part of the valley. The Rio Viejo Fault separates it from intrusive rocks on the north, and the Saba Fault separates it from intrusive rocks and the Valle de Angeles group on the east.

The intrusive rocks of Tertiary Age (Ki) occur along the littoral edge in a location that correspond to the central and easternmost parts of the valley. Those between Cretaceous and Tertiary (Kti) Ages occur mainly in the easternmost south margin of the valley.

The Nondifferentiated Volcanic Rocks (Tv) and the intrusive rocks (Ki, Kti) generally occur at higher elevations than the other rocks exposed in the area.

Tectonic Setting

The driving forces responsible for the present tectonics and major physiographic features of Central America and the Caribbean result from the interaction between the Caribbean and Cocos Plates and between them and their encircling plates (Gardner, 1987). The Caribbean Plate (Fig. 1-3) is bordered on the west by the Middle American Arc, on the northwest by the Cayman Trough, on the northeast and east by the West India Arc, and on the south by a less defined border which includes the Panama Fracture Zone on the southwest, and the seismic zone of northern South America (Molnar and Sykes, 1969). Ross and Scotese (1988) used a computer hierarchical tectonic analysis of the accumulated tectonic and geologic information to model the tectonic evolution of the Gulf of Mexico and the Caribbean region. They concluded that the evolution of this entire region is exclusively the result of the interaction of a rigid Caribbean Plate with the larger plates surrounding it.

Using the iterative fitting algorithm of Minster et al. (1974), Jordan (1975) calculated a spreading rate of 2.1 cm/yr along the mid-Cayman rise. Wadge and Burke (1983) suggested that the 1110 km relative displacement began about 30 Ma at a rate of 3.7 cm/yr and also proposed an anticlockwise rotation of Central America since this displacement could not be accommodated by rigid plate motion about a single pole. Rosencratz and Sclater (1986) proposed two spreading episodes to explain the 1100 km opening of the

Cayman Trough. They calculated a current low spreading rate of about 15 mm/yr during the last 30 my which followed an earlier faster episode. The spreading rate of the earlier episode is still unknown.

Gose (1985), using paleomagnetic data, concluded that the Caribbean Plate did not exist as a rigid unit until the Tertiary. He claims that during the Cretaceous period, the Chortis Block rotated independently of the rest of the Caribbean Plate.

High seismic activity characterizes the borders of the Caribbean-North America Plates and the Caribbean-Cocos Plates. On its west boundary, the Caribbean Plate is being subducted by the Cocos plate at the Middle America Arc, while on the northern boundary sinistral strike-slip motion characterizes the interaction of the Caribbean Plate with the North American Plate. This boundary is represented inland by the Motagua Fault, and seaward by the Cayman Trough (Molnar and Sykes, 1969; Schwartz et al., 1979; Winslow and McCann, 1985).

The northern boundary of the Caribbean Plate can be seen from Guatemala to northwest Honduras, where it is well expressed as the Polochic-Motagua and Jocotan-Chamelecon Fault systems. The fault system continues seaward, to the east, as the tectonically active Cayman Trough, which is a complex transform fault. Offsets of geomorphic and lithologic units along the Motagua Valley (Schwartz et al.,

1979), on northern Hispaniola (Malfait and Dinkleman, 1972; Winslow and McCann, 1985), and offshore Honduras (Pinet, 1972, 1975), indicate horizontal motion and vertical displacement along the margins between the North American and Caribbean Plates.

Horne et al. (1976) suggested that the Aguán Fault of northern Honduras is a continuation of the Jocotan-Chamelecon-Pueblo Nuevo zone. However, Manton (1987) proposed crustal flexuring instead of faulting accountable for the Jocotan and Chamelecon Valleys.

Manton's (1987) conclusions are based on the drainage system, topographic and geologic maps, and satellite imaging that indicate that northern and northwestern Honduras are controlled by the northern boundary of the Caribbean Plate. Manton (1987) further considered the Aguán Fault to be a strike-slip fault that could be dated from late-Oligocene to early-Miocene periods and to be the southernmost expression of the northern plate boundary represented by the Polochic-Motagua Fault system and the Cayman Trough. He considered the Aguán Fault to be an ancient fault system recently reactivated, as indicated by new faulting and the presence of hot springs along the valley.

Manton (1985) divided Honduras into two tectonic provinces: an older one along the north coast, where reverse faulting and uplift have created two fault systems parallel to the Cayman Trough without strike-slip motion,

and a younger province in the central part of the country with northeast trending strike-slip faulting and uplifted in Pliocene-Pleistocene times.

West of the Ulua Valley and the Rio Lean, northern Honduras is traversed by several, mostly northeast trending faults, which from north to south are: La Ceiba Fault which parallels the escarpments of the Cordillera Nombre de Dios on its northern margin; the Rio Viejo Fault across the heights of the same Cordillera; the continuation of the Aguán Fault along the Aguán River; the Saba Fault which runs northwest and divides the valley in two parts; and the La Esperanza Fault on the southern margin of the Aguán Valley along the escarpments of the Sierra la Esperanza and Montana de Botaderos (Manton, 1987; Kozuch, 1991).

Manton (1987) described new faults in northwestern and northern Honduras as resulting from new episodes of regional uplifting. He described the Quimistan Fault which extends from the base of the Sierra de Omoa where the fault meets the Motagua Fault in northwestern Honduras, across the Ulua Valley and continues in an east-northeast trend until its convergence with the Rio Viejo and La Ceiba Faults, on the southeast of the Rio Lean graben. As a result of this new described fault, the Sierra de Omoa would be part of an uplifted block separated from the general uplifting of the rest of the country. Manton (1987) also proposed the Saba Fault which divided the Aguán Valley into two parts as a

result of the first phase of new uplifting, and La Esperanza Fault on the southern margin of the Aguán Valley as the result of a second phase of recent uplifting.

Objectives of Study

The objectives of this study are:

1. To interpret the relative tectonic activity along the Aguan Valley using process-response models which combine morphotectonic indicators and soil-landscape relationships (Chapter II).
2. To describe the river morphology and the pedostratigraphy of some reaches of the Upper-Aguán floodplain and to decipher the fluvial response to climatic changes and tectonics during the Quaternary (Chapter III).
3. To characterize and classify the soils of a part of the Upper-Aguán Valley in order to understand the genesis of the soils and the relationship between the soils and the landscapes in this area (Chapter IV).
4. To use the knowledge acquired through the above objectives to develop a model for the overall geomorphologic evolution of the Upper-Aguán Valley (Chapter V).

CHAPTER II
MORPHOLOGY OF THE TECTONIC LANDSCAPES IN THE AGUÁN VALLEY

Introduction

The Aguán Valley extends subparallel to the north coast of Honduras and is controlled by a southwest-northeast trending fault system related to the northern boundary of the Caribbean Plate. Recent studies (Manton, 1985; 1987) confirmed that the Aguán Fault is a sinistral strike-slip fault developed during late-Oligocene to early-Miocene periods which recently has been reactivated. Strike-slip faults display predominantly horizontal displacement accompanied by less relevant vertical motions due to oblique movement between blocks. The complex interaction between blocks separated by strike-slip faults leads to periods of transpression and transtension displacements. The former causes thrust faulting, folding, and uplift. The latter causes the sinking of basins surrounded by normal faults (Reading, 1980; Ramsay and Huber, 1987).

Strike-slip faulting is normally associated with evidences of horizontal displacements indicated by the offset of geomorphic and geologic units, and by particular landforms such as pull-apart basins, beheaded streams, shutter ridges, linear fault escarps, and microtopography of

horsts and grabens (Keller and Rockwell, 1984). In central Honduras, Manton (1987) described several left-lateral pull-apart basins resulting from the strike-slip fault systems in the region. However, no evidence of offset or other landform characteristics of regions of strike-slip faulting have been identified along the Aguán Valley that can be used to calculate slip rates. This could be the result of lack of detail in geologic mapping due to the complex geology of the area. Recent vertical motion, however, seems to be obvious along the Aguán Valley.

Active uplifting along sections of the Aguán Valley is evident, at first glance, by the steep escarpments of some reaches of the mountain fronts. Further proof is the presence of triangular facets, and the general morphology of the mountain-piedmont junction along the valley.

Morphotectonic studies deal with the analysis of landforms originated and/or deformed by neotectonic activity (Doornkamp, 1986). Morphometric analyses of mountain-front structures enable the verification of fluvial and hillslope systems, adjustments to the relative intensity of uplifting during the Quaternary (Menges et al., 1987). Numerous approaches are used in this regard; their usefulness depending on the imprints left by the geomorphic processes.

Along mountain fronts, recent faulting and uplifting develop straight linear mountain-piedmont junctions which become increasingly sinuous when rates of denudation exceed

rates of uplift. Longitudinal stream profiles and morphometric indexes of profiles may reveal tendencies and irregularities indicative of the relative degree of river downcutting in response to base-level changes and/or the time elapsed since these changes occurred.

The posterior deformation of alluvial fans and alluvial piedmonts and the nonparallel construction of relative soil development on the distal and proximal sections of alluvial fans are also meaningful tools to assess tectonic activity and the location of such activity along tectonically active mountain fronts (Bull, 1984; Kesel and Spicer, 1985). As stated by Bull (1984), regions of arid and semiarid climates are ideal to study landforms influenced by Pleistocene and Holocene tectonic activity. These types of environments optimize preservation of the imprints of tectonic activity.

Objectives of Study

The main objective of this part of the study is to determine the relative tectonic activity and its spatial variation along the fault-bounded mountain fronts of the Aguán Valley and a part of the Caribbean coastline subparallel to the Aguán Valley, in northern Honduras. This objective has been addressed (a) through the determination of the sinuosity index of the mountain-piedmont junctions; (b) the concavity index of longitudinal stream profiles

across mountain-fronts; and (c) the morphology of the alluvial-fan piedmont. Morphometric analyses also were performed along the mountain-fronts bordering the north coast parallel to the valley, to make useful comparisons with the mountain-fronts along the valley and to confirm and/or detect the existence of distinct tectonic blocks in northern Honduras.

Materials and Methods

Location of the Study Area

The study area is located in northern Honduras. It comprises the Aguán Valley and surrounding mountains including the mountain fronts of the Cordillera Nombre de Dios that parallel the Aguán Valley along the north littoral of Honduras (Fig. 2-1). The area lies between approximately 85-25′ to 87-00′ west longitude and 15-20′ to 16-00′ north latitude. Elevations in the valley range from sea level at the mouth of the Aguán River to 300 m at the amphitheater formed at the beginning of the valley. The surrounding mountains reach altitudes that surpass 2000 m in the western portion of the valley, 1500 m in the middle, and about 1000 m in the eastern part (Fig. 2-2). The valley has a total length of approximately 160 km. The climate, geology, and general tectonic setting of the area were discussed previously in Chapter I.

Figure 2-1. Physiographic map of the Aguán Valley, surrounding mountains and the Caribbean coast of Honduras showing the segmented fronts. F1 through F17 equals mountain fronts (modified after Manton, 1987).

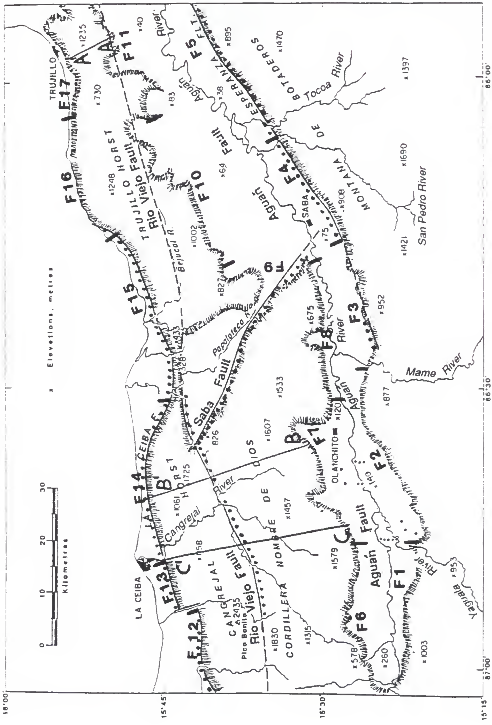
TRUJILLO
LA CEIBA
OLANCHITO
SABA
TRUJILLO HORST
Rio Viejo Fault
Saba Fault
Aguán Fault
ESPERANZA
BOTADEROS
CORDILLERA NOMBRE DE DIOS
MONTAÑA DE
Cangrejal River
Aguán River
Tocoa River
San Pedro River
Mame River
Bejucal R.
Papaloteca R.
Pico Bonito
F1
F2
F3
F4
F5
F6
F7
F8
F9
F10
F11
F12
F13
F14
F15
F16
F17
Kilometres
0
10
20
30
x Elevations, metres
16°00'
15°45'
15°30'
15°15'
87°00'
86°30'
86°00'

Figure 2-2. Topographic cross sections of three different sections on the mountain chain between north margin of Aguán Valley and north coast of Honduras. Location of the profiles indicated in Figure 2-1.

Cross-Section A-A'

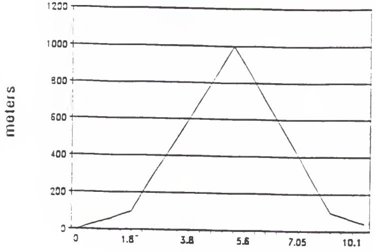

Cross-Section B-B'

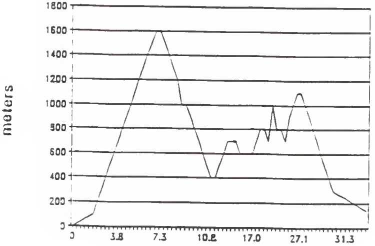

Cross-Section C-C'

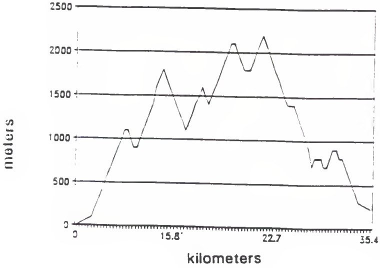

Physiography and Tectonic Setting

The physiography of the Aguán Valley and flanking mountains and the tectonic setting of Honduras have been recently described by Manton (1985; 1987). Based on the drainage network of Honduras, he proposed that the country is divided into three morphotectonic zones:

1. A zone in northern Honduras dominated by processes related to the north boundary of the Caribbean plate.
2. An interior zone with two domains, the northeast and northwest domains, decoupled from the northern zone by the Jocotan, Quimistan, Rio Viejo, and Aguán Faults.
3. A southern zone controlled by coastal flexure and separated from the interior zone by the Jalpatagua Fault of Nicaragua.

The Aguán Valley is located in the northern morphotectonic zone. Manton (1987) concluded that there are two phases of late Quaternary uplift around the Aguán Valley. One is an older phase of uplift represented by the Saba Fault, which divides the Aguán Valley into two parts. This fault is traced along the hills that parallel the Papaloteca River. The northern boundary of this phase of faulting encompass the Rio Viejo and Quimistan Faults. The younger, or second phase of uplift is postulated to follow the southern margin of the valley on the steep mountain

fronts of Sierra La Esperanza and Montana de Botaderos, which is proposed also as a distinct fault called La Esperanza Fault (Manton, 1987).

The northern range of the Cordillera Nombre de Dios embodies, according to Manton (1987), two Quaternary horsts, namely, the Cangrejal and the Trujillo horsts (Fig. 2-1). Although he only described the Cangrejal horst, both are bounded by the same faults, La Ceiba Fault in the north and the Rio Viejo Fault in the south. The horsts are separated by a point of convergence of the faults east of the Papaloteca River. The delineation of these two horsts by Manton (1987) implies that the Rio Viejo and the La Ceiba Faults have had recent activity. This is true, at least for the La Ceiba Fault, as evidenced by the steep slopes and abrupt contact between the Cordillera Nombre de Dios and the narrow Caribbean coastal plain. Huge boulders deposited on the coastal plain between the towns of La Ceiba and Jutiapa, evidently by gravity, further corroborate with the tectonic activity of La Ceiba Fault.

Manton (1987) considered the Aguán Fault as the southernmost extension in Honduras of the strike-slip fault system associated with the northern boundary of the Caribbean Plate (Fig. 1-2). This fault was active during late-Oligocene and early-Miocene times, paused during the rest of Miocene, and was reactivated during the Pliocene-Pleistocene periods as suggested by the hot springs along

this major fault. The reactivation of the Aguán Fault, however, was not incorporated by Manton (1987) into any of the morphotectonic units he postulated as created by two episodes of recent faulting and tectonism in northern Honduras.

Climate

The study area is situated within the trade winds belt. Most of the year the predominant winds along the north coast of Honduras are easterly. However, from October to December, strong north winds are common (Schramm, 1981).

The climate of the valley ranges from semiarid subtropical in the western section of the valley and surrounding mountains, subhumid at the center, to humid in western sections. There is, in fact, a west-east precipitation gradient along the valley with a mean rainfall of about 800 mm in the west, and >2000 mm in the extreme east. On the north littoral, the climate is similar to the eastern Aguán Valley. Precipitation is strongly seasonal in northern Honduras. The wet season extends from August to December, with maximum precipitation in September and October. The dry season extends from January to July, with maximum dryness occurring from February to May.

Mean annual air temperature is 27° C. Monthly mean temperatures range from a maximum of about 35° C during April, May, and June; to a minimum of about 18° C from

December to March. The three hottest months average 28° C, and the three coldest months 24° C.

Soil moisture regime ranges from ustic in the west to udic in the central part. The soil temperature regime is isohyperthermic in the whole valley.

Paleoclimatic information is not available in Honduras. Catt (1988, p. 25) speculated that major changes in temperature should not be expected during the Quaternary in the lowlands of low-latitude regions such as Central America. However, recent studies around the circum-Caribbean area reported the opposite. Significant climatic changes during late Pleistocene and Holocene have been reported in the Caribbean by several investigators (Hastenrath, 1976; Bradbury et al., 1981; Deevey et al., 1983; Leyden, 1984; 1985; Hodell et al., 1991; Higuera-Bundy, 1991; Curtis, 1992). There are unanimous conclusions that the climate was cooler and drier in late-Pleistocene Age and changed to warmer and wetter conditions at the onset of the Holocene. Chapter I offered a more detailed discussion about the paleoclimate of the area.

Morphometric Analyses

Fault-bounded mountain range morphology reflects the interaction between uplifting along a narrow zone (mountain-front-piedmont junction) and concurrent denudational processes (Bull, 1984). A diagrammatic sketch (Fig. 2-3)

Figure 2-3. Sketches of mountain front-piedmont characteristics that result from different uplift rates. The equations describe the interrelation of local base-level processes typical of different classes of tectonism (after Bull, 1984).

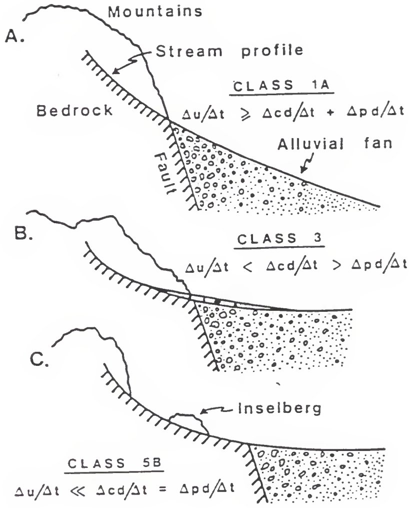

$\Delta u/\Delta t$=relative uplift

$\Delta pd/\Delta t$=piedmont degradation

$\Delta cd/\Delta t$=stream channel downcutting

describing three classes of relative tectonic activity along mountain-front piedmont junctions with their respective descriptive equations. Table 2-1 shows a classification of relative tectonic activity of mountain fronts in the Quaternary. Descriptive equations relate local base-level processes for fluvial systems immediately upstream and downstream of mountain-front-piedmont junctions (Bull, 1984).

Morphometric analyses were based on the study of landform arrays, evolution of landscapes, and in the development of process-response models aiming to explain the relationship between geomorphic processes, lithology, landforms, and pedogenesis through time. This study utilized quantitative parameters, measured on topographic maps, as a means to assess the relative tectonic activity of the faults that have generated the morphotectonic units, piedmonts, and mountain fronts surrounding the Aguán Valley (Fig. 2-4).

The geomorphic indices used in this study were mountain-front sinuosity (Bull, 1977b; Bull and McFadden, 1977; Bull, 1978) and the stream profile concavity index (K) as adapted by Menges et al. (1987), from Shepherd (1979) and Kelson (1986). This index is similar to the hypsometric integral of Strahler (1952).

Other morphometric parameters useful for the analyses of tectonic landforms on mountain fronts and potentially

Table 2-1. Classification of Quaternary relative tectonic activity of mountain fronts.

Relative Tectonic Activity	Rate of Activity	Typical Landforms at Mountain Fronts: Piedmont	Typical Landforms at Mountain Fronts: Mountain
Highly Active			
Class 1			
A	$\Delta u^{a}/\Delta t^{b} \geq \Delta cd^{c}/\Delta t + \Delta pa^{d}/\Delta t$		Unentrenched fanV-shaped cross-valley profile in bedrock
B	Same	Unentrenched fan	U-shaped cross-valley profile in alluvium
Moderately Active			
Class 2	$\Delta u/\Delta t < \Delta cd/\Delta t > \Delta pd^{e}/\Delta t$	Entrenched fan	V-shaped valley
Class 3	Same	Same	U-shaped valley
Class 4	Same	Same	Embayed mountain front
Inactive			
Class 5			
A	$\Delta u/\Delta t << \Delta cd/\Delta t > \Delta pd/\Delta t$	Dissected pediment	Dissected pediment embayment
B	$\Delta u/\Delta t << cd/\Delta t = \Delta pd/\Delta t$	Undissected pediment	Pediment embayment
C	$\Delta u/\Delta t << \Delta cd/\Delta t > \Delta pd/\Delta t$	Undissected pediment	May have characteristics of active mountain front

NOTE: From "Tectonic Geomorphology" by W. B. Bull. 1984. *Journal of Geological Education, 32*, 311.

[a] u = uplift
[b] t = time
[c] cd = channel downcutting
[d] pa = piedmont aggradation
[e] pd = piedmont degradation

Morphometric Parameters for Tectonic Analysis of Mountain Fronts

	Morphometric Parameters	
	S	K
Definition	Sinuosity of topographic mountain fronts	Stream profile concavity
Mathematical Derivation	LmF/Ls	∫Stream long profile, ie., area under % height - % distance longitudinal profile curve.
Measurement Procedure	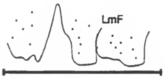 Ls *(plan view)*	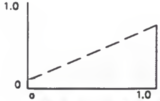 *(Plot derived from longitudinal profile measured from topographic maps)*
Source	Bull, 1978 Bull and McFadden, 1977	Adapted from Shepard, 1979 and Kelson, 1986

Figure 2-4. Morphometric parameters used in the morphological tectonic analysis of mountain fronts (modified after Menges et al., 1987).

usable in this study, were not used because the lack of resolution of the topographic maps. Such parameters include: percent faceting along mountain fronts, percent dissected mountain fronts, and percent dissected facets (Menges et al., 1987); and valley:floor-valley height ratios (Bull, 1978).

Changes of river patterns have been used to detect possible tectonic deformations along a valley (Schumm, 1985; 1986; Ouchi, 1985; Adams, 1980). However, this procedure does not seem reliable for the Aguán River. The river exhibits a continuous increase of meandering downstream that appears to be strongly related to the increasing discharge downstream of the river as the climate becomes wetter and larger tributaries join the main stream.

Mountain-front sinuosity (Smf) is defined as the ratio of the length of the mountain-piedmont junction (Lmf) to the straight length of the mountain front (Ls), or Smf = Lmf/Ls. Active and recent tectonic activities are characterized by straight mountain-piedmont junctions which translate to low Smf values. By contrast, when denudation processes exceed uplifting the mountain-piedmont becomes irregular and sinuous, generating high Smf values (Bull, 1984). The mountain-front sinuosity defines the morphology of the mountain fronts. Values of Smf are close to 1.0 for tectonically very active fronts; the value increases with time as the mountain front retreat due to erosional processes.

The Smf present some difficulties. The behavior of fluvial systems is not only the result of differential uplifting (changes of the baselevel), but changes in bedrock lithology. Smf does not offer enough sensitivity to detect temporal variation in uplift (i.e., rapid uplifting followed by stability or initial rapid uplifting followed by a regular decrease with time) and slow continuous uplifting. Finally, it has been found that a certain threshold of uplifting could be sufficient to determine low Smf values (Bull, 1978; Rockwell et al., 1985).

In this investigation mountain-front sinuosity was estimated along the two margins flanking the Aguán Valley and along the north front of the Cordillera Nombre de Dios bordering the Caribbean Coastal Plain. Each of these three lineaments was divided into discrete segments (fronts) according to similarities in geologic and geomorphic characteristics as indicated by changes in drainage pattern, known changes in lithology, and abrupt changes in front orientation. Special attention in measuring sinuosity was taken in defining the topographic mountain-piedmont junction and segmenting the mountain fronts (Menges et al., 1987).

Longitudinal profiles of third to fifth order streams draining the three lineaments were plotted in order to detect irregularities (i.e., nick points) along the channel slope and to generate a quantitative diagram of the overall shape of the stream profiles. In order to make

quantitatively sound comparisons among the fronts, a stream concavity index (K) was calculated. The longitudinal stream profiles were normalized by transforming the heights (h) and lengths (X) to percentages of the total height (H) and total length (L), respectively, and then calculating the area under the normalized curve (Menges et al., 1987). Low K values exhibited by concave-up profiles were characteristic of long periods of channel degradation and/or long time periods without baselevel changes. Conversely, high K values and associated convex-up profiles were identified with active baselevel changes.

A major problem interpreting the concavity parameter is related to possible changes of lithology along the stream channel that can be misinterpreted as indicating baselevel changes. Another limitation of the method is related to the resolution of the streams on the topographic maps.

The above discussed quantitative parameters, mountain-front sinuosity and stream profile concavity, were measured from 1:50,000 topographic maps covering northern Honduras.

To measure the sinuosity parameter, it was necessary to define the topographic junction. Field work and aerial photographs were extremely useful in assessing possible lithologic changes along the stream profiles not shown on the geologic map.

Results and Discussion

Morphometry of the Mountain-Piedmont Junctions

The location of the two valley margins and the Caribbean coastline as well as the mountain fronts on each one of these lineaments are shown in Figure 2-1. Each front will be discussed separately for the valley margins and the Caribbean coastline will be discussed as a whole. The results of the morphometric analyses will render a reconnaissance level of understanding about the tectonism of the study area and the relative degree of activity of the major faults associated with lineaments.

The Cordillera Nombre de Dios between the north margin of the valley and the Caribbean coastline reaches elevations that surpass 2000 m in the west but only 1000 m in the east. The topographic cross-section shown in Figure 2-2 indicates that there are more internal mountain fronts in the west than in the east.

Cross-section A-A′ apparently indicates a single mountain front resulting from one continuous orogenic process. Cross-sections B-B′ and C-C′ display subparallel mountain ranges with northwest-trending faults defining several mountain fronts. Cross-section B-B′ indicates that the mountain front in the northern part has experienced more rapid uplifting than the mountain fronts in the southern parts. Cross-section C-C′ shows a more complex pattern.

The Smf and K parameters and the morphology of the alluvial fans and fan piedmonts were determined from topographic maps with a scale of 1:50,000. This was the first approach to estimating the relative tectonic activity around the valley, and to making useful comparisons between and within the fronts.

Relative tectonic classes have been obtained in other places with different climatic conditions, where the Smf and K parameters were related to measured degrees of uplifting (southeast USA: Bull, 1978; Costa Rica: Menges et al., 1987). Left lateral slip rates have been calculated in the Motagua Valley, Guatemala, which is directly related to the Aguán Valley Fault system as part of the northern boundary of the Caribbean Tectonic Plate (Schwartz et al., 1979). But only uplift rates have been calculated in the eastern part of the boundary (Dodge et al., 1983; Bender et al., 1979). Both situations can be related to ascertain possible orders of magnitude of uplifting, based on Smf and K values, in northern Honduras.

South Margin of the Valley (SMV)

This margin runs along the active La Esperanza Fault (Fig. 2-1). This fault, postulated by Manton (1987) is depicted in the new geologic map of Honduras (Kozuch, 1991) parallel to the Aguán Fault along the south margin of the Aguán Valley. This margin was subdivided into five mountain

fronts according to criteria previously indicated, concavity index was computed on 12 third to fifth order streams along this boundary.

The first two mountain fronts along this margin of the valley are continuous east to west. The remaining three fronts are continuous in a southwest-northeast direction. The first four fronts of this margin show well developed alluvial fans. Front 5 is located at the end of the valley (the delta) where the floodplain of the Aguán River has occupied virtually the entire valley (lateral planation).

Uplifting is apparently very active and recent along this front. Figures 2-5 and 2-6 show the longitudinal and/or concavity profiles of four streams of this lineament.

Front 1: Macora River to Yaquala River

The bedrock of this front is composed of Paleozoic or pre-Jurassic metamorphic rocks corresponding to the Cacaguapa Schist Formation. The front extends for about 26 km. The first 5 km segment of this front does not exhibit alluvial fans. In fact, the Aguán River channel flows in a straight pattern along the south edge of the valley in direct contact with the bedrock of the front. The remainder of the river flows in a slightly braided pattern.

At first glance, one can think that the river location in this segment is the result of south-trending tilting, causing stronger uplifting in the north margin of the

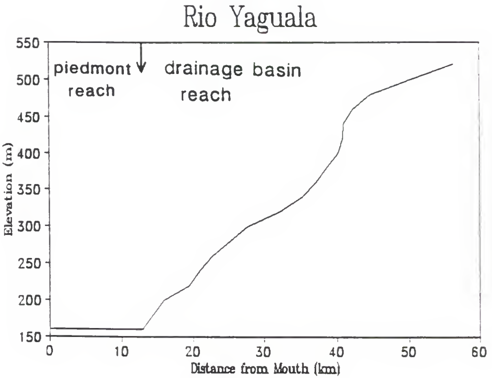

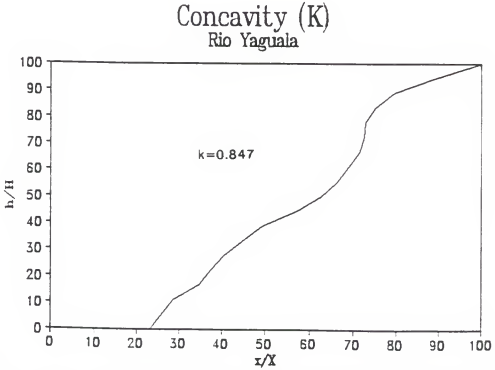

NOTE: h/H = measured heights/cumulative height of profile; x/X = plotting measure horizontal distance/total length of profile; K = concavity index.

Figure 2-5. Longitudinal profile and normalized concavity profile of the Yaguala River.

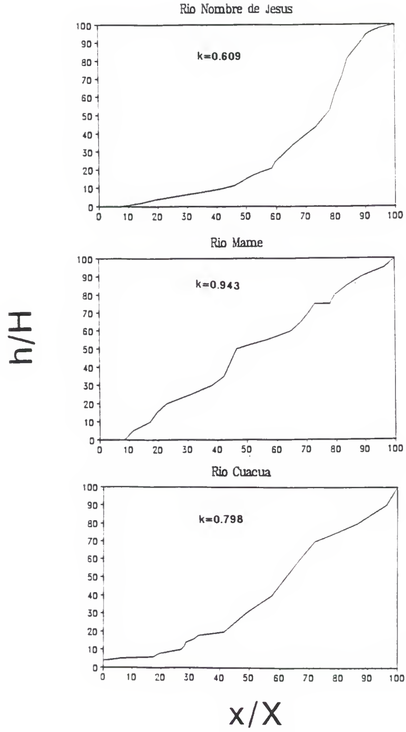

NOTE: h/H = measured heights/cumulative height of profile; x/X = plotting measure horizontal distance/total length of profile; K = concavity index.

Figure 2-6. Normalized concavity profile of three representative streams in the south margin of the valley.

valley, thus forcing the channel to the south side. This is unlikely. It seems more plausible that excess sediment from the north side is responsible for the situation. Tilting cannot be accounted for as other evidences will show that uplifting is actually greater in the south margin of the valley controlled by the more active La Esperanza Fault. Asymmetry in the sediment deposition should be considered the cause of the river shifting toward the south.

Along the first 5 km on the valley, the Aguán River has not formed a floodplain. It flows entrenched on the alluvial-fan piedmont formed by the streams draining from the mountains of the northern side of the valley.

Along the remaining 21 km of Front 1, small alluvial fans do occur. The fans increase in size toward the west as the Aguán River shifts to the middle of the valley. The river along this reach has already formed a narrow floodplain.

The alluvial fans of this last segment of Front 1 have a length up to 2.5 km. The piedmont is not formed by fan-shaped, individual alluvial fans, which coalesce to form a fan piedmont. It can be better described as an alluvial slope. This alluvial slope is unsegmented and unentrenched, and deposition continues along the whole piedmont.

The mountain front sinuosity of this front is 1.37 and the average concavity index of two streams is 0.690. These

values indicate active tectonism which agrees with the general morphology of the area.

Front 2: Yaguala River to Mame River

Yaguala and Mame Rivers are the two most competent streams of the valley's south margin. The bedrock of the Yaguala River comprises mainly the Cacaguapa Schists Formation; that of the Mame River comprises nondifferentiated volcanic rocks. La Esperanza Fault has been inferred in the geologic map of Honduras (Kozuch, 1991) to be located south of the front. This location of the fault could be due to problems of scale; the fault seems to coincide roughly with the mountain front-piedmont junction.

The alluvial fans in this front are relatively large, with an average length of 5 km, except for the western part, where the Aguán River gets closer to the mountain front and the fans are smaller as their ability to grow is limited by the river. The alluvial fans along this front also are unentrenched and unsegmented.

The floodplain of the Aguán River nearly begins in this reach of the valley and is separated from the alluvial fans of both sides of the valley by a steep alluvial escarp 10-20 m high.

The sinuosity of this segment of the mountain front is similar to that of Front 1; its value is 1.43. The average concavity index measured over four streams is 0.704. Both

values are close to those of Front 1, although there is a change in lithology.

Front 3: Mame River to Los Cocos Creek

The lithology of this front is constituted by the clastic red-beds of the upper member of the Valle de Angeles Group. This front has an extension of approximately 26 km bounded by a relatively wide piedmont with unentrenched and unsegmented alluvial fans.

Although the valley becomes narrower along this segment, the alluvial fans on this front exhibit large sizes as no fans occur in the opposite front. The reason is that the Aguán River in this reach has been forced to the northern edge of the valley by the abundance of sediments produced on this front. These sediments have been carried out primarily by the powerful Mame River. The lack of sediments from the opposite side of Front 2, is due in part to the shifting of the streams draining this front of the northern margin which have been diverted to the west by a small conjugated fault of the Saba Fault.

The Smf of this front is 1.68, the largest of this mountain front. Accordingly, the average of K calculated on two streams is the lowest (0.422). This value may indicate a significant change in activity along La Esperanza Fault.

Front 4: Los Cocos Creek to San Pedro River

Front 4 runs also along the La Esperanza Fault. This segment is composed of rocks of the Cacaguapa Schists Formation (as is Front 1) and has an extension of 19 km. The piedmont along this segment shows large unentrenched and unsegmented alluvial fans.

The activity of La Esperanza Fault seems to increase in these fronts as denoted by a low Smf of 1.13, which conforms very well with the general appearance of the area. The average of K measured on two streams is correspondingly high (0.798).

Front 5: San Pedro River to Corocito River

This front is located in the eastern end of this margin of the valley and has an extension of 32 km. This long segment exhibits a narrow piedmont without discernible alluvial fans. In fact, the floodplain of the Aguán River in some parts of this front binds directly with the steep escarpment of the Sierra de La Esperanza mountains. The bedrock is composed of granites, granodiorites, diorites, and tonalites of Cretaceous to Tertiary age.

The Smf in this segment is 1.23, and the average K of two streams is 0.599. These values comply with the abruptness in this section of the mountain front-piedmont junction, indicating very high activity of the La Esperanza Fault.

North Margin of the Valley (NMV)

This margin is encompassed by the Aguán Fault from which it has retreated considerably along most of its fronts, especially in the western fronts. This margin was divided into six fronts based on the standards of continuity, geology, drainage pattern, and change in orientation. Most of these fronts have an west-east orientation, except for Front 9 which has a south-north trend and Front 10 with a southeast-northwest direction.

Alluvial fans are present in Fronts 6 to 8, but Fronts 9 to 11 exhibit a large and apparently old pediment with several limestone knobs. The concavity index was calculated on 15 third to fifth order streams along this margin. Figure 2-6 shows the longitudinal profiles and k values of three streams of this lineament.

Front 6: San Marcos River to Santa Barbara River

At the very beginning of this front, in the northwestern corner of the valley, the Chiquito and San Marcos Rivers have formed narrow and rectangular-shaped drainage basins (mountain-valley fans) up to 4 km long, incised into the mountain front. The rest of the front has large unentrenched and unsegmented alluvial fans 5-7 km long. On the two larger alluvial fans of this front the trunk streams have shifted from the center to the western side of the fanheads. In the alluvial fan formed by the San

Felipe Creek, small streams are depositing new sediments on the east margin of this huge alluvial fan, creating a fan collar. The formation of the fan collar is a result of the trunk stream drifting to the west.

The bedrock lithology of this front corresponds to the Cacaguapa Schists Formation along an extension of 25 km. The Smf is 2.30, a relatively large value and the average K measured over four streams is 0.571, which does not correspond very well with the high sinuosity value of this front. It is because of the lack of sensitivity of K-index as influenced by changes in lithology.

Front 7: Santa Barbara River to Sabana Grande Creek

Front 7 is a continuation of Front 6 except for a major change in lithology. This front consists of undifferentiated volcanic rocks, mainly tuffs, andesite, and pyroclastic flows. The front extends for 28 km with coalescing alluvial fans, and long, rectangular, V-shaped basins. The alluvial fans are unentrenched and unsegmented with characteristic convex cross sections.

The Smf of the mountain-piedmont junction is 1.78 along this front, and the average K of three streams is 0.340.

Front 8: Sabana Grande Creek to Terrero Creek

Front 8 as a continuation of Front 7, presents the same lithology, but no piedmont is present in this front. The valley narrows in this reach from about 10 km in the previous reach to some 5-6 km in this one. The Aguán River, as a result of major uplifting and major sediment production in the corresponding front of the south margin, impinges directly on the mountain front along Front 8.

The sinuosity is, however, not much larger (1.56) than that of the correspondent south front (1.43 in Front 2). A major sediment production in Front 2 could be the reason for the shifting of the Aguán River to the north along this reach. The streams of Front 8, except the Uyuca River, drain to the west along a small conjugated fault of the Saba Fault, creating an asymmetry in the production of sediments in relation to Front 3.

Front 9: Terrero Creek to Rio de Piedras

Front 9 marks an abrupt change in direction along this lineament. It runs south-north on a lithology dominated by the red clast of the Valle de Angeles Group. The front extends for 24 km and its bounded to the west by an extensive pediment grading to the Aguán River floodplain, which in this reach runs southeast-northwest.

This front has large and numerous embayments resulting in a Smf of 2.66, the largest of any front in the

Aguán Valley. The average K of two streams of this front is consequently low 0.336.

Front 10: Rio de Piedras to La Cuchilla Hill

Front 10 is a continuation of Front 9 with a change in continuity to a southwest-northeast direction. The front extends for 28 km and its lithology is the same as Front 9. The front also is bounded by an broad pediment which grades to the Aguán Valley.

The Smf is also relatively high, 2.40, and the average K calculated on three of the front streams is correspondingly low with a value of 0.277.

Front 11: La Cuchilla Hill to Los Presos Creek

Moving eastward, Front 11 is the last front of the northern margin of the valley. It extends for 22 km along the Aguán formation which consists of fine-grained siliceous sediments, limestones, and interstratified volcanic ashes.

The sinuosity of the front is lower in relation to the antecedent fronts. Its value is still relatively high, i.e. 1.65. The average concavity index computed on two streams is 0.443.

Caribbean Coastline (CC)

This lineament corresponds to the eastern half of the junction between the Cordillera Nombre de Dios and the north

coastal plain of Honduras which approximately parallel to the Aguán Valley. This mountain front-piedmont junction has a general southwest-northeast direction and is bounded to the north by the active La Ceiba Fault. The width of the piedmont in this segment of the costal plain, which extends from Trapiche Creek to the Guaimoreto Lake, varies from 0 in places where the mountain front is directly in the sea to 11 km in the wider places corresponding to the basins of the Cangrejal River and the Papaloteca River.

Except in the distal and lowest parts of the wider plain segments, formed by the Cangrejal and the Papaloteca Rivers, the plain and the beds of the rivers and streams along this lineament are composed of very coarse debris of sand, cobbles, and boulders. Very large boulders, some of the size of a small house, are common in some parts of the coastal plain and seems to be deposited by gravity. All rivers and streams crossing these fronts show beds armored by cobbles and boulders.

The alignment was divided into six fronts based on the same criteria used for the Aguán valley margins. To calculate the concavity index, 13 rivers, of third to fifth order, were used. Figure 2-7 shows the longitudinal profiles and k values of three streams of this lineament.

The sinuosity is low along these fronts, varying from 1.0 to 1.11. One exception is Front 13 between the Bonito and the Cangrejal Rivers, which has a sinuosity of 1.60.

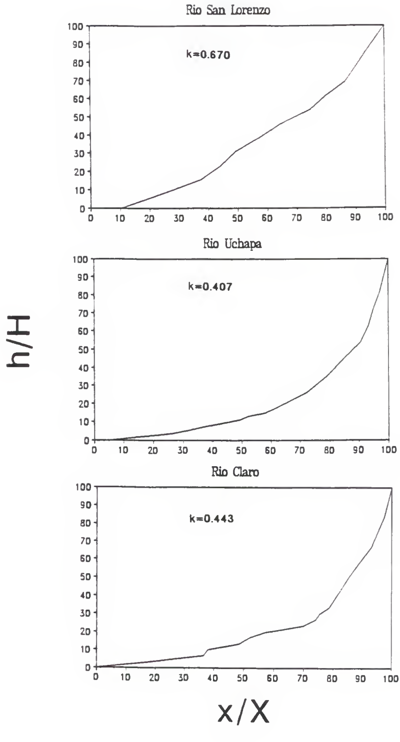

NOTE: h/H = measured heights/cumulative height of profile; x/X = plotting measure horizontal distance/total length of profile; K = concavity index.

Figure 2-7. Normalized concavity profile of three representative streams in the north margin of the valley.

The concavity index is relatively high, ranging from 0.47 to 0.75 with an average for the 13 plotted streams of 0.578 (Figure 2-8).

Tectonic Control on Mountain Fronts

The morphologic data obtained for the mountain fronts of the three lineaments are shown in Table 2-2. Values of sinuosity of fronts range from 1.0 to 2.66. Means of 1.37, 2.06, and 1.14 for the south margin of the valley (SMV), the north margin of the valley (NMV), and the Caribbean coastline (CC), respectively. These data indicate higher sinuosity values for the NMV, and lowest values for the CC.

Statistical tests indicate a significant difference between the mean sinuosity of fronts in both the CC and the SMV with respect to the fronts of the NMV. However, the mean sinuosities of the CC and SMV fronts were statistically indistinguishable (Table 2-3). The interpretation of the tests indicate that the mountain fronts of the NMV are more sinuous and dissected that those of the SMV and the CC.

Statistical tests for concavity index of the fronts render similar results (Table 2-4). No statistical significant differences existed between the fronts of the SMV and the CC. There were significant differences between CC and SMV and between CC and NMV.

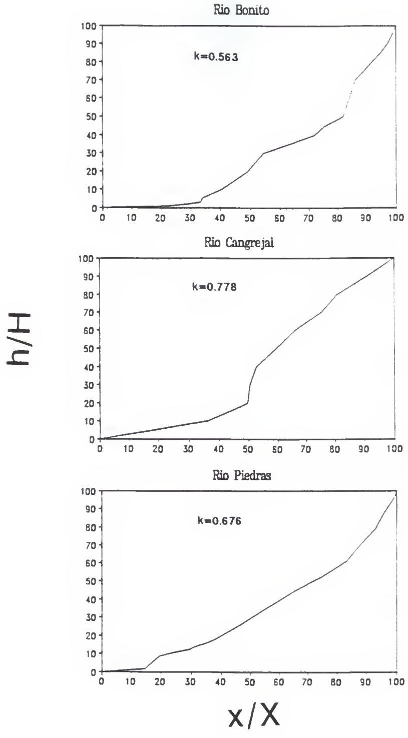

NOTE: h/H = measured heights/cumulative height of profile; x/X = plotting measure horizontal distance/total length of profile; K = concavity index.

Figure 2-8. Normalized concavity profile of three representative streams of the Caribbean coastline.

Table 2-2. Fluvial-geomorphic data for mountain fronts.

Mountain Front	Location	Orientation	Length	Sinuosity	Average K Index
SMV					
Front 1	Macora River to Yaguala River	E-W	26 km	1.37	0.69
Front 2	Yaguala River to Mame River	E-W	35 km	1.43	0.70
Front 3	Mame River to Los Cocos Creek	SW-NE	26 km	1.68	0.42
Front 4	Los Cocos Creek to San Pedro River	SW-NE	19 km	1.13	0.80
Front 5	San Pedro River to Corocito River	SW-NE	32 km	1.23	0.60
			Σ=148 km	$\bar{X}$=1.37	$\bar{X}$=0.64
NMV					
Front 6	San Marcos River to Santa Barbara River	E-W	25 km	2.30	0.57
Front 7	Santa Barbara River to Sabana Grande Creek	E-W	28 km	1.78	0.34
Front 8	Sabana Grande Creek to Terrero Creek	E-W	24 km	1.56	0.58
Front 9	Terrero Creek to Piedras River	S-N	15 km	2.66	0.34
Front 10	Piedras River to Calichal Hill	SW-NE	28 km	2.40	0.28
Front 11	Calichal Hill to Los Presos Creek	E-W	22 km	1.65	0.40
			Σ=142 km	$\bar{X}$=2.06	$\bar{X}$=0.42
CC					
Front 12	Trapiche Creek to Bonito River	E-W	16 km	1.00	0.47
Front 13	Bonito River to Cangrejal River	E-W	11 km	1.60	0.61
Front 14	Cangrejal River to Papaloteca River	E-W	30 km	1.01	0.54
Front 15	Papaloteca River to Bambu River	E-W	29 km	1.11	0.59
Front 16	Coco River to Corozo Alto River	E-W	27 km	1.00	0.75
Front 17	Mojaguay River to Guaimoreto Lake	E-W	11 km	1.09	0.52
			Σ=124 km	$\bar{X}$=1.14	$\bar{X}$=0.58

Table 2-3. Summary of statistical tests on morphometric data--Wilcoxon Rank Sum Test for statistical differences in the sinuosity index of the mountain fronts.

Test	Decision	Significance Level
Caribbean coastline (CC) vs. north margin of valley (NMV)	Reject	$\alpha = 0.05$
Caribbean coastline (CC) vs. south margin of valley (SMV)	Accept	$\alpha = 0.05$
South margin vs. north margin of valley	Reject	$\alpha = 0.05$

Table 2-4. Summary of statistical tests on morphometric data--Wilcoxon Rank Sum Test for statistical differences in the concavity index of the mountain fronts.

Test	Decision	Significance Level
Caribbean coastline (CC) vs. north margin of valley (NMV)	Reject Ho	$\alpha = 0.05$
Caribbean coastline (CC) vs. south margin of valley (SMV)	Accept Ho	$\alpha = 0.05$
South margin vs. north margin of valley	Reject Ho	$\alpha = 0.05$

Detailed observations of the morphological data suggest differences in the mean sinuosities among the fronts along the NMV which shows larger Smf values, as expected, for Fronts 9 and 10, which correspond to the section of the mountain front where the retreat of the mountain front-piedmont junction is obvious. However, it is important to note that these fronts occur in a wetter environment than that of the western fronts. Along the south margin of the valley, Fronts 4 and 5 show a lower mean sinuosity value than Fronts 1 to 3, indicating an opposite trend to the one on the north margin.

The concavity index values indicate that this parameter is less sensitive than the sinuosity as suggested by the standard deviations in Table 2-5. Also, the mean of concavity index for the CC shows a lower (.563) value than that of the SMV (.649) although the sinuosity mean of the SMV (1.37) is greater. Bull and McFadden (1977) related ranges of mountain front sinuosity (Smf) with classes of tectonic activity as follows: Class 1 for fronts with Smf values ranging from 1.0 to 1.6, Class 2 from 1.4 to 3.0 and Class 3 from 1.8 to more than 5. They specified that sinuosity values larger than 3 are characteristic of embayed and pedimented mountain fronts which have retreated for more than 1 km. from the original position. Bull (1978; 1984) expanded the tectonic activity classes to 5 (Table 2-1).

Table 2-5. Summary of mountain front sinuosity and concavity data.

Area	Number of Segments	Mountain segments sinuosity			Number of Streams	Concavity (k)		
		Range	Mean	Std. dev.		Range	Mean	Std. dev.
Caribbean coastline	6	1.00-1.60	1.14	0.23	13	0.367-0.778	0.563	0.123
North margin of valley	6	1.56-2.66	2.07	0.45	15	0.413-0.670	0.413	0.154
South margin of valley	5	1.13-1.68	1.37	0.21	12	0.403-0.943	0.649	0.187

Undoubtedly, to the mountain fronts of the north coastline of the valley, a Class 1 (Table 2-1) for tectonic activity can be assigned (Bull, 1977; 1978; 1984) due to the low Smf values of the fronts in this lineament (Smf close to 1). Only the relatively high value (Sm = 1.60) in Front 13 perhaps should be removed for the statistical tests since this front is affected by a small fault along the Bonito River. For the other two lineaments, the assignment of classes to the fronts was more difficult becasuse these classes were calibrated for uplift rates in areas of arid climate. Menges et al. (1987) preferred not to correlate their findings using morphological analysis in humid Costa Rica with the values obtained by Bull and McFadden (1977) and Bull (1978) in the arid landscapes of California. In this study the climatic difference is less marked, at least for the western half of the valley. Nevertheless, it is not unreasonable to assign Class 1 to all but Front 3 along the SMV. A Class 2 seems more adequate for Front 3.

To the mountain fronts of the NMV west of Saba Fault class 3-4 of tectonic activity were assigned. East of Saba Fault, the pediment along Fronts 8, 9, and 10 were considered tectonically inactive. These fronts are strongly embayed and had retreated considerably, they were, therefore, classified within class 3.

The relative classes of tectonic activity obtained from morphometric analyses are associated with descriptive

equations that interrelate local base processes to fluvial systems that cross mountain-piedmont junctions. Class 1, other than having low sinuosity values and high stream concavity values, is characterized by unentrenched fans. Also upstream of the front, uplifting is greater than the addition of channel downcutting and piedmont deposition. This situation is definitively the case along the south margin of the Aguán Valley.

Most difficult yet is to infer possible rates of uplifting based on morphometric analysis alone. Correlation with independently obtained uplift rates are necessary for determined regions. Bull (1978) determined rates of 1-5 m/1000 yrs to Class 1 fronts, 0.5 m/1000 yrs to Class 2 fronts, 0.05 m/1000 yrs to Class 3 fronts, and 0.005 m/1000 yrs to Classes 4 and 5 fronts. Rockwell et al. (1985), working along active faults in the California Ventura Basin, found Class 1 fronts with uplift rates as low as 0.5 m/1000 yrs. They concluded that in this region a threshold of 0.4 m/1000 yrs is enough to maintain low sinuosity values.

Vertical uplift associated with the northern Caribbean Plate boundary has not been determined in the area. In the eastern part of the boundary, uplift rates of 0.3 to 0.4 m/1000 yrs were calculated for raised marine terraces in northern Hispaniola (Dodge et al., 1983) and rates of 0.25 to 0.44 m/1000 yrs on terraces of Barbados (Bender et al., 1979).

The above discussion gives at least an idea of the order of magnitude of uplift in the Aguán Valley and surrounding area. Uplift rates from 1 to 5 m/1000 yrs possibly obtain along the La Esperanza Fault and Ceiba Fault. Along the western part of the Aguán Fault, rates are approximately 0.3 to 0.5 m/1000 yrs obtain, whereas one or two orders of magnitude less should be expected on the eastern part.

Summary and Conclusions

Seventeen mountain fronts corresponding to three lineaments occurring along known parallel faults in northern Honduras and their associated piedmonts were investigated morphometrically. Mountain-front sinuosity, longitudinal stream profiles, and concavity indices provided quantitative evidence of the relative tectonic activity along the mountain fronts and associated faults studied.

Statistical tests of the morphometric data show that the La Esperanza Fault along the south margin of the Aguán Valley and La Ceiba Fault along the Caribbean Coast parallel to the valley are more active tectonically than the Aguán Fault which runs along the NMV. The morphological data also suggest differences in tectonic activity along the lineaments. This is true especially for the NMV. Highly active fronts consistently render lower sinuosity values than less active fronts. These data also agree with the

morphology of the piedmont present in some of the fronts. The concavity index, although useful in differentiating the tectonic activity among lineaments, was less sensitive in detecting differences between fronts along the same lineament.

No information about rates of uplift along the fronts and lineaments studied is available. Such information is not even available for other associated fault systems in Honduras and Guatemala. Based on scarce data from the eastern section of the northern boundary of the Caribbean Plate and data from other areas where correlation between morphometric analysis of mountain fronts and uplift rates have been made, some speculation about the order of magnitude of uplift along the parallel faults of northern Honduras can be made. Along La Esperanza and La Ceiba Faults more than 1-5 m/1000 yrs of uplift is suggested. Along the Aguán Fault 0.3 to 0.5 m/1000 yrs is suggested east of the Saba Fault and less than 0.05 m/1000 yrs west of the Saba Fault.

Manton (1987) described and interpreted the eastern part of the Aguán Valley (Upper- and Middle-Aguán), west of the Saba Fault, as a parallel-sided depression in a wide fault zone that resulted from preferential erosion of more weatherable rocks and that the channel of the Aguán River runs along the major Aguán Fault. According to the new geologic map of Honduras (Kozuch, 1991), and direct field

observations during this investigation, at least the first third (from west to east) of the surrounding mountains at both margins of the valley are composed of the same lithology (i.e., graphitic mica schist of the Cacaguapa Schist formation (Pzm)). Furthermore, the rest of the northern margin up to the Saba Fault, and a considerable part of the rest of the south margin, are underlain by nondifferentiated volcanic rocks of unknown age (tuffs, andesites, and pyroclastic rocks) (Tv). Only the last third of the south margin, in this half of the valley, exhibits a lithology different from the northern counterpart. This section is underlain by the Valle de Angeles Group.

Due to the orographic effect of the Cordillera Nombre de Dios, the northern side of the western part of the valley is significantly drier than its southern counterpart. This can be seen by the lower number of large streams draining the northern margin of the western part of the valley. However, the Caribbean side mountain fronts are much more embayed than the southern margin as demonstrated by the morphological analysis.

Another interpretation clearly is demanded. Differential weathering due to different lithology cannot explain the geometry of this half of the valley. Based mainly on the morphologic data obtained in this investigation, it is proposed that the morphology of the western part of the valley is due to different tectonic

activity along both sides. The northern mountain front of the western part of the valley was aligned with the Aguán Fault from which it has retreated due to the relative moderate and older activity of this fault. The southern mountain front corresponds to the prolongation of the most active La Esperanza Fault. The recent activity of this fault has precluded the embayment and retreatment of the mountain fronts along it.

The Aguán Fault was considered an undifferentiated fault. Later, it was considered as a strike-slip fault related to the northern boundary of the Caribbean Plate. Manton (1987) proposed the La Esperanza Fault as running only along the eastern part of the south margin of the valley (Fig. 2-9). This study suggests that the La Esperanza Fault covers the entire SMV and the Aguán Fault covers the north margin. The earlier phase of regional uplift identified with the Saba Fault (Manton, 1987) also includes the northern margin (west of Saba Fault) of the Aguán Valley controlled by the Aguán Fault. Also, it is proposed that the Pleistocene-Holocene activity of the Aguán Fault is limited to its approximate western half (west of the Saba Fault) of the valley.

Manton (1987) postulated two phases of regional uplifting in the Aguán Valley. An earlier phase represented by the Saba Fault and a younger phase represented by the SMV east of Saba Fault (La Esperanza Fault). The results

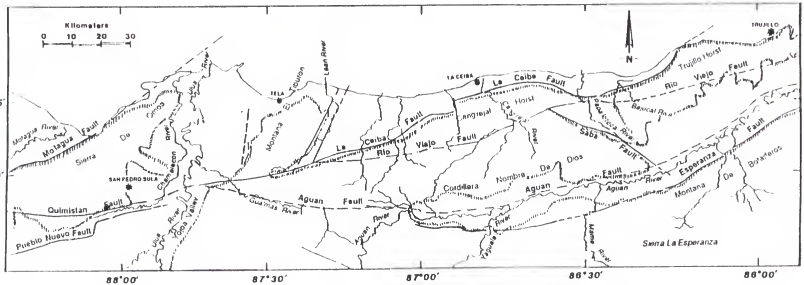

Figure 2-9. Physiographic map of north-central Honduras and adjacent eastern Guatemala showing major topographic features and faults of the region (compiled after Manton, 1987).

obtained from this study lead to the inclusion of the western part of the SMV (continuation of La Esperanza Fault) with the younger phase of uplift, and the western part of the Aguán Fault (reactivation of the Aguán Fault) with the earlier phase of uplift.

CHAPTER III
THE FLOODPLAIN OF THE UPPER-AGUÁN VALLEY

Introduction

Published literature concerning river regimes, and fluvial landscapes is extensive. Rivers are among the most active erosional agents in nature, and their associated deposition landforms provide, in many cases, the stratigraphic records necessary to understand the history of rivers's regime.

Most studies on floodplains have been conducted in the temperate regions of North America and Europe. Relatively few studies have been performed in the tropical and subtropical areas of Latin America. However, since hydrologic processes and the physical laws that support them are similar everywhere, it is reasonable to assume that fluvial landscapes and landforms are similar worldwide.

An expected difference of alluvial landscapes of the tropics in relation to alluvial landscapes and landforms of other latitudes, other conditions being equal, should be the faster weathering of deposited sediments and faster development of their associated soils. This is especially true for terraces of middle-Holocene age or older, but less relevant for younger terraces and floodplains. In most cases, differences among floodplains of different regions

have been related to the variability of the annual flows and annual floods, and to the frequency of moderate and catastrophic flood events.

Lateral accretion of active migrating streams has been considered the most important fluvial process in the formation of floodplains. Wolman and Leopold (1957), stated that floodplains essentially constitute by coarse lateral accretion deposits overlain by a veneer of fine vertical accretion materials deposited by overbank flows. Nanson (1986), based on his studies in New South Wales, proposed a model in which confined streams form slowly by vertical accretion units and then are destroyed by infrequent catastrophic floods.

Schumm (1991) estimated that the problem of lateral vs. vertical accretion predominance is one of time scale. In a short term, a floodplain can be seen as mainly formed vertically by overbank deposition. In a long term, the lateral migration of the channel will eventually rework the floodplain and deposit alluvium by lateral accretion. Brakenridge (1988) considered that as a result of both processes of fluvial development two distinct sedimentary facies developed in floodplains. A bottom stratum of coarse sediments deposited on the channel bed mainly by lateral accretion and a top stratum of fine materials deposited by overbank deposition during rare high river stages.

The predominance and thickness of the top stratum will depend on the contrast between bankfull discharge and modal discharge, the capability of stream channels to adjust to higher than normal discharges, and the rapidness of channel migration (Brakenridge, 1988). He recognized, however, that his model of bottom stratum-top stratum does not cover all the complexities found in floodplain sequences.

As an example, the Aguán Valley, Honduras, as discussed in the preceding chapters, occurs in an active tectonic location and within a region where drastic climatic changes have taken place during late-Pleistocene and Holocene times. Two faults parallel the valley. The older and least active of them, the Aguán Fault, has been considered as controlling the Aguán River.

The study of a river's floodplain basically focuses on the relationships between a river's and floodplain stratigraphy (Brakenridge, 1988). Numerous studies on floodplains center on fluvial processes as influenced by climatic changes during late-Pleistocene and Holocene times (Kozarski and Rotnicki, 1977; McDowell, 1983; Knox 1983; 1985; Brakenridge, 1980; 1983; 1984; 1985; 1988). Major changes in rivers' morphology and floodplains, as a consequence of climatic changes for periods of up to 50 years, have been studied in Australia (Erskine and Warner, 1988; Riley, 1988) and in USA (Hereford, 1984). Schumm and Litchy (1963) studied the significant changes in river

morphology and construction of the floodplain of the Cimarron River in Kansas over a period of 12 years.

Changes in river morphology and floodplain geomorphology may occur in different time spans or even during a single event. The transformation caused by events of considerable magnitude on floodplains will persist depending on the magnitude of the phenomena that cause the changes and on the aftermath climatic conditions. In arid regions these changes are usually irreversible. In more humid conditions the land returns to the original form and that may do so in a matter of a few years or decades.

Except for the study of Schwartz et al. (1979) on the fluvial terraces of the Tambor River in Guatemala, no systematic research has been done on the valleys that encompass the major faults of northern Guatemala and northeastern Honduras. These faults constitute the Caribbean-North America Plate boundary in Central America.

In this study, possible influence of tectonism and climatic changes during the late-Pleistocene and Holocene Ages to the development of the Upper-Aguán River and Valley will be considered. Also, based on limited information, recent historical behavior of the river and associated geomorphic processes will be estimated.

Justification and Objectives of Study

The study reported in this chapter was focused mainly along four reaches located on a 24 km long segment of the Aguán River floodplain in the Upper-Aguán Valley, Honduras. The selection of the floodplain segment studied was based on geomorphic considerations indicating that this segment is most expressive of the geomorphic history of the valley floor.

First, this segment encompasses reaches of the Aguán River floodplain which apparently represents different positions of the river in relation to its floodplain or different geomorphic conditions. The segment chosen includes two reaches of the floodplain which occur immediately before and after the junction of the first major tributary to the main stream. It also includes reaches where the stream channel is eroding opposing walls of the the scarp that separates the floodplain from the alluvial-fan piedmonts and where the channel is flowing in the center of the floodplain. Secondly, in this segment the floodplain has been aggraded after considerable incision and widening of the river channel into sediments deposited on both sides of the valley in the form of alluvial-fan piedmonts.

The objectives of this study were to (a) decipher the relative timing and nature of the fluvial processes that resulted in the incision, widening, and development of the Aguán River floodplain inset into the fan-piedmont alluvium

in the Aguán Valley; (b) examine modern tendencies of river channel patterns, morphology, and mode of operation; (c) interpret the influence of past climatic changes and possible tectonic perturbations in the history of the floodplain.

Materials and Methods

Location of the Study Area

The study area reported in this chapter corresponds to a 24 km long segment of the floodplain of the Upper-Aguán River, northern Honduras (Fig. 3-1). The segment lies approximately between the banana farm locally known as El Cayo and the town Olanchito (between 86°-35′ and 86°-44′ west longitude and 15°-24′ and 15°-28′ north latitude). Elevations at this segment of the floodplain range from 120 to 260 m, decreasing downstream from the southwest to the northeast.

Physiographic and Environmental Settings

The Aguán River runs east-west along the Aguán Fault for approximately 260 km after flowing for approximately 60 km in the valley. The total basin area is 10,640 km^2 and the altitudes of the watershed range from 700 m at the headwaters on the heights of the Cordillera Nombre de Dios, Department of Yoro, Honduras, to 280 m at the

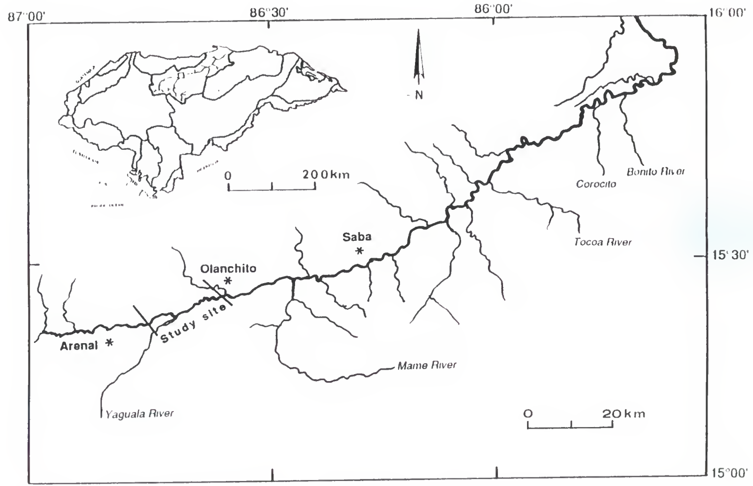

Figure 3-1. Location of the Aguán River along the Aguán Valley and the study site.

beginning of the Aguán Valley. The valley is approximately 160 km long. The width varies from less than 4 to 5 km in the upper valley to more than 15 km in the last reaches near the mouth of the river.

Along the first 26 to 27 km, within the valley, and upstream from the study site, the river flows along the valley floor incised into alluvium deposited on one or both sides of the valley in the form of alluvial fans and coalescent fan piedmonts. Approximately 10 km before the confluence of the Aguán River with its first major tributary, the Yaguala River, a relatively wide floodplain has been developed. The floodplain continues until it becomes a delta at the river's mouth in the Caribbean Sea. The provenance of the alluvium along the reaches studied mainly is constituted by metamorphic rocks of the Cacaguapa Schists group and nondifferentiated volcanic rocks (volcanic, andesitic, rhyolitic, and tuffs).

The area falls within the "Tpo" world flood climatic region of Hayden (1989), characterized by flood-generating rainfalls coming from organized convective systems, namely, easterly waves in the trade wind streams and tropical storms. In northern Honduras invasions of cold air from the north ("temporales") characterized by large amounts of rain in large areas are also responsible for considerable floods of higher frequency than those created by the trade winds (Portig, 1976).

Three meteorological phenomena are responsible for the climate in northern Honduras; (1) the intertropical convergence zone of the trade winds, (2) presence of high pressure centers with anticyclone systems, and (3) the Bermudas' anticyclone. Tropical storms and hurricanes are relatively frequent along the northern coast of Honduras. Using data from the National Hurricane Center in Miami, Schramm (1981) calculated that tropical storms have a frequency of 4.5 yrs, and hurricanes a frequency of 12 yrs in this area of Honduras. Rainfall associated with these phenomena produces significant landslides and catastrophic floods.

Hurricane Fifi, with winds of 175 km/hr, struck the north coast of Honduras in 1974. Its associated rainfall caused the worst historical flood in the Aguán Valley. Schramm (1981) estimated, using relatively long rainfall records of northwestern Honduras, a recurrence interval of about 50 yrs for an event as severe as Hurricane Fifi.

Significant and minor climatic changes during late-Pleistocene and the Holocene Epochs that have been documented in Central America and around the circum-Caribbean area were discussed in Chapter I.

Research Methods

Soil transects were performed along four reaches of the floodplain in the upper part of the Aguán Valley

(Fig. 3-2). A topographic representation of the study area is shown in Figure 3-3.

The soil transects on cross-sections were located on four morphologically different reaches of the Aguán River floodplain. The reaches were named after the banana farms where they occur, from west to east as Cayo, (A-A′); Palo Verde, (B-B′); Naranjo, (C-C′); and Rosario, (D-D′).

These reaches were selected for the following reasons: In the first reach (Cayo Reach) the floodplain lies between the Yaguala and Aguán Rivers which are impinging the south wall and the north wall, respectively, of the alluvial scarp that separates the floodplain from the alluvial-fan piedmonts. In two other reaches the Aguán River is migrating apparently to opposite directions, toward the south in the second reach, Palo Verde Reach, and toward the north in the fourth reach, Rosario Reach. In the third reach, Naranjo Reach, the river flows near the center of the floodplain and is apparently migrating to the north.

In making the soil transects, advantage was taken of recent shallow trenches excavated as part of a drainage net at the banana farms and of other observations made during a soil survey conducted in the area. The observations were made down to 2 and 2.5 m depths from the soil surface using boring augers to determine the spatial distribution of soil strata. The soil horizons and/or deposition beds were described in the field. Selected soils were sampled

Figure 3-2. Geomorphic map of the study site showing major landscapes and the four cross-sections of the floodplain.

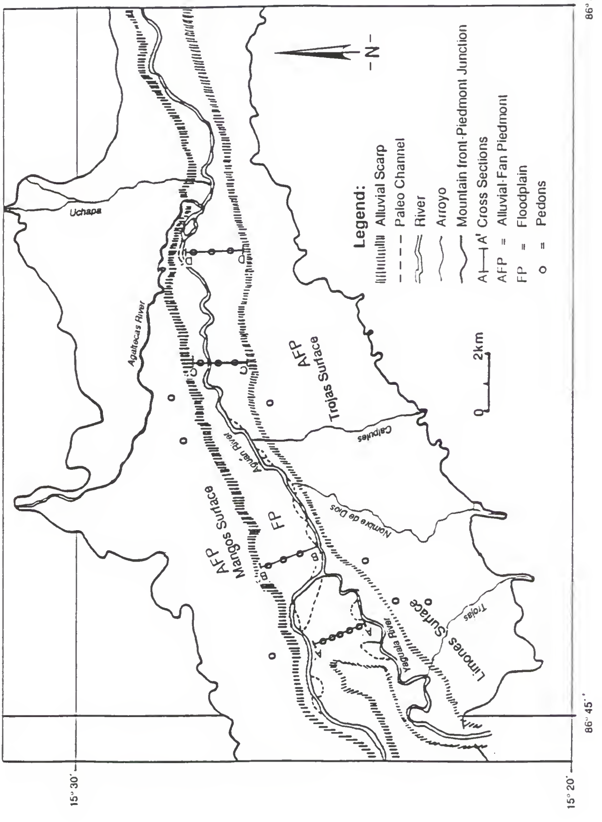
Uchapa
Agalteca River
AFP
Mangos Surface
FP
Aguán River
AFP
Trojas Surface
Calpules
Nombre de Dios
Yaguala River
Trojas
Limones Surface
Legend:
Alluvial Scarp
Paleo Channel
River
Arroyo
Mountain front-Piedmont Junction
A—A' Cross Sections
AFP = Alluvial-Fan Piedmont
FP = Floodplain
o = Pedons
0
2km
N
15° 30'
15° 20'
86° 45'
86° 30'

Figure 3-3. Computer-generated topographic surface map (A) and contour map (B) of the Upper-Aguán Valley (altitude measured in meters above sea level; contour lines measured every 20 meters.)

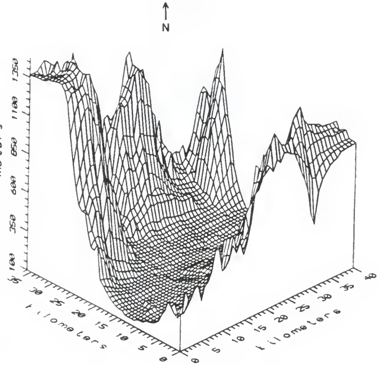
N
meters
kilometers
kilometers

A.

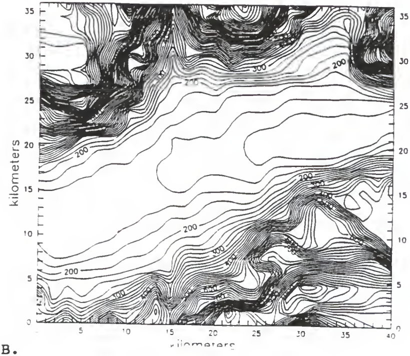
kilometers
kilometers
200
300

B.

and analyzed following standard soil survey procedures (Soil Survey Staff, 1981; Soil Survey Staff, 1991).

Aerial photographs (scale 1:6,000) taken in the late 1960s, and photographs taken in 1987, were used to observe possible recent historical changes in river patterns and the migrating trend of the stream channel along these stream reaches.

The scarcity of datable materials in the floodplain sediments (wood and carbon) deeper than 1 m and economic constraints preclude acceptable absolute dating of the strata. Wood and carbon samples found within the first meter were avoided because of the great disturbance in the area. A common practice on the banana farms was to put into the ground wood sticks to support the banana plants. In this study, only one wood sample that was found at approximately 180 cm in the Rosario Reach was dated.

Results and Discussion

Channel Pattern

The Aguán River is a polyzonal stream which flows from a semiarid through a subhumid to a humid climatic area as the valley runs west to east along a rainfall gradient. As in many streams the sinuosity of the river increases downstream as the discharge increases in this direction (Table 3-1). Along the first 70 km (approximately) the

Table 3-1. The Aguán River channel sinuosity and channel bed slope.

Location	Valley Distance (Km)	River Distance (Km)	Channel Sinuosity	Channel Slope m/m
Beginning to Yaguala River	32.0	38.0	1.19	0.0027
Yaguala River to Mame River	28.5	32.0	1.13	0.0014
Mame River to Saba Fault	23.0	32.5	1.41	0.0013
Saba Fault to Tocoa River	27.0	44.0	1.63	0.00048
Tocoa River to Corocito River	30.0	50.0	1.67	0.00076
Corocito River to Mouth	33.0	61.0	1.85	0.00016

river shows a straight to slightly braided river pattern. It is within this segment of the river that the two major tributaries of the Aguán River, the Yaguala and the Mame Rivers merge with the main drainage of the valley.

After this segment the river channel gradually increases its sinuosity. The valley slope decreases gradually downstream except for one segment (between the Tocoa and Corocito Rivers) in which the slope has a slight increase in relation to the reach before (Table 3-1).

The overall picture can be seen in the long profile of the Aguán River along the valley (Fig. 3-4) which shows convex profile anomalies, which may suggest differences in tectonic activity along the valley (Chapter II). These irregularities also indicate that the river has not reached an equilibrium profile after past climatic and/or tectonic perturbations. However, the attempt to relate differential uplifting along the valley with changes in river pattern (Adams, 1980; Ouchi, 1985; Schumm, 1986) was prevented by the overwhelming effect of the downstream increase in discharge caused by the rainfall gradient. A geomorphic map shown on 1987 aerial photography of the study area is shown in Figure 3-5. This map covers the entire study site represented by Figures 3-6b, 3-7b, and 3-8b.

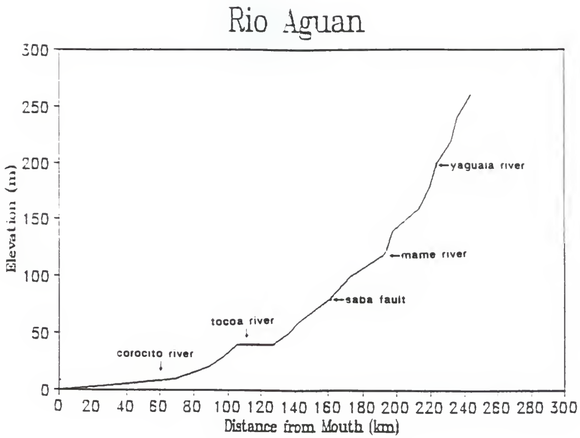

Figure 3-4. Longitudinal profile of the Aguán River along the valley displaying major stream junctions and the Saba Fault.

Figure 3-5. Aerial photograph of the study site showing the geomorphic surfaces of the area (photo taken in 1987).


Legend:
F P = Flood Plain
P C = Paleo Channel
C B = Channel Belt
M B = Meander Belt
AFP = Alluvial-Fan Piedmont
0
2 km
AFP
FP
CB
MB

Figure 3-6a. Aerial photograph of the Cayo Reach displaying the geomorphic surfaces of the area (photo taken in 1970). Legend same as in Figure 3-5.

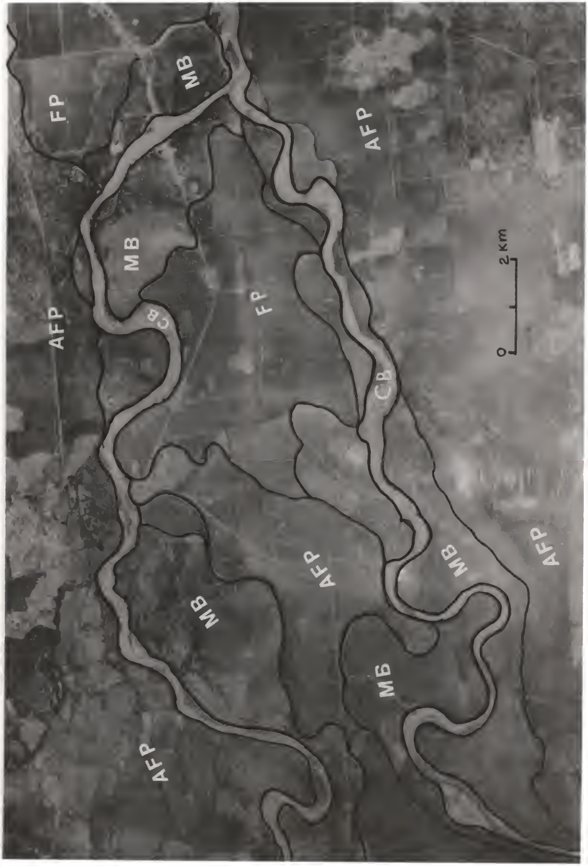
FP
MB
AFP
MB
FP
AFP
CB
CB
MB
AFP
MB
AFP
MB
AFP
0
2 KM

Figure 3-6b. Aerial photograph of the Cayo Reach displaying the geomorphic surfaces of the area (photo taken in 1987). Legend same as in Figure 3-5.


0
2 km
AFP
FP
CB
MB
MB
MB
FP
AFP
MB
AFP
MB
AFP

Figure 3-7a. Aerial photograph covering Palo Verde Reach and part of Naranjo Reach (photo taken in 1970). Legend same as in Figure 3-5.


AFP
FP
MB
MB
FP
AFP
PC
CB
MB
AFP
AFP
PC
MB
FP
0
2 km

Figure 3-7b. Aerial photograph covering approximately the same area as in Figure 3-7a (photo taken in 1987). Legend same as in Figure 3-5.

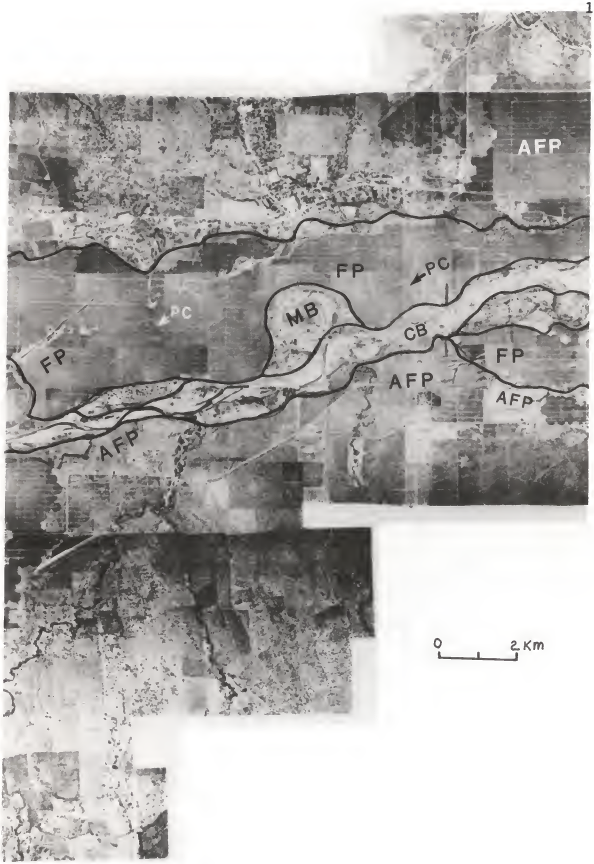
AFP
FP
PC
PC
MB
CB
FP
FP
AFP
AFP
AFP
0
2 Km

Figure 3-8a. Aerial photograph covering part of Naranjo Reach and Rosario Reach (photo taken in 1970). Legend same as in Figure 3-5.

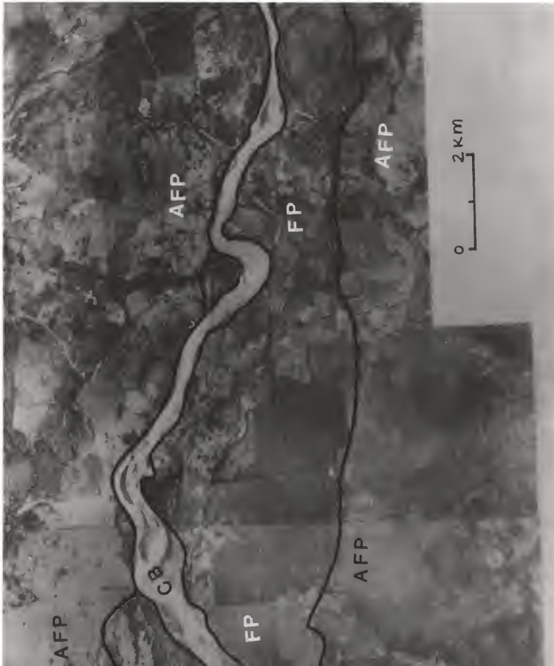
AFP
FP
CB
FP
AFP
AFP
FP
AFP
0
2 KM

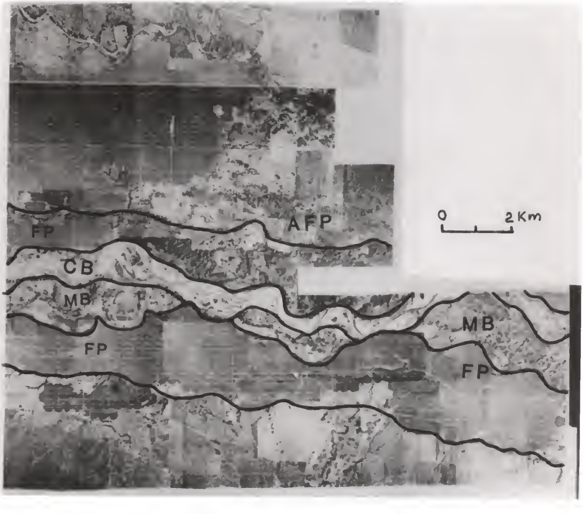

Figure 3-8b. Aerial photograph covering approximately the same area as in Figure 3-8a (photo taken in 1987). Legend same as in Figure 3-5.

Cayo Reach

On the Cayo Reach, the Yaguala River enters the valley and flows northward in a straight pattern for approximately 2 km. It then approximately parallels the Aguán River for about 12 km in a clearly sinuous pattern (Fig. 3-6a,b). Between the two rivers there is a large area of alluvial-fan piedmont. The Yaguala River has cut part of the southern piedmont, almost isolating it from the rest of the piedmont.

The sinuosity of the Yaguala River is near 1.50 along its short flow into the valley. A comparison of the river between 1970 and 1987, shows a slight increase in sinuosity during this time due to a slight increase of amplitude of the existing meanders. The width of the meander belt, and the amplitude and wavelength of the Yaguala River meanders, decrease toward the junction of the river with the Aguán River.

The past pattern of the Yaguala can still be seen in the sinuous contact between the remaining alluvial-fan materials and the recent floodplain of the Yaguala River. Also, some fresh meander scars can be seen on the aerial photographs on the right side of the channel. These features indicate no significant recent changes of pattern of the Yaguala River channel.

The intensive agricultural use of the floodplain at this location together with relatively thick overbank

deposited sediments obscure the ancient signs of river channel migration.

The irregular characteristics of the site where the Yaguala River incises into the valley and the narrow floodplain built by this river insinuate that it has enhanced its drainage basin, perhaps through channel piracy. There is no available chronology of the Yaguala floodplain, but the fresh meander scarps and other features indicate that little time has passed since its formation. Along the short flow of its channel in the valley, before joining the main stream, the floodplain formed by the Yaguala River is virtually a narrow meander belt. The large floodplain between the two rivers has been built essentially by the Aguán River.

The Aguán River channel in this reach shows a different morphology from that of the Yaguala River. In this reach the Aguán River flows first west to east paralleling the Yaguala River and then abruptly changes direction to the south until its confluence with the Yaguala River. The channel is currently braided slightly with some vegetated islands between secondary channels. The river, in the west to east direction, before changing direction to the south to join the Yaguala River, shows a clear tendency of northward migration and is eroding the northern alluvial-scarp wall.

As evidenced by abandoned meanders and paleochannels, the Aguán River used to join the Yaguala River at a more acute angle in earlier times (Fig. 3-2). The confluence angle was approximately 30° and almost 1 km downstream of today's junction. The junction is at approximately 90°, mainly as a result of northward migration of the flowing west to east channel approximately 2 km before the confluence.

Comparison of early 1970 with more recent 1987 aerial photographs (Figs. 3-6a and 3-6b) shows that the large abandoned meander of the Aguán River in the middle of this reach was still active less than two decades ago. The cutoff possibly occurred during the large flood caused by Hurricane Fifi in 1974. Two other plan-rounded landforms, which are relatively fresh abandoned meanders, at both sides of the Aguán channel are located shortly before the confluence. They also appear in the early photographs indicating that although their apparent freshness was evident, they were abandoned (cutoff) earlier than the upstream meander cutoff caused by the 1974 flood.

Past evidence of a more sinuous pattern of the Aguán River, in this reach, can be seen in the curving contact between the meander belt and in the remaining piedmont located between the two rivers and through a barely visible paleochannel which has been partially used as a drain.

Palo Verde Reach

At the Palo Verde Reach, the Aguán River is directly influenced by the discharge and sediment load provided by the Yaguala River. The river flows near the south wall of the alluvial scarp. This scarp is being undercut by the river. Over the course of the reach, the channel shows a straight and slightly braided pattern. This is probably a result of channel adjustment to the sediment load and discharge supplied by the Yaguala River. For the same reasons the Aguán channel also becomes wider after the confluence.

In comparison to the aerial photographs of 1970 this reach of the river has been notably shortened (first two-thirds of Figs. 3-7a,b). Small meanders at the beginning of the reach have had chute cutoffs. A more drastic change can be seen near the end of this reach where a S-shaped large meander is present on the earlier aerial photographs but has now been cut off.

Approximately midway between the river channel and the alluvial scarp (600 to 1,200 m north of the current channel), a paleochannel can be seen on the aerial photographs. This paleochannel is interrupted at the large S-shaped abandoned meander (Fig. 3-7a,b). This paleochannel evidences a less powerful stream and a former meandering pattern of this reach of the Aguán channel.

Naranjo Reach

At the Naranjo reach the river flows in the middle of the floodplain (last one-third of Figs. 3-6a and 3-6b and last one-fourth of Figs. 3-7a and 3-7b). The current channel is meandering pattern along this reach. The contemporary larger sinuosity and the most frequent appearance of abandoned meanders can be at least partially attributed to the fact that the channel is not adjacent to any of the scarp wall along this reach. The clear tendency of the channel to migrate to the north is indicated by the several coalescent, fresh, abandoned meanders on the south margin of the channel. Some of the meanders were abandoned very recently, probably by floods caused by Hurricane Fifi, as they still were active on the earlier aerial photographs.

Rosario Reach

The easternmost reach studied, the Rosario Reach, is not covered completely by the recent aerial photographs, so meaningful comparison cannot be made with the earlier photographs and Figures 3-8a and 3-8b. It seems, however, based on field observations, that no major changes have occurred in this part of the channel in the last two decades. The river channel at this reach is eroding mainly the north wall of the alluvial scarp. The channel pattern is essentially straight, with some slight braided

characteristics at the beginning and some slight meandric characteristics at the end.

Geomorphology of the Floodplain and Surrounding Areas

The geomorphologic map of the floodplain at the site studied is shown in Figure 3-3. The major landscapes are the floodplain of the Aguán River and alluvial-fan piedmonts flanking the valley. The piedmonts are undissected and abruptly separated from the floodplain by an alluvial scarp that varies in elevation from 10 to 20 m in the study area. The north wall of the scarp is currently being impinged by the Aguán River at the Cayo and Rosario Reaches. The south wall is being eroded by the Yaguala River in the Cayo Reach and by the Aguán River in the Palo Verde Reach. The width of the floodplain varies from approximately 3.3 km in the west part of the Cayo Reach to 2.3 km in the Rosario Reach.

The floodplain begins approximately 4 km upstream from the confluence of the Aguán River with the Yaguala River. Upstream from the study area, the river is entrenched into alluvial-fan piedmont sediments with only small areas of floodplain. The floodplain in the Cayo Reach is limited to the eastern side of the reach with a part of the southern alluvial-fan piedmont further east. This piedmont has almost been isolated from the rest of the south alluvial-fan piedmont by the incision of the Yaguala River (Fig. 3-4). Eastward, at the point where the rivers are closer to each

other, the floodplains of both rivers are separated by a very narrow part of the almost isolated southern piedmont. Probably not far in the future and triggered by a large flood event, this area will be the point of confluence of the two rivers and major changes downstream will occur.

The piedmonts at both sides of the floodplain and between the Yaguala and Aguán Rivers may be mistaken as paired terraces-called "false terraces" by Frye and Leonard (1954), terraces left by the river after incision. Careful observation indicates that the slope of the piedmonts rises continuously toward the flanking mountains indicating that they are not related to the rivers. Also, in many parts of the piedmonts, there are clear signs of continuous recent and earlier depositions on these surfaces as evidenced by the freshness of the upper sediments which show limited soil development.

The river is incised into alluvial materials deposited in the form of alluvial fans from the mountains on both sides of the valley. The point where the floodplain begins, i.e., where the channel has had the power to build a floodplain by lateral erosion, resembles a nickpoint zone migrating upstream.

Three distinct landforms can be separated on the floodplain: (1) A fine colluvium landform around some boundaries of the alluvial scarp, (2) the floodplain basin, and (3) the meander belt. In the reaches where the river is

not eroding the alluvial scarp wall, fine colluvium material has been deposited on the edges of the floodplain. In some floodplains such colluvium can be field identified and morphologically separated from the rest of the floodplain by the presence of a colluvial scarp (Frye and Leonard, 1954). In the Aguán floodplain, although the colluvium is slightly steeper than the rest of the floodplain, subsurface data were required in order to separate these landforms since the colluvium grades conform with the floodplain basin.

The floodplain basin covers most of the floodplains area. Except for the existence of some channel fills and paleochannels this landform exhibits a very uniform surface.

The third major landform is the meander belt which indicates the migration pattern and represents the more recent changes of the Aguán River.

There are also some small remnants of a terrace 3 to 4 m higher than the floodplain. These small terrace vestiges are located mainly in protected areas near the alluvial-fan piedmont. The terrace areas are situated between the Yaguala and Aguán Rivers in the Cayo Reach. The most extensive relict of this cut terrace is occupied by the village of Cayo.

In general, the width of the meander belt changes downstream in relation to the total width of the floodplain. It represents approximately one-fourth of the area in the Palo Verde Reach to one-half of the area in the Naranjo

Reach. All abandoned meanders in the study area have been chute cutoff (as opposed to neck cut off). This indicates that the threshold responsible for a meander is not intrinsic, but caused by flood events (extrinsic threshold). Except for the larger "S"-shaped abandoned meander of the Palo Verde Reach with an 1,300 m amplitude, most current and abandoned meanders are less than one kilometer of amplitude. It seems that the amplitude of the meanders is determined by the frequency of large floods (apparently every 50 yrs). The "S"-shaped meander of the Palo Verde Reach was abandoned during the 1974 flood.

Episodes of large discharges seem to be responsible for meander cutoff (extrinsic threshold) because the amplitude and shape of the most recent abandoned meanders are similar to those already abandoned before the 1974 large flood.

Soil Stratigraphy and Sedimentology

Cross-sections of the four reaches of the study area are shown in Figures 3-9 to 3-12. This information is based on intensive mapping of the area, but limited to the 2.0 to 2.5 m depth. Only one absolute date was obtained at the Naranjo Reach which corresponded to transect C-C′. The available evidence indicates that the floodplain of the Upper-Aguán Valley is very recent.

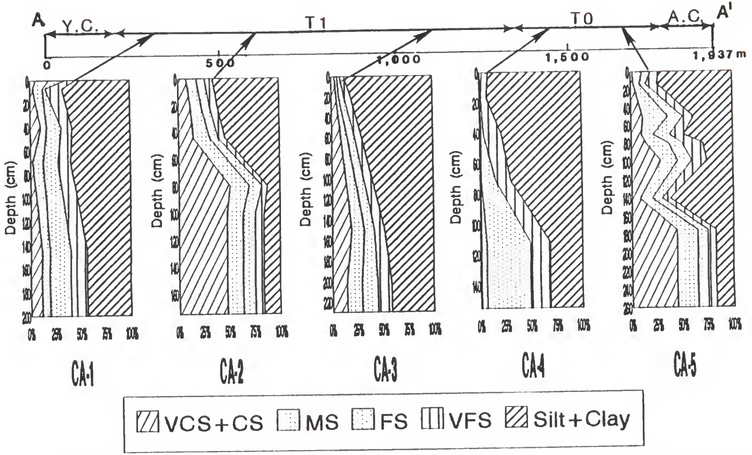

Figure 3-9. Cross-section of the Cayo Reach illustrating the particle size of the floodplain basin (T1), and the meander belt (TO). Y.C. = Yaguala channel; A.C. = Aguán channel. Scale is in meters. VCS = very coarse sand; CS = coarse sand; MS = medium sand; FS = fine sand; VFS = very fine sand.

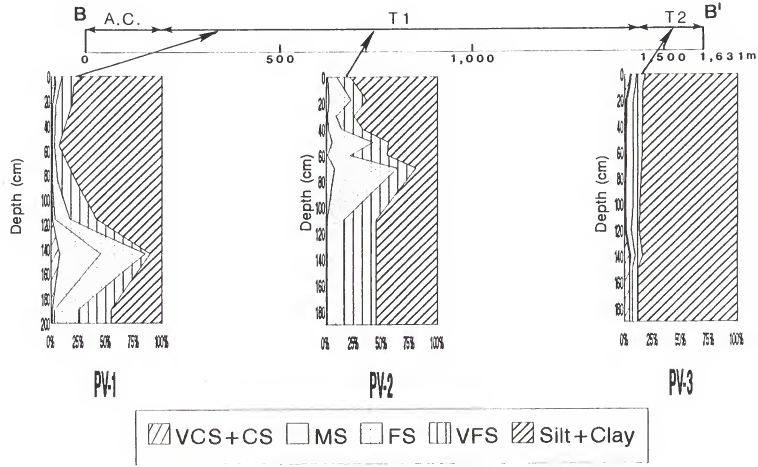

Figure 3-10. Cross-section of the Palo Verde Reach illustrating the particle size of the fine colluvium (T2) and the floodplain basin (T1). A.C. = Aguán channel. Scale is in meters. VCS = Very coarse sand; CS = coarse sand; MS = medium sand; FS = medium sand; FS = fine sand; VFS = very fine sand.

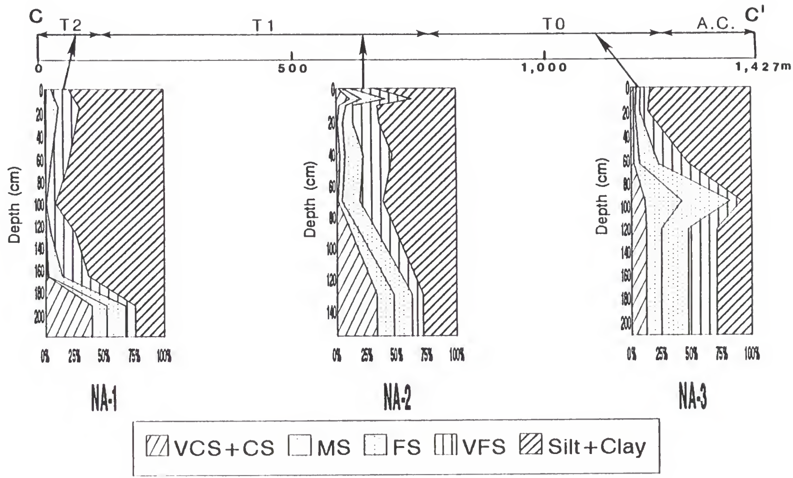

Figure 3-11. Cross-section of the Naranjo Reach illustrating the particle size of the fine colluvium (T2), the floodplain basin (T1), and the meander belt (TO). Scale is in meters. VCS = Very coarse sand; CS = coarse sand; MS = medium sand; FS = fine sand; VFS = very fine sand.

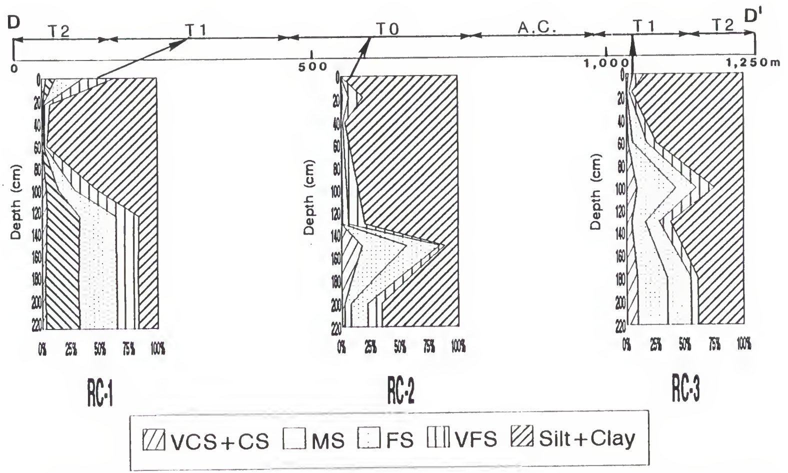

Figure 3-12. Cross-section of the Rosario Reach illustrating the particle size of the floodplain basin (T1) and the meander belt (TO). Scale is in meters. VCS = Very coarse sand; CS = coarse sand; MS = medium sand; FS = fine sand; VFS = very fine sand.

The stratigraphy of the floodplains is studied in three different aspects, namely, (a) soil stratigraphy, (b) lithostratigraphy, and (c) morphostratigraphy (Brakenridge, 1988). A chronology is established through absolute and relative dating and correlation, which permits one to assemble the fluvial history including the geomorphic variables that regulate such history.

Morphostratigraphy

In fluvial landscapes morphostratigraphy is related to different terrace levels associated with cut-and-fill events. Stratigraphic principles regard each level as different formations which decrease in age with decreasing altitude. In many floodplains, however, terraces are not detected topographically, no matter whether cut-and-fill episodes have occurred (Brakenridge, 1988). More frequently detected is the display of successive horizontal sequences of sediments that develop by the consecutive accretion of point bar sediments as the river migrates laterally. By this process, fills of different ages will be displayed laterally without significant vertical differences or even the same fill will exhibit different age depending on how close or far it is from the channel (Kozarski and Rotnicki, 1977). In this regard, the relative age of each fill is not determined by its relative altitude, but by its relative distance from the stream.

In some floodplains the result of the above process will be an undular surface of levees and backswamps; in others a planar surface. The results will depend on the presence or absence of a veneer of vertically accreted sediments posteriorly deposited on the floodplain (Hickin, 1974).

The floodplain of the Upper-Aguán River does not present discernible terrace levels. The only morphologically distinguishable surface is displayed as a narrow band adjacent to the alluvial scarp constituting a colluvial landform slightly steeper than the adjacent floodplain basin. The surface of the floodplain is rather level and continuous with simple morphology. It implies that overbank deposition has covered former in-channel deposition. The different depositions (fills) are conformable which makes it difficult to detect former river banks. The conformable nature of the deposition fills and the covering veneer obscure the former river banks.

If a more complex stratigraphy actually is present in this floodplain, continuous trenches with deeper subsurface data are needed to decipher it. At present, with the available data, the stratigraphy seems to be simple and corresponds to a bottom stratum formed by coarse materials deposited as point bars and a top stratum formed by fine materials deposited by vertical accretion in the floodplain. In many parts of the meander belts and in the few small

channel islands between secondary stream channels, only the bottom stratum of recent point bar deposition is present.

Using the fluvial geomorphic "T" (Brakenridge, 1988) nomenclature, in the area studied, three units can be morphostratigraphically separated. A T0 which exists in the areas included within the meander belt, a T1 surface which constitutes the floodplain basin, and a T2 surface formed by colluvium eroded from the alluvial-scarp wall in the places where the channels are not actively eroding it. The T2 surface exists in a narrow band along the wall, which grade conformably with the T1 surface (Fig. 3-12).

Lithostratigraphy

Weathering *in situ*, changes in the sediment provenance, and changes in channel patterns can produce different lithological units on floodplains (Brakenridge, 1988). The freshness-youthfulness of the sediments in the Upper-River Aguán floodplain precludes significant changes in the sediments through weathering and diagenesis.

Changes in color and texture, presence of color mottles and concretions in the sediments, as well as the formation of pedogenic structure are not apparent in the sediments of the reaches in the floodplain studied. Changes in the sediments from decomposition of the organic matter cause small differences in the soils of the floodplain.

A possible cause for different lithologies should be the presence of two different streams (different sources) in the studied area. However, both major rivers seem to carry sediments from the same geologic formation, the Cacaguapa Schists. The sediments transported by the Yaguala River are graphitic mica schists of this formation. The Aguán River also carries other materials. The predominance of the Aguán River results from its much larger drainage basin area. Overbank discharges of the Yaguala River do not always coincide with Aguán River floods. However, beds that can be traced as being deposited by the Yaguala River can be identified in the stratigraphic column. These layers consist of fine (predominantly silty clay) particles, dark olive color, and graphitic (greasy) "texture" which can be easily related to the graphitic mica schists of the Cacaguapa Schists Formation. These layers are very similar to the upper horizons in the soils located on the eastern part of the south alluvial-fan piedmont (Chapter IV). However, after intensive mapping, these beds were detected only as single beds in some nonmappable spots of the Cayo Reach and therefore, do not constitute a lithological unit.

Three lithological units were identified in the study area, and they correspond with the three morphostratigraphic units. These lithological units are differentiated by textural distribution with depth in the profile (Figs. 3-9 to 3-12).

Lithological Unit 1 underlies the colluvium materials adjacent to the alluvial scarp (T2). The color ranges from dark-brown (10YR 3/3) to dark yellowish brown (10YR 4/4), it is massive with silty clay to clay loam texture. This unit can be distinguished based on its fine texture and the regular decrease of organic carbon with depth (total absence of buried A horizons and absence of coarse layers in the upper layers). This unit is present in the south part of the Palo Verde Reach, in both the south and north boundaries of the Naranjo Reach and in the south margin of the Rosario Reach. Unit 1 is only absent in the Cayos Reach where both rivers are impinging the north and south alluvial-scarp wall and therefore, no colluvium from the alluvial scarp has been deposited.

Lithological Unit 2 underlies the floodplain basin (T1) and covers the majority of the floodplain. The colors are similar to those of Unit 1, ranging from dark-brown to dark yellowish brown. The texture is somewhat coarser than that of Unit 1. It varies from silty clay loam to silt loam. In some places, especially near the meander belt, a sandy loam layer 10 to 20 cm thick, perhaps deposited during the extensive 1974 flood, is identified in the soil and exhibits clear stratification (2 to 3 cm thick beds). A distinct characteristic of Unit 2 from Unit 1 is the common presence of buried A horizons at different depths in the

layer. This unit lies between Units 1 and 3 and is present in all four of the reaches studied.

Lithological Unit 3 underlies the meander belt (T0); its colors are slightly lighter than the other two units, ranging from brown to yellowish-brown. The texture is coarser than that of the other two units varying from fine and medium sand to sandy loam near the surface and medium and coarse sand with gravel and pebbles with depth.

Stratigraphic Units 1 and 2 were defined by upper stratum characteristics and the dominance of were vertical sediment accretion. Unit 3 sediments were deposited mainly by lateral accretion and correspond to the bottom stratum facies.

The bottom stratum was not very well investigated due to the limited depth of the observations and the lack of suitable exposures. It consists mainly of coarse sand, gravel, and pebbles of variable mineralogy, and is similar to the current bed of the Yaguala and Aguán Rivers and the lower layers of stratigraphic Unit 3.

Soil Stratigraphy

The soils of the floodplain are described in detail in Chapter IV. The reaches of the floodplain studied exhibit soils of limited development. All soils of the floodplain were classified as Entisols. No diagnostic subsurface horizons were identified in these soils. Rather than

horizons, the layers in the soils studied are depositional beds. The abrupt boundary between these layers and the absence or weakly pedogenic structures further testify the lack of pedogenic development.

At the great group level, most soils of the colluvium deposits (T2) were classified as Ustifluvents and Ustorthents; the soils of the floodplain basin (T1) as Ustifluvents; and those of the meander belt (T0) as Ustipsamments and Ustifluvents, depending on sand content. No paleosols were identified. Buried, thin "A" horizons that cannot be traced horizontally are common in the floodplain basin (T1-Ustifluvents). These buried horizons do not indicate periods of considerable relative stability since an "A" horizon in this environment can be formed with relative rapidity.

Depositional Processes

The existence of paleochannels and paleomeanders along these reaches in the Upper-Aguán floodplain, as well as the evidences of meander cutoffs when comparing 1970 with 1987 aerial photographs, indicate moderately rapid lateral migration of the Aguán River channel. The lack of soil development in the floodplain supports this interpretation. However, the floodplain does not exhibit the typical surface of many floodplains where lateral migration is the dominant fluvial process. The characteristic levee-swale surface of

such floodplains is not exhibited in the studied floodplain. The above arguments lead to the conclusion that a veneer of overbank sediments covers the floodplain. If this is the case, the deposition of this top-stratum facies occurred rapidly and recently.

The only absolute dating available in this study was performed on a fossil wood fragment found 180 cm deep in pedon NA-1 of the Naranjo Reach. The wood fragment was located exactly at the intersection of the top-stratum with the bottom-stratum. It yielded 310 +/- 70 ^{14}C yrs B.P.

If it is assumed that the river steadily migrated from the place where the fossil wood was located toward its current position (northward) which is approximately 800 m from the river channel, then the river has moved at an average rate of 2.68 m per year (2.2 to 3.3 m/year). By similar reasoning, the river deposits approximately 60 cm of sediments per 100 year (0.60 cm/year). Overbank deposition surely has increased during the last few centuries due to human impact. Both increase in sediment yields and flash-floods have been noted in northern Honduras as a result of extensive modern deforestation.

Figures 3-9 to 3-12 show particle-size distribution with depth in the landform of the reaches studied. The typical variability, characteristic of floodplains sedimentation is evident. A general tendency to upward fining is obvious in all of the profiles. For the colluvial

landform (T2), fine materials are dominant down to 180 cm or deeper without interbedded sandy layers (PV-3 in Figure 3-10 and NA-1 in Figure 3-11). In the floodplain basin (T1) and in the meander belt (TO) the top-stratum of fine materials (silt and clay) is sometimes interbedded by sand textured horizons resulting from major flood events. The thickness of the top-stratum on these landforms depends on the closeness to the river channel and the presence of paleomeanders.

Climate, Tectonics and Fluvial History

Climate, directly or indirectly, is the major force generating geomorphic changes. Episodic erosional and depositional processes in fluvial systems are largely related to reversals of climatic conditions. Knox (1983; 1984), based on alluvial chronologies, concluded that changes to drier conditions generally cause drainage basin erosion and deposition in channels and floodplains; in contrast, a shift to wetter conditions commonly enhances basin stability and channel and valley erosion and entrenchment.

Whether increasing rates of channel/valley erosion caused by wetter climatic conditions are due to larger magnitudes of very frequent floods or to more frequent events of very high magnitude is equivocal (Knox, 1985). Schumm and Lichty (1963) discovered that the floodplain of

the Cimarron River, Oklahoma was destroyed by an extremely large flood that was followed by frequent moderate to large floods. Afterwards, a new floodplain was built, mainly by vertical accretion, during a 12-year period of low magnitude floods. Nanson (1986) described floodplains in southeastern Australia which were gradually built by vertical accretion to be obliterated later by a catastrophic large flood or several large floods.

Changes in fluvial systems are not only accomplished through shifts of climatic conditions. Tectonics, sea-level changes, human-induced changes through land use, and intrinsic thresholds are also responsible for erosion-sedimentation episodes. In some cases, changes in one of the external variables are reflected clearly in the fluvial system. In many instances a complex response is more likely, as natural systems are complex themselves (Schumm and Parker, 1973).

The entrenchment and widening of the Upper-Aguán Valley floor into the piedmont sediments without any vestige of previous depositional surfaces (terraces) indicate a significant change in one or more external variables. Sea-level changes can be discounted, as in this region the sea-level has been rising, at least during the Holocene period. Intrinsic thresholds and human factors cannot be the main cause of such spectacular and long-lasting

processes. It leaves climatic and tectonic changes as possible causes for the genesis of the valley floor.

Recent tectonic activity along the Aguán Valley has been described (Chapter II; Manton, 1987). The Aguán River and the mountain fronts of the north margin of the valley seem to be controlled by the Aguán Fault, which is less active than the La Esperanza Fault occurring at the south margin of the valley. If intermittent uplifting, with consequent river downcutting, has occurred, any geomorphic evidence (e.g. cut-terraces, tectonic scarps) has been obliterated by posterior erosion, and/or insufficient time has evolved since the last tectonic episode.

Climate, or more specifically climatic change, seems to be the major factor responsible for the geomorphic history of the valley floor (floodplain) in the Upper-Aguán Valley. Currently, and at least during the last hundred years, the floodplain is being aggraded. The lack of soil development, the absence of developed paleosols, and the only absolute date obtained, indicate recent deposition of sediments at least to 2.5 m depth in the floodplain.

As stated before, no paleoclimatic reconstruction near the Aguán Valley presently is available. Not even long present-day climatic records of the study site exist. Several paleoclimatic reconstructions around the Caribbean including places as close to the study site as eastern Guatemala show very similar trends (Chapter I). Especially

noteworthy, is a change from colder and drier conditions in the late-Pleistocene Age to warmer and wetter conditions from early- to late-Holocene periods.

The presence of a paleosol exposed in the western part of the southern scarp wall of the valley can contribute to the possible explanation of the development of the valley floor. This paleosol can be traced several hundred meters in the western-most part of the study site, approximately in the middle part ofthe southern alluvial scarp. The paleosol is buried by approximately 10 m of piedmont material and exhibits a well-structured natric horizon. A natric horizon has the characteristics of an argillic horizon plus strong prismatic or columnar structure and high sodium saturation (Soil Survey Staff, 1992). Natric horizons in many parts of the world commonly develop in sediments of the late-Pleistocene in playas or around the margins of present or Pleistocene lakes with arid climate (Soil Survey Staff, 1975). This type of environment can be visualized along the vertex of converging alluvial-fan piedmonts during the late Pleistocene in northern Honduras.

The paleosol indicates a considerable period of stability in the piedmont providing a pause of sediment accumulation during its formation. It also might indicate a considerable dry period at the final stages of its evolution. Unfortunately neither the material underlying

the paleosol nor the material overlying it could be dated because of the lack of datable material.

Model

Based on the evidence available the following model for the development of the valley floor is considered. This portion of Upper-Aguán River, probably during late Pleistocene, flowed along the vertex of the fan piedmonts deposited on both sides of the valley in the same manner that the Aguán River flows currently in the first reaches of the valley. The climate was arid at the time as suggested by the paleoclimate reconstructions and the paleosol. At the onset of the Holocene period, the climate became warmer and wetter and perhaps large floods were more frequent. As water discharges increased, the sediment supply decreased due to a change in natural vegetation and an increase in vegetative covering. The river, with these conditions, incised the piedmont and began to erode very large amounts of sediments that were deposited downstream.

This period of river incision and rapid valley widening lasted until at least 3,500 yr B.P. when the climate became dryer. The climate became dryer between 2,500 to 1,000 yr B.P. and, thus, decreased water discharge of the streams and increased sediment yield promoted some alluviation and slower widening of the valley. These conditions have continued into the present when conditions

are perhaps slightly wetter than during the middle-Holocene period.

The early- to late-Holocene, as suggested by the paleoclimatic reconstruction, were periods of continued warmer and wetter conditions. Frequent large floods and relatively frequent extreme floods whould characterize this period. During this 6,500 yrs, the river basically eroded the piedmont sediments and widened the floodplain. As is typical of erosion cycles, the only signs of this erosion period are the abrupt alluvial scarps that separate the fan-piedmonts from the floodplain. Any possible geomorphic surfaces created by river response to tectonism were obliterated during this period.

At present, the climate is semiarid, and deforestation of the drainage basin facilitates erosion in the upper mountains and subsequent aggradation in the floodplain. The river, in the reaches studied, is still migrating and eroding the scarp walls. It is, however, more stable and rates of lateral migration are relatively slower. It can be seen by comparing early to recent aerial photographs, that when the meanders reach certain limited amplitude, chute cutoff occurs (sinuosity threshold). It seems that large floods are responsible for these cutoffs. As the river is more laterally stable, overbank deposition seems to prevail upon lateral accretion.

Concurrently with the valley floor aggradation, the piedmont was possibly aggraded as the rate of uplift of the mountain front exceeded the rate of downcutting for the relatively small streams draining the piedmonts. During accumulation on the piedmonts the paleosol was buried.

Tilting along the Aguán Valley floor should be contemplated as a consequence of differential uplift between both margin of the valley. In this regard, the major activity of the SMV along the La Esperanza Fault would incline the valley toward the north. Also, symmetry in sediment deposition will force the Aguán River channel preferentially toward the north since the major tributary streams of the Aguán River drain the SMV (i.e., Yaguala, Mame, and Tocoa Rivers). The combined effect of the above factors causes the river channel to preferentially migrate toward the north. Other factors seem to be effective as in some reaches (i.e., first valley reach and Palo Verde reach in the study site) the river channel is actually migrating toward the south.

Summary and Conclusions

The first segment of the Upper-Aguán River floodplain is entrenched between alluvial-fan piedmonts at both margins of the valley. Downstream, where the floodplain starts, an abrupt scarp, 10-20 m high, separates the floodplain from the piedmonts which were left as paired false terraces.

Upstream on the reaches studied, the river is incised into the piedmont sediments without building a significant floodplain. Downstream, the valley floor has evolved by lateral planation. In these places the river has deposited very large amounts of sediments mainly eroded from the alluvium of the first segments of the valley.

In the study area, the Yaguala River, the first important tributary of the Aguán River, flows in a meandering pattern that has not changed significantly in late-Holocene and recent times as evidenced by paleochannels, paleomeanders, and comparison of historical early to recent aerial photographs.

Comparison of aerial photographs of 1970 and 1987 (Figs. 3-6a,b to 3-8a,b), shows that the Aguán River has straightened its channel by means of chute cut offs, probably during the extreme flooding caused by Hurricane Fifi in 1974. The recent and former paleomeanders are circular in shape and their amplitude is relatively small. Older abandoned meanders (already appeared abandoned in early 1970 photographs) exhibit the same pattern.

The floodplain shows a relatively narrow meander belt as compared to the floodplain basin. It indicates that the lateral migration of the river, particularly in the reaches where the river currently is impinging the floodplain walls, is rather restricted or relatively slow. The floodplain is formed primarily by vertically accreted sediments which

covers a bottom-stratum formed by point-bar sedimentation. No developed buried soil was identified in spite of intensive mapping. Buried A horizons were locally recognized mainly on the floodplain basin.

On the margins where the river is not presently eroding the alluvial-scarp walls, the floodplain has been subjected to local deposition from erosion of the scarp caused by local wash, tributary rills and mass movement. A relatively narrow colluvial landform is covering the floodplain at these sites, leaving the impression that the false paired-terraces have been slightly uplifted at the sides.

Other than the anomalies shown by the longitudinal profile of the Aguán River, no indication of tectonism was recognized in the floodplain. The absence of alluvial faulting on the piedmonts indicate that faulting is limited to the mountain front-piedmont junctions. The lack of terraces is indicative of the youthfulness of these landscapes. If river downcutting, in response to uplift, has occurred, subsequent erosion has obliterated any geomorphic record of such episodes.

The observed influence of tectonism in the development of the valley floor is related to the course of the main stream. It is reasonable to believe that the differential activity of both faults along the valley has influenced the

type and amount of lateral migration of the river along the valley.

Based on a paleoclimatic reconstruction of the circum-Caribbean, the characteristics of a paleosol displayed on the south wall of the alluvial scarp, and the geomorphology and soil stratigraphy of the floodplain, a model for the development of the valley floor was envisaged. During the latest Pleistocene Age when the climate was cooler and dryer than at present (Younger Dryas), the Aguán River at the study site basically flowed along the conjunction of the alluvial-fan piedmonts at both margins of the valley. During this time of relative stability and arid conditions, together with poor drainage at the toe slope position, the paleosol at the scarp wall acquired its arid character (development of a natric horizon). The powerful influence of climate has obscured any possible tectonic control in the development of the valley floor.

At the onset of the Holocene Age with the shift to warmer and wetter conditions, the vegetation density of the drainage basin increased, the sediment yield decreased and the river began to incise and erode the alluvial fan sediments. This climate lasted for almost 7000 yr, and during this time the river had the power to erode and widen the valley floor. Approximately 3,000 yr B.P., the climate shifted to dryer conditions until approximately 1,000 yr B.P. As a consequence, hillslope erosion increased and

runoff decreased, and the river began the alluviation of the valley floor.

Since 1,000 yr B.P., the climate first became wetter for a short period of time, and then became dry again until the present time. During this time, aggradation of the valley floor continues as a predominant process. As channel widening and floodplain construction occur in sandy rivers of semiarid regions (Schumm and Litchy, 1963), the channel of the Aguán River has continued the lateral expansion of the floodplain through lateral migration.

Table 3-2 offers a synopsis of the main weather trends during the last 15,000 yrs, as inferred from several paleoclimatic studies in the circum-Caribbean region discussed in Chapter 1.

The Yaguala River seems to have reached its current recently by increasing its drainage basin. It has incised and eroded the south alluvial-fan piedmont leaving piedmont remnant almost disconnected from the upper mountain front. This alluvial-fan remnant is narrow at some point between the Yaguala and Aguán Rivers just before the beginning of the Aguán floodplain. It seems likely that the Yaguala River will join the Aguán River at approximately 10-12 km upstream from the present confluence.

Table 3-2. General late-Quaternary paleoclimatic changes in the Caribbean.

Age	Years before present	Changes relative to present	
		Temperature	Precipitation
Late Holocene	2,500-1,000	Warmer	Dryer
	1,000		Moisture slightly increased, then began to dry until present.
Middle Holocene	7,000-3,500	Warmer	Wetter
	3,000		Dry
Early Holocene	10,000-7,000	Warmer	Wetter
Latest Pleistocene	15,000-10,000	Cooler	Dryer

NOTE: Based on paleoclimatic studies of Bradbury et al. 1981; Bindford, 1982; Leyden, 1984, 1985; Markgraff, 1989; Piperno et al., 1990; Curtis, 1992.

CHAPTER IV
SOIL GENESIS IN THE UPPER-AGUÁN VALLEY, HONDURAS

Introduction

Alluvial soils of fluvial origin occur in several types of landforms including terraces, deltas, alluvial fans, and floodplains. Depending on the kind and the age of fluvial landscape where they occur, soils with different degrees of development will result. Soils developed in fluvial terraces may vary widely according to the age of these landforms. In most cases, fluvial terraces have formed during the Pleistocene and have relatively well-developed soils, even in areas of arid to semiarid climate. Generally, soils formed on floodplains, show restricted development no matter what their location, type of parent alluvial material, and the climatic conditions of the site. Geomorphic evolution governs the development of the floodplains and associated soils.

Like fluvial terraces, alluvial fans exhibit geomorphic surfaces of variable age. Soils on alluvial fans have been studied mostly in arid and semiarid regions of temperate latitudes. In these areas Entisols, specifically Fluvents and Orthents, are usually the typical soils of the late-Holocene age surfaces, whereas Aridisols (mostly

Argids) are found on early Holocene and Pleistocene surfaces. Well-developed soils that occur in arid and semiarid regions have experienced different climate conditions than the present climate, thus explaining their development. These soils are labeled polygenetic soils since different pedogenetic processes have taken place in their evolution as a consequence of different types of climate.

The Upper-Aguán Valley, as previously stated, geomorphically consists of alluvial-fan piedmonts which parallel the mountain fronts that surround the valley. Incised in the former vertex, where the piedmonts converged, a floodplain has been developed by the main river of the valley, the Aguán River. Therefore, the soils of the Upper-Aguán Valley occur basically on two types of broad landforms, namely, a floodplain, occurring approximately along the axis of the valley, and alluvial-fan piedmonts on both sides of the valley.

The evolution and pedogenesis on the piedmonts of the Upper-Aguán Valley are, to some extent, related to the tectonic activity along the mountain fronts and to the predominance of particular types of rocks in the sediments deposited on these geomorphic surfaces. In the floodplain, soil development is associated mainly with fluvial geomorphic processes.

River valleys frequently offer the opportunity to study soil chrono-sequences, defined as a sequence of related soils that differ in some important properties due to the isolated action of time, a major soil forming factor (Stevens and Walker, 1970). This is not the case in the study site, where fluvial terraces are absent.

Classic approaches to study the degree of soil development focus on the development of textural B horizons, rubefication, clay illuviation, clay mineralogical transformations, carbonate translocation, and other pedogenic processes (Birkeland, 1984). A soil development index based on morphological characteristics that reflect these chemical and mineralogical changes has been depicted (Harden, 1982).

In the young alluvial soils of floodplains, as soil formation and sedimentation overlap, other kind of processes are of major importance. The ripening of the organic matter and the biotic obliteration of depositional stratification have been considered in the pedogenetic studies of young alluvial soils (Hoeksema, 1953). In arid and semiarid regions, different soil properties are considered to interpret and understand soil evolution. They include increased pH, and translocation, accumulation, and stages of maturity of precipitates (Harden et al., 1991).

In contrast with the river sediments of temperate areas, which are derived in many cases from fresh and coarse

glacial and periglacial deposits, the characteristics of the parent material deposited by streams in the tropics and subtropics are highly variable. They range from fresh sediments of different sizes derived from steep mountain ranges to fine sediments originating on deeply weathered surfaces.

Paleosols are excellent stratigraphic markers which indicate periods of stability between depositional and erosional episodes. They also reflect paleoenvironmental conditions useful in interpreting geomorphic processes. The scarp that separates the floodplain from the southern alluvial fan piedmonts in the study area displays a prominent paleosol which indicates a considerable period of equilibrium in the depositional environment on the piedmont located at the south margin of the valley. The weathering and pedogenesis reflected by the characteristics of this paleosol can be useful in estimating past environmental conditions in the area and for evaluating the estimated paleoclimate of the region.

The objectives of this part of the study were:

1. to characterize the morphological, physical, chemical and mineralogical properties of the soils developing in the landscapes and landforms present in the study area and those of a paleosol displayed on the fluvial scarp.

2. to interpret, based on those properties, the pedogenesis of the soils developed on these landscapes and its relationship with the climate and tectonics conditions of the area and the geomorphic evolution of the Aguán Valley.

Materials and Methods

Study Area

The location, geology, physiography, and climate of the Aguán Valley were discussed in Chapters I and II. In Chapter III, the location and physiographic and environmental setting of the specific study area in the Upper-Aguán Valley were addressed.

Field and Laboratory Methods

The pedons described in this study were selected from the pedons described during a recent soil survey, performed by the author at the banana plantation of Coyoles, Yoro Department, Honduras. These pedons are representative of the soils that are associated with the major landscapes of the area, initially identified on aerial photographs (i.e., alluvial fan piedmonts and floodplain), and local landforms identified during field work.

Previous photointerpretations, using 1:6000 panchromatic aerial photographs, permitted the separation of the

major landscapes. Further photointerpretation with direct field observations enabled the separation of the major landscapes into their component landforms.

These landforms were identified mostly in the floodplain, and described in Chapter III. Changes in soils associated with subtle lateral variations of the individual coalesced alluvial fans were identifiable only through subsurface examination during the soil survey.

Field Investigations

Soils were described and sampled according to standard soil survey procedures (Soil Survey Staff, 1981). Soil descriptions included horizon thickness, nature of the boundary between horizons, structure, moist consistence, color, texture class, reaction to diluted HCl, root distribution, and the presence of particular pedogenic or biogenic features.

Twenty-one pedons, representing different landforms of the floodplain, and changes in the parent material associated with individual fans on the coalesced alluvial fans that form the piedmonts, were studied in detail. Fourteen pedons are located along four reaches of the floodplain and seven on the piedmonts located on both sides of the floodplain. The paleosol studied is displayed on the scarp wall that separates the floodplain from the piedmont in the southwestern part of the study area.

Physical and Chemical Analyses

Particle-size distribution was determined by the pipette method (Soil Survey Staff, 1991). The silt fraction additionally was fractionated into coarse silt (53-16μ), medium silt (16-4μ) and fine silt (4-2μ).

Cation-exchange capacity (CEC) was determined using a modification of the method described by Rhoades (1986), which was particularly well-suited for soils of arid and semiarid regions containing carbonates and more soluble salts. Previous determination of the CEC on some of the soils samples using 1 N NH_4OAc buffered at pH 7, rendered questionable high values and were suspected to be caused by carbonate dissolution of ammonium acetate. In the method used, the saturating solution was composed of 0.4 N NaOAc, 0.1 N NaCl, and 60% ethanol, which was subsequently diluted during the saturating procedure. The extracting solution was 0.25 M $Mg(NO_3)_2$. Finally, the CEC was calculated by measuring the saturating Na cation using flame emission spectroscopy.

Other chemical analyses were performed using standard procedures (Soil Survey Staff, 1991) and included organic carbon by acid-dichromate digestion, soil pH 1:1 in water, 1 M KCL and 0.01 M $CaCl_2$ suspensions. Exchangeable bases were extracted by 1 M NH_4OAc at pH 7; Na and K quantities from the extracting solution were measured by flame emission spectroscopy, and Ca and Mg by atomic absorption

spectroscopy. Calcium cation of the pedons studied was calculated by subtracting the summation of the remaining cations Mg, Na, and K from the CEC except for the Paleosol studied. Overestimated Ca amounts were obtained by extraction with NH_4OAc buffered at pH 7 and were due to calcium carbonate dissolution.

Calcium carbonate ($CaCO_3$) equivalent was determined by the acid-neutralization method and electrical conductivity was measured in a 1:1 soil/water suspension.

Mineralogical Analysis

Samples for mineralogical analysis were limited to selected horizons of some of the pedons studied. The subsamples were not pretreated. Sand, silt and clay separates were obtained by sieving and centrifugation after adjustment to pH 10 with Na_2CO_3.

Oriented mounts of clay were prepared for X-ray diffraction (XRD) analysis by depositing (under suction) approximately 250 mg from suspension unto a ceramic tile, saturating with Mg or K, washing free of salts, and adding glycerol to the Mg saturated subsamples. The XRD analyses were conducted using a computer-controlled XRD system. The oriented mounts were scanned at a fixed counting time of 2° θ per min using Cu radiation and a graphite crystal monochromator. Voltage and current for XRD scans were set at 35 kV and 20 mÃ, respectively. All samples were scanned at

room temperature, and K-saturated samples also were scanned following 4-h heat treatments at 110°, 300°, and 550° C. Magnesium-saturated subsamples also were scanned following 4-h treatment at 110° C.

Clay minerals were identified from XRD patterns using differentiation criteria outlined by Whittig and Allardice (1986). Relative quantities of clay minerals were assessed based on peak height. Absolute quantification was not attempted.

Radiocarbon Dating

One radiocarbon dating analysis was performed on a wood fragment sample found 180 cm deep in the floodplain basin at pedon RC-2. The analysis was performed by Beta Analytic Inc. of Coral Gables, Florida; it is reported as radiocarbon years before present (YBP). Another radiocarbon analysis was attempted on the base of the paleosol, but failed to give reliable results because of a lack of sufficient organic carbon.

Results and Discussion

Geomorphology of the Study Area

The major landscapes of the study area were already identified in previous chapters and the geomorphological characteristics of the floodplain were discussed in detail

in Chapter III. The alluvial-fan piedmont landscapes, situated on both sides of the floodplain and paralleling the mountain fronts, have not been discussed yet in detail. It is on these surfaces where the most developed soils of the study occurred.

The piedmonts on both sides of the valley present remarkable similarities. Their altitude, slopes, and surface morphology are exceedingly analogous, indicating that these surfaces are coeval. Soils on both sides are remarkably similar morphologically and in degree of development, which supports the postulated contemporaneous deposition of these surfaces.

Studies of alluvial-fan sequences in southwestern USA, particularly in the Basin and Range province, have demonstrated that age of alluvial-fan surfaces varies within a single fan and between adjacent alluvial fans on an alluvial-fan piedmont (Christenson and Purcell, 1985). Summarizing the extensive work done by several investigators, Christenson and Purcell (1985) successfully used several diagnostic criteria to separate alluvial-fan surfaces by age. Included in the diagnostic criteria are drainage pattern, surface morphology and soil development.

The alluvial-fan surfaces in the study area meet the distinctive conditions of young alluvial-fan deposits as determined by Christenson and Purcell (1985). Distributory types of drainage pattern, weakly developed soils without

substantially developed B and calcic horizons, and channel incision less than 1 m, characterize the alluvial fans in the study area. These characteristics correspond with those of the young alluvial-fan sequences as defined by these authors. However, the smooth and flat surfaces of the fans studied conform with those alluvial fans classified as intermediate in age. The reason for these discrepancies could be the different climatic conditions and the fineness of the sediments at the study site.

Differences in local base-level processes and in size of individual fans and/or fan drainage basins are responsible for differences between adjacent alluvial fans. The latter can better explain the differences observed in the alluvial-fan piedmont located in the northern margin of the study area and discussed below.

Geomorphic Surfaces and Field Morphology

The location of the pedons studied are shown in Figure 3-2, and the pedon morphological descriptions are presented in Appendix A. Complete particle-size characterization data are given in Appendix B. Selected morphological and physical properties of the pedons are given in Table 4-1.

As stated before, the pedons studied are representative of the soils on major geomorphic surfaces in the study area. In this sense, some pedons represent the

Table 4-1. Selected morphological properties of the pedons studied.

Pedon	Horizon[a]	Depth (cm)	Color (moist)	Texture[b]	Structure[c]	Effervescence to HCl[d]
CA-1	Ap	0-13	10YR 4/3	CL	MA	2
	A	13-50	10YR 4/3	CL	MA	3
	C1	50-70	10YR 4/3	SL	SGR	3
	C2	70-80	7.5YR 4/2	SL	SGR	3
	C3	80-99	7.5YR 4/2	SL	SGR	3
	C4	99-140	10YR 5/3	GRSL	SGR	3
	Ab	140-175	7.5YR 4/2	L	MA	3
	C	175-260	10YR 4/3	GRLS	SGR	1
CA-2	Ap	0-16	10YR 4/2	SICL	1 COSBK	1
	C1	16-41	10YR 4/3	SIL	MA	3
	C2	41-72	10YR 4/2	SIL	MA	3
	C3	72-112	10YR 4/3	SIL	MA	4
	C4	112-155	10YR 5/3	LS	MA	1
CA-3	Ap	0-20	10YR 4/3	SICL	1 MSBK	1
	C1	20-60	10YR 4/4	CL	1 MCSBK	1
	C2	60-150	10YR 3/4	CL	MA	1
	C3	150-200	10YR 3/4	SCL	MA	1
	C4	200-230	10YR 4/4	SL	MA	1
CA-4	Ap	0-20	10YR 4/3	L	1 MCSBK	1
	C1	10-45	10YR 5/4	L	1 MCSBK	1
	C2	45-80	10YR 5/4	L	MA	3
	C3	80-100	10YR 5/4	CBCOS	SGR	1
	C4	100-140	Cobbles	-	-	-
	C5	140-175	10YR 5/4	LS	SGR	0
	C6	175+	Cobbles & boulders		-	-

Table 4-1. Continued.

Pedon	Horizon[a]	Depth (cm)	Color (moist)	Texture[b]	Structure[c]	Effervescence to HCl[d]
CA-5	Ap	0-7	10YR 4/4	SCL	1 MCSBK	1
	A	7-40	10YR 3/3	SCL	1 MCSBK	1
	C1	40-70	10YR 4/3	SCL	1 MCSBK	1
	C2	70-145	10YR 6/4	SCL	MA	3
	C3	145-185	10YR 6/6	SL	SGR	1
	C4	185-195	10YR 5/4	FS	SGR	1
	C5	195-260	10YR 5/4	LS	SGR	3
	C6	260-320	10YR 5/3	S	SGR	1
PV-1	Ap	0-7	10YR 5/2	SIL	2 TNPL	1
	A1	7-24	10YR 4/2	SIL	1 MSBK	3
	A2	24-56	10YR 4/2	SIL	1 MSBK	1
	C1	56-85	10YR 4/3	SIL	MA	1
	C2	85-116	10YR 4/2	SIL	MA	3
	C3	116-144	10YR 5/3	SL	MA	1
	C4	144-189	10YR 6/4	S	SGR	1
	C5	189-220	10YR 6/4	GRSL	MA	1
PV-2	Ap	0-18	10YR 3/3	CL	1 TKPL	1
	C1	18-41	10YR 5/3	SCL	1 MCSBK	1
	C2	41-75	10YR 3/4	L	1 MCSBK	1
	C3	74-170	10YR 5/4	LS	SGR	3
	C4	170-190	10YR 4/4	LS	SGR	3
PV-3	Ap	0-20	10YR 4/3	SIL	1 CSBK	1
	C1	20-58	10YR 5/3	SIL	1 MSBK	1
	C2	58-100	10YR 5/4	SIL	MA	3
	C3	100-235	10YR 4/4	SIL	MA	3

Table 4-1. Continued.

Pedon	Horizon[a]	Depth (cm)	Color (moist)	Texture[b]	Structure[c]	Effervescence to HCl[d]
NA-1	Ap	0-15	10YR 3/2	SIL	1 CSBK	1
	C1	15-66	10YR 4/2	L	MA	3
	C2	66-100	10YR 5/2	SIL	MA	3
	C3	100-127	10YR 4/4	SIL	MA	3
	C4	127-166	10YR 5/3	SIL	MA	3
	C5	166-192	10YR 5/4	L	MA	3
	C6	192-220	10YR 5/4	CBLS	SGR	3
NA-2	Ap	0-6	10YR 3/3	L	1 VKPL	0
	C	6-10	10YR 5/3	SL	SGR	0
	Ab	10-20	10YR 3/2	L	1 MCSBK	1
	C1	20-70	10YR 5/4	SL	SGR	3
	C2	70-130	10YR 4/3	L	MA	1
	C3	130-155	10YR 4/3	GRSL	SGR	1
NA-3	Ap	0-19	10YR 3/3	SIL	1 FMSBK	1
	C1	19-63	10YR 4/3	SIL	MA	3
	C2	63-95	10YR 5/4	SL	MA	1
	C3	95-120	10YR 4/4	S	SGR	1
	C4	120-210	10YR 5/4	SL	MA	1
RC-1	Ap	0-15	10YR 3/3	CL	1 MCSBK	1
	C1	15-60	10YR 4/3	SICL	MA	1
	C2	60-100	10YR 4/4	CL	MA	3
	C3	100-130	10YR 5/4	LS	SGR	1
	C4	130-180	10YR 4/4	SCL	MA	3
	C5	180-200	10YR 4/4	SL	MA	1
RC-2	Ap	0-23	10YR 5/4	SL	1 THPL	1
	Ab	23-60	10YR 4/2	SICL	1 CBSK	1
	C1	60-100	10YR 4/3	SICL	MA	3
	C2	100-125	10YR 4/4	SCL	MA	3
	C3	125-190	10YR 6/4	SCL	MA	3
	C4	190-225	10YR 6/4	LS	SGR	1
	C5	225+	Cobbles & stones		-	-

Table 4-1. Continued.

Pedon	Horizon[a]	Depth (cm)	Color (moist)	Texture[b]	Structure[c]	Effervescence to HCl[d]
RC-3	Ap	0-18	10YR 4/2	SICL	1 FMGR	1
	C1	18-40	10YR 4/3	CL	1 FMGR	1
	C2	40-130	10YR 4/4	SICL	MA	3
	C3	130-150	10YR 5/4	L	MA	1
	C4	150-200	10YR 4/4	S	SGR	3
	C5	200+	Pebbles, cobbles, stones		-	-
LA-1	A1	0-30	5YR 3/1	SIL	1 MSBK	1
	A2	30-56	7.5YR 3/2	SIL	1 MSBK	1
	2C1	56-70	10YR 3/1	GRL	MA	1
	3C2	70-95	7.5YR 3/2	SIL	MA	1
	4C3	95-140	7.5YR 3/0	SL	MA	1
LA-2	Ap	0-19	10YR 3/2	C	1 CSBk	1
	A	19-70	10YR 3/1	C	MA	2
	Bw	70-90	10YR 4/4	C	2 MCSBK	2
	2C1	90-150	10YR 5/3	SIC	MA	3
	2C2	150-230	10YR 5/4	SIC	MA	3
TB-1	Ap	0-12	7.5YR 4/4	CL	MA	1
	Bt	12-42	7.5YR 5/4	SICL	MA	1
	Btk	42-80	10YR 5/4	SIL	1 MCSBK	4
	Ck	80-120	10YR 6/4	L	1 MCSBK	4
	2C1	120-152	2.5Y 5/4	S	SGR	1
	2C2	152-180	2.5Y 5/4	LFS	SGR	1
	3C3	180-225	10YR 5/4	SICL	MA	1
	4C4	225-245	Gravel	-	-	0
	5C5	245-280	2.5Y 4/4	CS	-	1
	6C6	280-295	Gravel	-	-	0
	7Ck	295-340	2.5Y 5/4	SICL	-	3

Table 4-1. Continued.

Pedon	Horizon[a]	Depth (cm)	Color (moist)	Texture[b]	Structure[c]	Effervescence to HCl[d]
TB-2	Ap	0-20	10YR 4/3	L	1 CSBK	0
	Bt	20-52	7.5YR 4/4	L	1 CSBK	1
	Bk1	52-73	10YR 4/4	SL	MA	3
	Bk2	73-122	10YR 4/4	SIL	MA	3
	2Ck1	122-144	10YR 4/4	LS	SGR	3
	3Ck2	144-190	10YR 5/4	SIL	MA	3
MA-1	Ap	0-22	7.5YR 3/2	SIL	2 MSBK	0
	Bt	22-57	5YR 4/4	SIL	2 MSBK	1
	Bk	57-90	10YR 5/4	SIL	3 MCSBK	4
	Ck1	90-142	10YR 5/6	SIL	1 MCSBK	3
	Ck2	142-200	10YR 5/8	SIL	MA	3
MA-2	Ap	0-23	5YR 3/2	SIL	2 MCSBK	0
	Bt	23-70	10YR 4/3	SIL	2 MCSBK	0
	Bk	70-130	5YR 4/4	SIL	2 FMSBK	3
	Ckm	130-200	7.5YR 4/4	SIL	MA	4
MA-3	Ap	0-19	5YR 3/3	L	1 FMSBK	0
	Bt	19-46	5YR 4/3	L	2 FMSBK	0
	C1	46-65	7.5YR 4/2	SL	MA	0
	C2	65-170	7.5YR 4/4	GRS	SGR	0

[a]Horizons with the same designation were subsampled.

[b]LC = clay; L = loam; S = sand; SI = silt; LS = loamy sand; SL = sandy loam; SCL = sandy clay loam; LFS = loamy fine sand; SICL = silty clay loam; GRLS = gravelly loamy sand; GRSL = gravelly sandy loam.

[c]1 = weak; 2 = moderate; S = strong; C = coarse; M = medium; F = fine; SBK = subangular blocky; PL = platy; MA = massive; SGR = single grain.

[d]0 = noneffervescent; 1 = very slightly effervescent; 2 = slightly effervescent; 3 = strongly effervescent; 4 = violently effervescent.

floodplain basin, the meander belt, and the colluvial soils adjacent to the fluvial scarp in the floodplain. At the alluvial-fan piedmonts, four pedons represent the two geomorphic surfaces formed by the alluvial-fan piedmonts on the south margin of the valley at the study area, and three pedons represent the soils located on the alluvial-fan piedmont situated at the north margin of the valley.

Three geomorphic surfaces were identified on the alluvial-fan piedmonts encompassed within the study area. Two geomorphic surfaces corresponded to the south margin and were separated solely based on soil properties since no discernible topographic or surface features, other than the color of the soil's surface, distinguished them. These two surfaces indicated changes in the parent material, possibly related to a lateral change from an assembly of coalescent alluvial fans. The two geomorphic surfaces were given the names Limones Surface and Trojas Surface.

The western-most surface in the study area consists of soils which parent material provenance is related to the Cacaguapa Schists Formation. This surface also shows recent and continuous aggradation activity. It is designated the Limones Surface. The eastern surface is more stable and its sediments are related to a more variable stratigraphic unit defined in the geological map of Honduras (Kozuch, 1991) as "non-differentiated volcanic rocks of unknown age; generally tuffs, andesites, and pyroclastic rocks." This unit is

symbolized as Tv in the geologic map (Chapter I). This geomorphic surface is labeled as the Trojas Surface.

Mangos Surface, the alluvial-fan piedmont at the northern margin, of the study area, is not further subdivided and it is, therefore, considered as a single unit. The parent material is similar to that of the Trojas Surface of the southern piedmont (same geological unit) and the sediments deposited on it also correspond to the geologic formation noted as Tv in the geologic map exhibit in Chapter I. Field observations indicate that andesite is the prevalent rock in the beds of the streams draining this surface and in the coarse materials underlying the soils.

The floodplain geomorphic surfaces were already discussed in Chapter III and subdivided as floodplain, floodplain meander belt, and fine-colluvium adjacent to and eroded from the fluvial scarp. The 14 pedons studied on this landscape are located on the transects across four reaches studied in Chapter III.

Soils of the Limones Surface

Soils on this unit are formed in alluvial deposits originating from the Cacaguapa Schist Formation. Pedons LA-1 and LA-2 represent two soils occurring on the mid- and distal parts of coalescent alluvial fans located at the easternmost part of the southern margin.

Pedon LA-1 represents soils on this surface, close to and strongly influenced by ephemeral small streams, that have not developed a cambic horizon. These soils are characterized by dark surface horizons with colors that range from dark olive gray (5Y 3/2) to very dark grayish brown (10YR 3/2) (Table 4-1). In many cases two or three weakly structured or massive A horizons without evidence of stratification form the surface layers. The lack of structure and/or the hardness preclude the surface horizons from being mollic or pachic epipedons. Some of these soils contain layers of angular gravel consisting of mica schist alone or embedded in a fine matrix. Very dark gray and very dark grayish brown C horizons, reflecting the color of the parent material, are characteristic in these soils.

Pedon LA-2 exemplifies those soils on this surface that exhibit more pedogenic evolution. A cambic subsurface horizon underlies the A horizon(s) with colors ranging from yellowish red (5YR 4/6) to dark yellowish brown (10YR 4/4). The top of the cambic horizon is generally between 40 and 70 cm from the surface, but in some cases it is as deep as 150 cm. In these instances an AB horizon lies between the A and Bt horizon.

Deep C horizons are usually high in gravel with variable proportions of coarse angular fragments. The fragments invariably consist of both fresh and partially weathered mica schist.

Soils of the Trojas Surface

Soils of the Trojas Surface are formed from mixed alluvial mainly of andesitic nature. These soils have developed some pedogenetic features not evident by the soils on the Limones Surface. Pedons TB-1 and TB-2 represent the soils developed and mapped on this surface.

The following sequence of horizons characterize the soils on the Trojas Surface. A massive (ochric) Ap horizon with a color hue ranging from 10YR to 7.5YR and a value and chroma between 2 to 4 is underlain by a cambic Bt horizon that has not experienced enough clay illuviation to be ruled as an argillic horizon. The color of the cambic horizon was a 7.5YR hue with both value and chroma ranging from 4 to 5. Lime enriched Btk, Bk and Ck horizons follow the sequence. As shown in the TB-1 pedon, several sedimentation layers with lower carbonate content continues with depth, and some of these layers are gravelly. The TB-1 pedon presents another lime-enriched (Ck) horizon between 295 and 340 cm.

Soils of the Mangos Surface

The northern alluvial fans encompassed within the study area constitute a single geomorphic surface. Neither surface topographic features nor the parent material present significant differences in the area. The soils exhibit some variability considered normal within a geomorphic surface. The soils developed on this surface are analogous to those

of the Trojas Surface with similar parent materials consisting of mixed fine alluvium from the same geological formation and similar sequence of soil horizons.

The most relevant morphological feature in the majority of these soils is the presence of calcic horizons at a relatively constant depth between 50 to 75 cm. Overlying the calcic horizons is a textural cambic horizon which may evolve into an argillic horizon with time. Surface and subsurface horizons show dark reddish-brown and dark brown colors with 5YR and 7.5YR hues and value and chroma ranging from 2 to 3. Subsurface horizons present reddish brown (5YR 4/3, 4/4) and yellowish brown (10YR 5/4, 5/6) colors.

Pedons MA-1, MA-2, and MA-3 adequately represent the range of properties of the soils on the Mangos Surface. Most pedons have a calcic horizon between 50-75 cm. Some calcic horizons are moderately indurated as the Ckm horizon in the MA-2 pedon whereas others do not have a calcic horizon at all (Pedon MA-3). Pedons without calcic horizons and with moderately indurated calcic horizon occur intermingled in the landscape and could not be separated at the scale of the soil survey for the Coyoles Farm.

Soils on the Floodplain

Three geomorphic surfaces were separated in the floodplain (Chapter III). These correspond to the floodplain meander belt, floodplain basin, and floodplain fine colluvium. The floodplain basin covers the majority of the floodplain area. Both the floodplain meander belt and the floodplain fine colluvium are restricted to narrow belts along the river and along the fluvial scarps that separate the floodplain from the alluvial-fan piedmonts, respectively.

The soils of the floodplain basin have developed by vertical accretion deposition and stratigraphically present a relatively thick top-stratum facie formed by fine sediments, predominantly silt, clay, and in less proportion fine and very fine sand. Occasionally, sand layers are interbedded within the top-stratum.

Sediments of the Floodplain Meander Belt have been deposited mainly by lateral accretion. These soils have a thinner fine top-stratum and a thicker and coarser bottom-stratum consisting mainly of coarse sand with variable quantities of gravel and cobbles especially in the deeper layers.

Soils on the floodplain fine colluvium which are nonmappable at the scale used, are similar to those of the floodplain basin except that they have a finer particle-size top-stratum that continues deeper in the sediments and

rarely do they have a sandy layer interstratified with the finer layers of the upper parts of the sediments.

Color of most soil horizons in the floodplain are of 10YR hue. Value and chroma range between 2 to 4 for the A and the Ab horizons and mostly between 2 to 5 for the C horizons.

The soils showed little development and were classified as Entisols. They do not have any diagnostic subsurface horizons. Some pedons have developed a mollic epipedon. The most important diagnostic characteristic of these soils is the irregular distribution of the organic carbon with depth and/or amounts of more than 2 g/kg of organic carbon at 1.25 m depth. Because of this characteristic these soils were classified as Ustifluvents. Some Ustipsamments occur in parts of the meander belt, as well as in miscellaneous areas.

Chemical Properties

Tables 4-2 and 4-3 present the chemical properties of the soils studied. Soil water pH in most soil horizons ranges from mild to strongly alkaline. A few soil horizons in the pedons studied present pH values near neutrality and most of them are moderately alkaline. No trends were observed either with depth or with calcium carbonate equivalent content in the pedons studied. The only tendency in regard to soil pH in water was that a half pH unit lower

Table 4-2. Acidity, electrical conductivity, and organic carbon content for the soils studied in the Upper-Aguán Valley

Horizon[a]	Depth (cm)	pH KCl	pH H_2O 1:1	pH $CaCl_2$	EC[b] dS/m	OC[c] g/kg
Pedon CA-1 (floodplain basin)						
Ap	0-13	7.0	8.0	7.2	0.75	27.6
A	13-50	7.1	8.3	7.3	0.67	9.0
C1	50-70	7.1	8.4	7.4	0.41	3.4
C2	70-80	7.2	8.5	7.4	0.30	3.4
C3	80-99	7.3	8.5	7.5	0.34	2.1
C4	99-140	7.2	8.6	7.7	0.25	1.0
Ab	140-175	7.1	8.4	7.5	0.59	6.2
C	175-250	7.3	8.6	7.6	0.27	1.4
Pedon CA-2 (floodplain basin)						
Ap	0-16	6.8	7.9	7.3	0.27	19.2
C1	16-41	7.1	8.0	7.5	0.13	11.5
C2	41-72	7.0	8.2	7.4	0.16	6.4
C3	72-112	6.9	8.0	7.3	0.14	6.5
C4	112-155	6.8	7.9	7.3	0.12	5.1
Pedon CA-3 (floodplain basin)						
Ap	0-20	6.9	8.0	7.2	1.28	17.3
C1	20-60	7.1	8.2	7.3	1.00	9.0
C2	60-150	7.2	8.4	7.4	0.42	4.1
C3	150-200	7.0	8.5	7.3	0.38	4.1
C4	200-230	7.1	8.4	7.4	0.15	2.1
Pedon CA-4 (floodplain meander belt)						
Ap	0-20	7.0	8.0	7.1	0.79	14.5
C1	20-45	7.2	8.4	7.3	0.72	11.7
C2	45-80	7.1	8.3	7.5	0.89	6.9
C3	80-100	7.1	8.6	7.4	0.22	1.7
C4	100-140	nd[d]	nd	nd	nd	nd
C5	140-175	7.0	8.3	7.3	0.27	1.3
Pedon CA-5 (floodplain meander belt)						
A1	0-7	7.1	7.5	6.4	0.84	9.7
A2	7-40	7.0	8.4	7.3	0.77	9.7
C1	40-70	7.1	7.4	6.5	1.64	2.8
C2	70-145	7.3	8.5	7.4	0.73	1.4
C3	145-185	7.1	8.4	7.2	0.53	1.4
C4	185-195	nd	nd	nd	nd	nd
C5	195-260	nd	nd	nd	nd	nd
C6	260-330	nd	nd	nd	nd	nd

Table 4-2.--Continued

Horizon[a]	Depth (cm)	pH KCl	pH H_2O 1:1	pH $CaCl_2$	EC[b] dS/m	OC[c] g/kg
Pedon PV-1 (floodplain basin)						
Ap	0-7	6.6	7.1	6.7	0.35	34.4
A1	7-24	6.7	7.4	6.8	0.31	20.8
A2	24-56	6.7	7.0	7.0	0.32	13.3
C1	56-85	6.6	7.6	7.1	0.22	7.7
C2	85-116	6.7	7.2	7.2	0.27	7.0
C3	116-144	6.7	7.6	7.2	0.24	5.0
C4	144-189	6.2	7.6	7.1	0.19	3.9
C5	189-220	6.6	7.5	7.2	0.27	5.8
Pedon PV-2 (floodplain basin)						
Ap	0-18	7.0	8.2	7.4	0.92	22.8
C1	18-30	7.1	8.2	7.5	0.80	18.6
C1	30-41	7.0	8.2	7.4	0.88	10.4
C2	41-50	7.3	8.3	7.5	0.82	9.7
C2	50-60	7.5	7.9	7.5	0.47	3.8
C2	60-75	7.4	7.9	7.6	0.41	4.1
C3	75-170	7.1	7.8	6.9	0.33	1.4
C4	170-190	6.9	8.6	7.1	nd	4.8
Pedon PV-3 (floodplain fine colluvium)						
Ap	0-10	6.9	7.8	7.2	0.81	43.5
Ap	10-20	6.8	7.6	7.1	0.52	17.9
C1	20-30	6.9	7.6	7.2	0.35	4.8
C2	30-58	6.9	8.2	7.1	0.40	3.5
C2	58-80	7.1	8.3	7.3	0.74	2.1
C3	80-100	7.0	8.5	7.3	0.56	0.7
C3	100-120	7.2	8.4	7.3	0.61	4.8
C3	120-140	7.1	8.5	7.3	0.57	6.2
C3	140-150	7.1	8.5	7.2	0.72	4.1
C3	150-190	7.0	8.4	7.4	0.69	3.5
Pedon NA-1 (floodplain fine colluvium)						
Ap	0-15	6.7	7.9	7.1	0.16	14.4
C1	15-66	6.7	7.8	7.2	0.21	10.4
C2	66-100	6.9	8.0	7.3	0.16	9.7
C3	100-127	6.8	8.0	7.3	0.18	9.9
C4	127-166	6.8	7.8	7.3	0.20	9.4
C5	166-192	6.8	7.9	7.3	0.16	5.7
C6	192-220	6.6	8.1	7.3	0.14	4.3

Table 4-2.--Continued

Horizon[a]	Depth (cm)	pH KCl	pH H_2O 1:1	pH $CaCl_2$	EC[b] dS/m	OC[c] g/kg
Pedon NA-2 (floodplain basin)						
Ap	0-6	7.1	7.9	7.5	0.43	15.9
C	6-10	7.2	7.7	6.1	0.54	12.8
Ab	10-20	7.3	7.9	7.6	0.45	26.9
C2	20-40	7.2	8.3	7.7	0.39	7.0
C2	40-70	7.2	8.4	7.5	0.44	2.1
C3	70-130	7.3	8.4	7.3	0.37	2.1
C4	130-155	7.2	8.6	7.4	0.36	1.4
Pedon NA-3 (floodplain meander belt)						
Ap	0-19	7.1	7.4	6.6	0.68	16.8
C1	19-63	7.0	7.6	6.6	0.68	9.8
C2	63-95	7.3	7.5	6.5	0.29	5.8
C3	95-120	7.4	7.5	6.4	0.99	3.7
C4	120-210	7.1	7.5	6.7	0.31	3.1
Pedon RC-1 (floodplain basin)						
Ap	0-15	7.4	7.8	7.5	1.12	32.4
C1	15-60	6.9	8.0	7.2	0.65	9.7
C2	60-100	7.2	8.4	7.5	0.62	3.5
C3	100-130	7.1	8.5	7.4	0.54	2.4
C4	130-180	7.1	8.4	7.3	0.49	1.4
C5	180-220	7.0	8.3	7.4	0.51	1.4
Pedon RC-2 (floodplain meander belt)						
C	0-23	7.2	7.5	6.3	3.84	29.0
Ab	23-60	7.0	8.0	7.4	0.82	45.5
C1	60-100	7.1	8.3	7.5	0.88	9.7
C2	100-125	7.2	8.4	7.4	0.54	5.5
C3	125-190	7.1	8.3	7.6	nd	0.7
C4	190-225	7.2	8.5	7.7	nd	0.6
Pedon RC-3 (floodplain basin)						
Ap	0-18	7.4	7.5	6.1	3.84	29.0
C1	18-40	7.1	8.0	7.2	0.82	nd
C2	40-60	7.1	8.3	7.2	0.88	9.7
C3	60-130	7.1	8.4	7.3	0.54	5.5
C4	130-150	7.0	8.3	7.2	nd	0.7
C5	150-200	7.2	8.5	7.4	nd	nd

Table 4-2.--Continued

Horizon[a]	Depth (cm)	pH KCl	pH H_2O 1:1	pH $CaCl_2$	EC[b] dS/m	OC[c] g/kg
Pedon LA-1 (alluvial fan piedmont-Limones Surface)						
A1	0-33	6.6	7.5	7.1	1.44	6.9
A2	33-56	6.6	7.5	7.1	1.06	0.3
2C1	56-70	6.8	7.3	7.2	0.62	6.9
3C2	70-95	7.0	8.1	6.7	0.53	4.8
4C3	95-140	6.5	7.9	7.1	0.45	6.9
Pedon LA-2 (alluvial fan piedmont-Limones Surface)						
Ap	0-19	6.7	7.5	7.2	0.59	27.6
A	19-70	7.1	7.9	7.3	0.62	16.0
Bw	70-90	7.2	8.1	7.1	0.49	6.2
2C1	90-150	7.2	8.3	7.4	0.29	2.8
2C2	150-230	7.1	8.3	7.3	0.26	1.5
Pedon TB-1 (alluvial fan piedmont-Trojas Surface)						
Ap	0-12	6.2	7.0	5.7	0.35	16.5
Bt	12-42	6.4	7.1	6.0	0.28	9.0
Bk	42-80	6.7	7.5	6.2	0.23	4.3
C1	80-120	7.1	7.7	6.4	0.12	1.4
2C2	120-152	7.3	8.0	6.6	0.73	0.6
2C3	152-180	6.9	7.7	6.6	0.92	1.0
3C4	180-225	7.1	7.9	6.7	1.07	1.0
4C5	225-245	nd	nd	nd	nd	nd
5C6	245-280	7.2	8.0	6.7	0.17	0.9
6C7	280-295	nd	nd	nd	nd	nd
7C7	295-340	6.7	7.6	6.6	1.94	1.3
Pedon TB-2 (alluvial fan piedmont-Trojas Surface0						
Ap	0-20	6.7	7.6	7.1	0.19	11.9
Bt	20-52	6.1	7.7	6.8	0.12	5.3
Bk1	52-73	6.9	7.9	7.2	0.18	5.2
Bk2	73-122	7.2	8.0	7.1	0.15	5.0
Ck1	122-144	7.3	8.4	7.4	0.11	3.8
Ck2	144-190	7.2	8.4	7.5	0.15	3.9
Pedon MA-1 (alluvial fan piedmont-Mangos Surface)						
Ap	0-22	6.9	8.1	7.3	0.23	19.5
Bt	22-57	6.9	8.0	7.3	0.17	7.1
Bk	57-90	7.4	7.9	7.7	1.29	5.5
Ck1	90-142	7.5	8.1	7.8	1.63	4.5
Ck2	142-200	7.5	7.9	7.7	0.99	3.3

Table 4-2.--Continued

Horizon[a]	Depth (cm)	pH KCl	pH H_2O 1:1	pH $CaCl_2$	EC[b] dS/m	OC[c] g/kg
Pedon MA-2 (alluvial fan piedmont-Mangos Surface)						
Ap	0-23	7.2	7.3	6.4	0.33	23.7
Bt	23-70	7.0	7.8	6.7	0.24	7.9
Bk	70-130	7.3	7.5	6.3	0.14	2.2
Ckm	130-200	7.0	7.5	6.7	0.11	1.1
Pedon MA-3 (alluvial fan piedmont-Mangos Surface)						
Ap	0-19	7.3	7.5	6.1	0.23	21.3
Bt	19-46	7.1	7.3	6.4	0.19	6.0
C1	46-65	7.3	7.4	6.5	0.14	3.7
C2	65-170	nd	7.8	6.7	0.58	0.4

[a]Horizons with the same designation were subsamples.
[b]EC = Electrical Conductivity.
[c]OC = Organic Carbon.
[d]nd = Not determined.

Table 4-3. Selected chemical properties for the soils studied in Upper-Aguán Valley

Horizon[a]	Depth (cm)	Extractable Bases Ca	Mg	Na	K	CEC	$CaCO_3$ g/kg
		cmol(+)/kg soil					
Pedon CA-1 (floodplain basin)							
Ap	0-13	15.61	3.62	0.15	0.82	20.20	14.3
A	13-50	14.62	3.51	0.14	0.42	18.69	15.0
C1	50-70	15.48	3.36	0.19	0.49	19.52	16.3
C2	70-80	8.81	3.14	0.15	0.39	12.49	43.5
C3	80-99	8.75	1.30	0.08	0.15	10.28	18.8
C4	99-140	3.91	1.41	0.09	0.10	5.51	10.0
Ab	140-175	nd	2.04	0.12	0.21	nd	32.5
C	175-250	nd	1.16	0.10	0.11	nd	8.8
Pedon CA-2 (floodplain basin)							
Ap	0-16	21.69	3.14	0.18	0.32	25.33	39.0
C1	16-41	21.86	3.36	0.15	0.36	25.73	30.0
C2	41-72	16.22	2.04	0.12	0.22	18.60	30.0
C3	72-112	16.38	2.12	0.11	0.19	18.80	51.1
C4	112-155	8.89	1.30	0.08	0.15	10.42	54.2
Pedon CA-3 (floodplain basin)							
Ap	0-20	16.27	2.85	0.11	0.56	19.75	8.0
C1	20-60	15.63	2.34	0.10	0.21	18.28	8.2
C2	60-150	19.59	1.06	0.11	0.23	20.99	8.4
C3	150-200	nd	0.92	0.08	0.24	nd	8.5
C4	200-230	nd	0.98	0.09	0.21	nd	8.4
Pedon CA-4 (floodplain meander belt)							
Ap	0-20	12.82	3.27	0.12	1.75	17.96	2.8
C1	20-45	9.55	2.16	0.11	0.25	12.07	7.5
C2	45-80	8.33	1.31	0.10	0.19	9.93	6.3
C3	80-100	3.96	0.87	0.09	0.11	5.03	1.3
C4	100-140	nd	nd	nd	nd	nd	nd
C5	140-175	nd	0.91	0.09	0.10	nd	1.5
Pedon CA-5 (floodplain meander belt)							
A1	0-7	11.04	1.84	0.12	0.84	13.84	2.5
A2	7-40	14.68	1.01	0.11	0.39	16.19	10.0
C1	40-70	11.51	0.97	0.10	0.55	13.13	13.0
C2	70-145	9.23	1.05	0.06	0.36	10.70	42.5
C3	145-185	8.36	1.10	0.05	0.30	9.81	13.0
C4	185-195	nd	nd	nd	nd	nd	nd
C5	195-260	nd	nd	nd	nd	nd	nd
C6	260-320	nd	nd	nd	nd	nd	nd

Table 4-3.--Continued

Horizon[a]	Depth (cm)	Extractable Bases Ca	Mg	Na	K	CEC	$CaCO_3$ g/kg
		cmol(+)/kg soil					
Pedon PV-1 (floodplain basin)							
Ap	0-7	21.25	3.60	0.12	1.74	26.71	30.0
A1	7-24	20.48	2.34	0.11	0.65	23.58	46.0
A2	24-56	18.23	1.84	0.11	0.31	20.49	30.0
C1	58-85	13.31	0.65	0.09	0.16	14.21	18.0
C2	85-116	15.01	2.38	0.10	0.21	17.70	38.0
C3	116-144	8.85	1.06	0.06	0.11	10.08	19.0
C4	144-189	6.47	0.58	0.04	0.07	7.16	10.0
C5	189-220	12.09	1.36	0.08	0.15	13.68	23.0
Pedon PV-2 (floodplain basin)							
Ap	0-18	16.21	2.11	0.10	0.73	19.15	13.2
C1	18-30	12.81	1.72	0.11	0.36	15.00	3.5
C1	30-41	13.91	1.34	0.10	0.24	15.59	18.0
C2	41-50	24.68	1.61	0.12	0.31	26.72	1.0
C2	50-60	11.18	1.22	0.10	0.29	12.79	0.8
C2	60-75	13.71	1.11	0.08	0.25	15.15	4.1
C3	75-170	6.12	0.76	0.06	0.27	7.21	24.3
C4	170-190	nd	1.15	0.10	0.23	nd	28.5
Pedon PV-3 (floodplain fine colluvium)							
Ap	0-10	20.83	3.60	0.13	1.23	25.79	14.0
Ap	10-20	17.49	2.73	0.13	0.79	21.14	1.0
C1	30-30	15.78	1.89	0.12	0.74	18.53	0.8
C1	30-58	14.34	1.75	0.11	0.61	16.81	25.9
C2	58-80	11.93	1.63	0.10	0.55	14.21	18.0
C2	80-100	18.87	1.77	0.11	0.56	19.31	44.0
C3	100-120	nd	nd	nd	nd	20.12	55.5
C3	120-140	17.06	3.36	0.16	0.55	21.13	82.0
C3	140-150	11.02	3.66	0.13	0.59	15.4	55.0
C3	150-190	10.83	2.78	0.13	0.56	14.3	55.5
Pedon NA-1 (floodplain fine colluvium)							
Ap	0-15	14.27	2.29	0.17	0.55	17.28	36.0
C1	15.66	12.74	1.54	0.15	0.27	14.70	25.0
C2	66-100	13.31	1.39	0.14	0.21	15.05	45.0
C3	100-127	16.71	1.63	0.13	0.28	18.75	42.0
C4	127-166	15.05	1.40	0.13	0.16	16.74	54.0
C5	166-192	9.46	1.19	0.11	0.13	10.89	54.0
C6	192-220	7.65	0.87	0.09	0.10	8.71	nd

Table 4-3.--Continued

Horizon[a]	Depth (cm)	Extractable Bases Ca	Mg	Na	K	CEC	$CaCO_3$ g/kg
		cmol(+)/kg soil					
Pedon NA-2 (floodplain basin)							
Ap	0-6	14.22	1.83	0.09	0.36	16.50	1.42
C	6-10	7.36	1.52	0.09	0.29	9.26	1.19
Ab	10-20	16.78	1.73	0.08	0.35	18.94	7.43
C2	10-40	11.39	1.45	0.06	0.30	13.20	10.22
C2	40-70	7.95	1.65	0.14	0.20	9.91	10.56
C3	70-130	nd	nd	nd	nd	nd	3.0
C4	130-155	nd	nd	nd	nd	nd	1.80
Pedon NA-3 (floodplain meander belt)							
Ap	0-19	10.31	3.01	0.35	0.43	14.10[b]	42.5
C1	19-63	9.9	3.18	0.28	0.33	13.69	62.7
C2	63-95	6.12	1.57	0.12	0.31	8.12	44.4
C3	94-120	4.34	0.54	0.07	0.16	5.12	29.2
C4	120-210	7.29	1.20	0.13	0.19	8.81	33.9
Pedon RC-1 (floodplain basin)							
Ap	0-15	23.51	3.24	0.12	2.09	28.96	10.3
C1	15-60	17.75	2.33	0.11	0.63	20.82	2.5
C2	60-100	11.16	1.63	0.09	0.24	13.12	15.5
C3	100-130	6.06	0.89	0.11	0.24	7.30	2.5
C4	130-180	9.84	1.12	0.08	0.27	11.31	13.8
C5	180-220	9.19	0.74	0.09	0.18	10.20	5.0
Pedon RC-2 (floodplain meander belt)							
C	0-23	9.32	0.65	0.08	0.13	10.18	11.3
Ab	23-60	21.47	0.87	0.09	0.15	22.58	5.0
C1	60-100	18.71	0.46	0.06	0.08	19.31	13.0
C2	100-125	16.25	0.65	0.07	0.13	17.10	13.8
C3	125-190	nd	nd	nd	nd	nd	2.8
C4	190-225	nd	nd	nd	nd	nd	2.5
Pedon RC-3 (floodplain basin)							
Ap	0-18	19.47	2.79	0.11	0.39	22.76	6.0
C1	18-40	15.78	1.62	0.12	0.20	17.72	9.3
C2	40-60	19.93	1.21	0.07	0.15	21.36	12.5
C3	60-130	13.86	0.72	0.10	0.12	14.80	11.0
C4	130-150	nd	0.54	0.02	0.06	nd	2.5
C5	150-200	nd	0.32	0.03	0.09	nd	11.3

Table 4-3.--Continued

Horizon[a]	Depth (cm)	Extractable Bases Ca	Mg	Na	K	CEC	$CaCO_3$ g/kg
		cmol(+)/kg soil					
Pedon LA-1 (alluvial fan piedmont-Limones Surface)							
A1	0-33	7.45	1.66	0.12	0.86	10.10	19.0
A2	33-56	8.22	1.16	0.10	0.34	9.82	23.0
2C1	56-70	5.42	0.86	0.07	0.30	6.65	19.0
3C2	70-95	5.31	0.92	0.09	0.26	6.58	21.0
4C3	95-140	3.31	0.98	0.06	0.16	4.51	22.0
Pedon LA-2 (alluvial fan piedmont-Limones Surface)							
Ap	0-19	23.3	7.62	0.11	2.70	nd	28.73
A	19-70	16.54	2.93	0.12	1.63	nd	21.22
Bw	70-90	19.52	3.28	0.15	0.97	nd	23.92
2C1	90-150	4.53	0.62	0.07	0.13	12.27	5.35
2C2	150-230	3.85	0.37	0.04	0.06	8.02	4.32
Pedon TB-1 (alluvial fan piedmont-Trojas Surface)							
Ap	0-12	8.20	3.03	0.11	3.00	14.34	55.8
Bt	12-42	9.80	2.99	0.12	2.20	15.11	53.6
Bk	42-80	7.89	2.00	0.09	0.83	10.81	232.0
Ck	80-120	4.86	1.53	0.06	0.47	6.92	160.7
2C2	120-152	2.93	0.81	0.04	0.20	3.98	41.5
2C3	152-180	3.57	1.21	0.06	0.25	5.09	62.9
3C4	180-225	5.11	2.57	0.07	0.52	8.27	52.2
4C5	225-245	nd[b]	nd	nd	nd	nd	nd
5C6	245-280	16.42	1.23	0.04	0.35	18.04	28.5
6C7	280-295	nd	nd	nd	nd	nd	nd
7C8	295-340	0.81	4.98	0.10	1.31	7.2	132.5
Pedon TB-2 (alluvial fan piedmont-Trojas Surface)							
Ap	0-70	12.73	1.65	0.05	0.46	14.89	18.0
Bt	20.52	12.39	2.13	0.06	0.39	14.97	18.0
Bk1	52-73	12.31	2.71	0.14	0.33	15.49	113.0
Bk2	73-122	11.83	2.25	0.15	0.41	14.64	98.0
Ck1	122-144	6.01	1.67	0.08	0.20	7.96	39.0
Ck2	144-190	7.58	3.88	0.17	0.31	11.94	104.0
Pedon MA-1 (alluvial fan piedmont-Mangos Surface)							
Ap	0-72	16.10	3.74	0.11	1.89	21.84	21.0
Bt	22.57	15.47	2.77	0.18	0.56	18.98	24.0
BK	57-90	7.52	4.80	2.17	0.32	14.81	200.0
CK1	90-142	9.79	6.77	1.10	1.37	19.03	94.0
CK2	142-200	9.02	6.48	1.11	1.03	17.64	81.0

Table 4-3.--Continued

Horizon[a]	Depth (cm)	Extractable Bases Ca	Mg	Na	K	CEC	$CaCO_3$ g/kg
		cmol(+)/kg soil					
Pedon MA-2 (alluvial fan piedmont-Mangos Surface)							
Ap	0-23	12.07	4.61	0.14	1.35	18.17	56.2
Bt	23-70	9.92	3.63	0.17	0.84	14.56	33.4
BK	70-130	9.82	3.48	0.18	0.68	14.16	74.3
Ckm	130-200	5.87	3.76	0.12	0.61	10.36	123.9
Pedon MA-3 (alluvial fan piedmont-Mangos Surface)							
Ap	0-19	11.64	3.52	0.18	1.54	16.88	35.1
Bt	19-46	10.85	3.05	0.18	0.61	14.69	47.7
C1	46-65	10.08	2.96	0.15	0.45	13.64	42.9
C2	65-170	3.78	1.24	0.06	0.31	5.39	28.2

[a]Horizons with the same designation were subsampled.
[b]nd = Not determined.

was observed in some surface Ap horizons with respect to their immediate underlying horizons perhaps due to agronomic manipulations. The high pH values undoubtedly are caused by the calcium carbonate content of these soils.

Organic carbon content is higher in the surface A horizons except in some soils of the floodplain basin relatively close to the river channel (i.e. pedon RC-2) where newly deposited C horizons may overlie the A horizons. Many soils on the floodplain show irregular decrease in organic matter content with depth which is typical of soils formed in floodplains. The amount of organic carbon is also relatively high at considerable depths in these soils due to the continuous depositional processes characteristic of fluvial soils. Even some pedons on the alluvial-fan piedmonts present irregularities in the distribution of the organic carbon with relatively high values with depth.

All the soils are base saturated and, consistently, Ca is the major cation in the exchangeable complex. Cation exchange capacity is high generally in the surface horizons which is mainly due to the presence of high organic matter in these horizons. The clay mineralogy partially contributes to this tendency.

Salts more soluble than calcium carbonate are relatively low in these soils. Exceptions are the Ap horizons of pedons RC-2 and RC-3, as indicated by the electrical conductivity values, which reach the level of

saline soils. It could be attributed to local concentration of fertilizers.

Soil Mineralogy

Mineralogy of the clay-sized fraction in these soils indicates that no significant mineralogical changes have taken place. This is true for the most developed soils on the alluvial-fan piedmont. In fact, the mineralogy of the soils seems to be inherited from the parent materials which add to the limited evolution of the soils in the Upper-Aguán Valley. XRD patterns from select horizons for some of the pedons studied that are considered to be typical of the soils at this study site are presented in Figures 4-1 to 4-5. No attempt was made to quantify the minerals and any remark about the predominance or abundance of a particular mineral is based upon the relative intensity of the peaks.

Floodplain

Soils on the floodplain present similar clay mineralogical suites. The A and C horizons in these soils are dominated by muscovite, kaolinite, vermiculite, smectite and calcite. Muscovite is present in all the horizons of the floodplain soils studied. It was identified by 1.0, 0.50 and 0.33 nm peaks. Undoubtedly, the muscovite is inherited directly from the original rocks where these

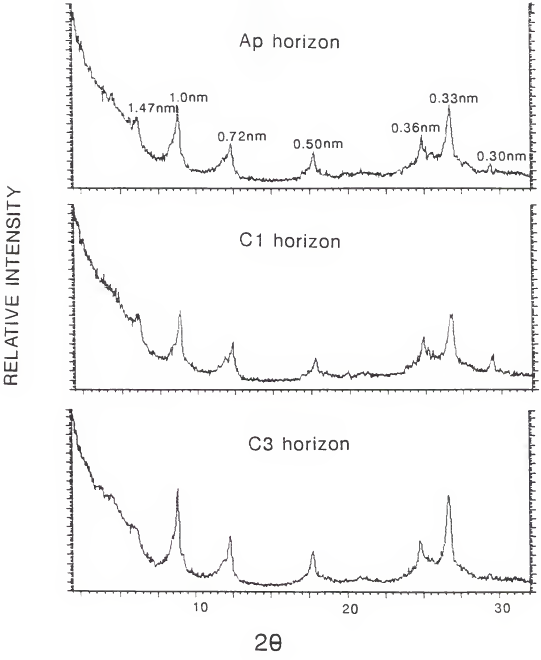

Figure 4-1. Pedon PV-1 X-ray diffraction patterns of parallel-oriented total clay (Mg-saturated and glycerol solvated) from selected horizons. Minerals identified include: vermiculite (1.47 nm peak); muscovite (1.0, 0.50, and 0.33 nm peaks); kaolinite (0.72 and 0.36 nm peaks); and calcite (0.30 nm peak).

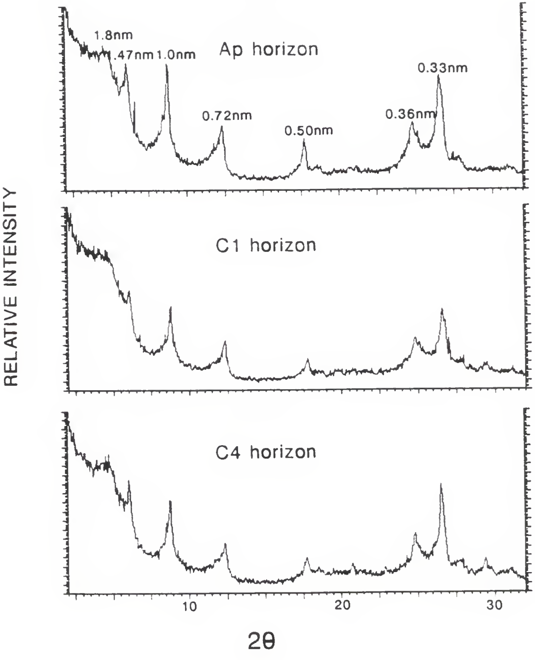

Figure 4-2. Pedon NA-3 X-ray diffraction patterns of parallel-oriented total clay (mg-saturated and glycerol solvated) from selected horizons. Minerals identified include: smectite (1.8 nm peak); vermiculite (1.47 nm peak); muscovite (1.0, 0.50, and 0.33 nm peaks); and kaolinite (0.72 and 0.36 nm peaks).

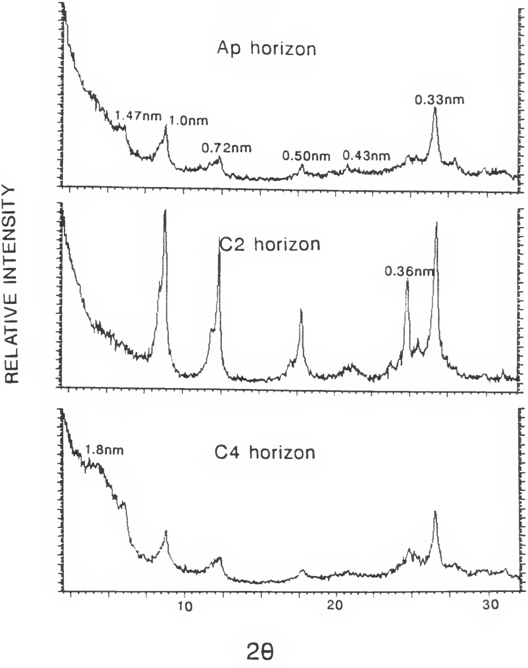

Figure 4-3. Pedon CA-1 X-ray diffraction patterns of parallel-oriented total clay (Mg-saturated and glycerol solvated) from selected horizons. Minerals identified include: smectite (1.8 nm peak); vermiculite (1.47 nm peak); muscovite (1.0, 0.50, and 0.33 peaks); and kaolinite (0.72 and 0.36 nm peaks).

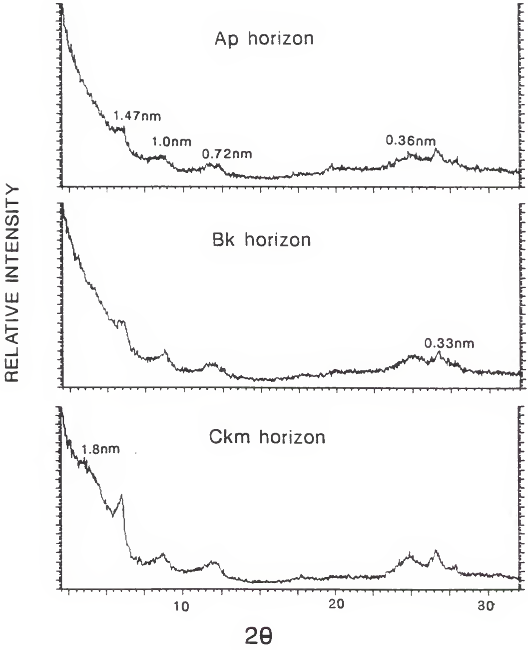

Figure 4-4. Pedon MA-2 X-ray diffraction patterns of parallel-oriented total clay (Mg-saturated and glycerol solvated) from selected horizons. Minerals identified include: smectite (1.8 nm peak); vermiculite (1.47 nm peak); muscovite (1.0 and 0.33 nm peaks), and kaolinite (0.72 and 0.36 nm peaks).

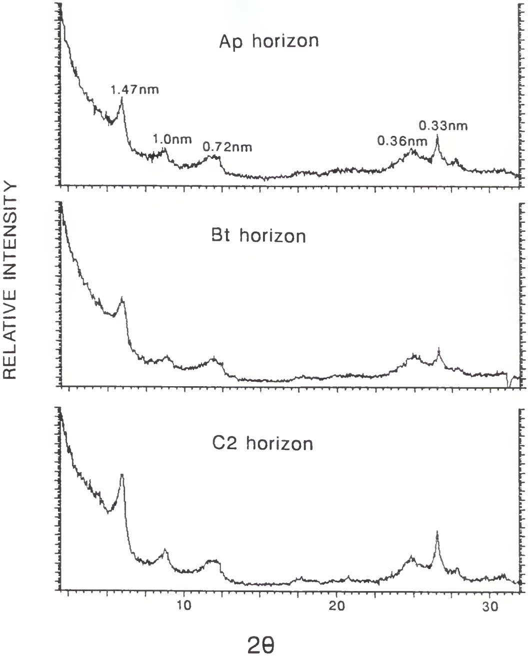

Figure 4-5. Pedon MA-3 X-ray diffraction patterns of parallel-oriented total clay (Mg-saturated and glycerol solvated) from selected horizons. Minerals identified include: vermiculite (1.47 nm peak); muscovite (1.0 and 0.33 nm peaks); and kaolinite (0.72 and 0.36 nm peaks).

sediments originated. Both the characteristics of the sand-sized mica flakes and the diffractograms point to dioctahedral mica. The dioctahedral character of the mica in the soil samples studied was suspected because the strong 0.50 nm peak and later confirmed for selected samples by looking at the 060 spacing which for dioctahedral forms is close to 0.15 nm. Mica flakes were observed in the field in virtually all soil horizons. The finer sand fractions obtained during particle-size fractionation also invariably contained mica flakes.

Kaolinite is also ubiquitous in the soils of the study site. It was identified by the 0.72 and 0.36 nm peaks. The origin of kaolinite in these soils can be traced to preweathering of the sediments before deposition on the floodplain in the well-drained soils of the drainage basin presumably from feldspar in the andesitic rocks and albite from the mica schists rich parent material.

Another pervasive clay mineral in the soils of the floodplain is vermiculite, identified by a 1.47 nm peak with Mg-saturation and glycerol solvation which shifted toward 1.0 nm upon K-saturation. The genesis of this mineral and is linked to the previously described muscovite. The intensity of the vermiculite peak in the soils of the floodplain varies among the soil horizons but no particular trend was detected.

More peculiar is the case of smectite identified by a 1.8 nm peak in Mg-saturated glycerol-solvated subsamples. Smectites are present in some soils of the floodplain, e.g,. NA-1 pedon (Fig. 4-2) but not in others, e.g., pedon PV-1 (Fig. 4-1). It is interpreted as due to random, or in any event irregular, deposition of smectite-bearing sediments along the floodplain.

Calcite is represented by a 0.30 nm peak and shows an inconsistency in its presence and peak intensity among the soil horizons of the soils studied. It is due to its preferential occurrence in the silt fraction.

Alluvial fans

The mineralogy of the soils located on the alluvial fans present basically a similar mineralogy suite to the soils of the floodplain. This is specially true for the soils of the Limones Surface, for example pedon CA-1 (Fig. 4-3). The soils on the Trojas and Mangos Surfaces, however, present some differences with respect to the rest of soils (Figs. 4-4 and 4-5). Most importantly is the lower and broader peaks characteristic for both mica and kaolinite.

Bcause the samples were not pretreated for removal of carbonates and organic matter, possible interference of these "contaminants" was suspected. Organic matter influence can be discounted, however, since soil horizons with large amounts of organic carbon presented sharp XRD

peaks, indicating little interference. Carbonates, especially acting as a cementing agent interfering in the parallel orientation of the particles, might affect XRD peak appearance. This possibility also was discounted since the XRD peaks for calcic horizons (shown later) in a paleosol studied are remarkably sharp. Another possibility was the presence of Na carbonates which also have a 0.30 nm peak. The simple comparison of the two horizons of the mentioned paleosol discount this possibility.

A possible explanation for the broad and low XRD peaks for mica and kaolinite in the soils of Trojas and Mangoes surfaces is a poor crystallinity of these minerals in these soils. The high intensity and sharpness of the 1.47 vermiculite XRD peaks for these soils also differentiate them from the remaining soils at the study site. An example is well expressed in the MA-3 pedon (Fig. 4-5).

Pedogenesis

Frequent and large sedimentation seems to be the depositional character of the floodplain sediments in the Upper-Aguán Valley. The strong sedimentary stratification expected in these kinds of materials is not evident in the soils except for very recently deposited layers on the top of the soils in some areas of the floodplain basin. It seems that homogenization of fluvial deposits (Hoeksema, 1953) can occur rapidly in some cases. Scholer (1974)

observed that fresh, fine deposits on the floodplain of the Hawkesbury River, New South Wales, lost stratification in about one year due to runoff and biological activity. The oldest sediment sequences of the floodplain in the Upper Aguán Valley seem to be not older than a few hundred years old. Surface horizons are not more than a few decades old. These soils on the floodplain are in the stratic and cumulic stages discussed by Walker and Coventry (1976).

Pedogenetic processes have little expression in the soils of the floodplain because sedimentation has overlapped with soil formation. They have been classified within the Fluvent suborder of Entisols. Only A horizons have pedogenetically developed in these soils, and in some cases a mollic epipedon has developed. The soils were classified in the Mollic Ustifluvent subgroup. The scarcity of traceable buried A horizon indicates periodic aggradation at least during the last few hundred years.

Many morphological, chemical, and physical properties in the soils of the alluvial-fan piedmont are the result of pedogenetic pathways. These soils present weakly developed textural and color B horizons (cambic horizons). Evidence that clay illuviation has occurred is not significant as these soils do not have argillic horizons.

The most important pedogenetic process expressed by these soils is the formation of calcic horizons. Only the soils of the Limones Surfaces, developed mainly from mica

schist sediments of the Cacaguapa Schists Formation, have not developed calcic horizons. The origin of $CaCO_3$ in the soils of the Trojas and Mangos Surfaces is associated with Ca-bearing minerals contained in the source rocks, mainly andesites. Ca has already been released from the primary minerals in considerable amounts before sedimentation as evidenced in the $CaCO_3$ content of the soils of the floodplain. Preweathered carbonates, *in situ* dissolution of calcium on deposited sediments, and subsequent precipitation in the soils look to be the predominant processes of calcium carbonate accumulation in these soils.

Most calcic horizons observed in Trojas and Mangos Surfaces conform with the stage I of the morphologic sequence of calcic soils originally defined by Gile et al. (1966) and later modified by Bachman and Machette (1977) and Machette (1985). A few soil horizons like the Ckm horizon of the NC-1 pedon correspond better to stage II. The depth, morphologic characteristics, and $CaCO_3$ distribution and content of each of the stages depends on the texture of the parent material and current and past climates (Arkley, 1963; Gile et al., 1966; Bachman and Machette, 1977; Birkeland, 1984).

For gravelly soils the requirements for each carbonate stage are lower than for finer soils. Gile (1975; 1977) observed in stage I carbonate soils of Holocene age that finer-textured horizons have slower downward movement of

soil moisture and consequently result in carbonate accumulation. Soils on the Mangos Surface, e.g., pedon MA-2, show coarser subsurface horizons. This may explain the lack of calcic horizons in these soils.

Trojas Paleosol

Root traces, soil structure, and soil horizons are the three primary features to distinguish paleosols (Retallack, 1988). These three features are displayed prominently in conspicuous stratigraphic layers arrayed approximately in the middle of the fluvial scarp in the southwestern part of the study site. The Trojas Paleosol can be traced for more than 1 km along a segment of the scarp currently being eroded by the Yaguala River, first, and then by the Aguán River downstream.

Morphological, chemical, and physical properties of the paleosol horizons are given in Tables 4-4, 4-5, 4-6, and 4-7. Clay mineralogical X-ray patterns for the two horizons are shown in Figure 4-6.

The most remarkable property in this paleosol is its natric horizon. Strong prismatic structure and high Na saturation of both horizons confirm the existence of a natric horizon. Relatively little information in regard to the formation of natric horizons exists in the pedologic literature. Poor drainage seems to be an indispensable

Table 4-4. Morphological description of the Trojas paleosol in the Upper-Aguán Valley (beginning at approximately 10 m from the surface).

Horizon	Depth (cm)	Description
Btn	0-70	Reddish brown (5YR 4/4) clay; strong very coarse prismatic structure; very hard; few fine root traces; strongly effervescent to HCl; strongly alkaline; clear smooth boundary.
Ckn	70-130	Light yellowish brown (10YR 6/4) loam, moderate coarse and very coarse prismatic structure; very hard; many fine root traces; violently effervescent to HCl; mildly alkaline; abrupt smooth boundary.

Table 4-5. Particle-size data of the Trojas paleosol studied in the Upper-Aguán Valley.

Horizon	VCS	CS	MS	FS	VFS	TS	CSi	MSi	FSi	TSi	Clay
Btn	0.7	1.5	2.4	2.7	2.6	9.8	19.2	9.4	12.4	40.0	50.2
Ckn	5.9	7.7	5.1	4.7	3.9	27.3	19.2	16.6	10.1	45.9	26.8

NOTE: VCS = very coarse sand, CS = coarse sand, MS = medium sand, FS = fine sand, VFS = very fine sand, TS = total sand, CSi = coarse silt, MSi = medium silt, FSi = fine silt, TSi = total silt.

Table 4-6. Selected chemical properties for the Trojas paleosol studied in the Upper-Aguán Valley.

Horizon	Extractable Bases Ca	Mg	Na	K	CEC[a]	$CaCO_3$ g/kg
	cmol(+)/kg soil					
Btn	25.1	10.7	29.6	1.31	20.9	34.4
Ckn	44.4	7.4	22.2	0.4	8.5	292.0

[a]CEC = cation exchange capacity

Table 4-7. Acidity, electrical conductivity and organic carbon content for the Trojas paleosol studied in the Upper-Aguán Valley.

Horizon	pH KCl	pH H_2O 1:1	pH $CaCl_2$	EC[a] dS/m	OC[b] g/kg
Btn	7.2	8.5	7.2	3.15	4.8
Ckn	7.4	7.7	7.1	0.22	2.2

[a]EC = electrical conductivity

[b]OC = organic carbon

Figure 4-6. Trojas paleosol X-ray diffraction patterns of parallel-oriented total clay (Mg-saturated and glycerol solvated) from the horizons. Minerals identified included: smectite (1.8 nm peak); muscovite (1.0, 0.50, 0.33, and 0.20 nm peaks); kaolinite (0.72 and 0.36 nm peaks); and calcite (0.30 nm peak).

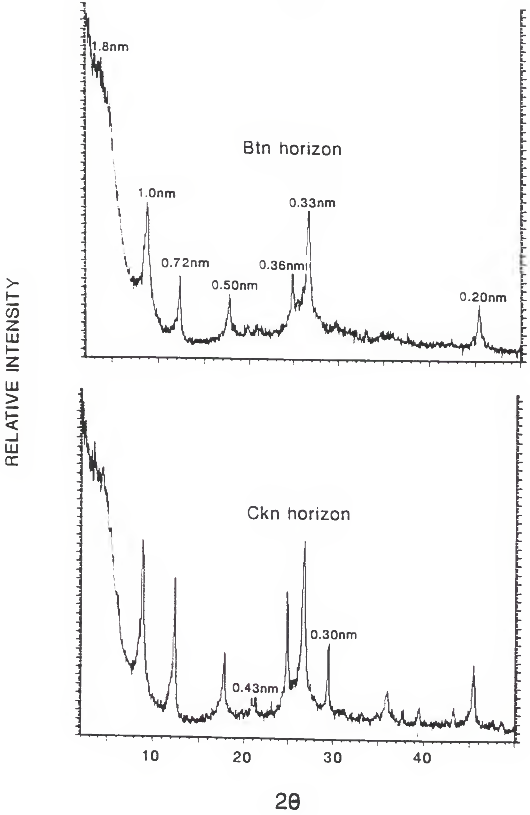
RELATIVE INTENSITY
1.8nm
Btn horizon
1.0nm
0.33nm
0.72nm
0.36nm
0.50nm
0.20nm
Ckn horizon
0.30nm
0.43nm
10
20
30
40
2θ

condition for its genesis. Most natric soils form in arid and semiarid conditions.

Ca and Na cations may be overestimated in Table 4-6, due to carbonate dissolution. Calcium cation in this case was directly measured since Na cation value is higher than the CEC values in the two horizons.

Generally, the mineralogy is similar for both horizons and similar to the clay mineralogy of the soils of the Limones Surface. Sharp high intensity XRD peaks characterize the diffractograms. Mica identified by 1.0, 0.50, 0.33, and 0.20 nm peaks predominates. Kaolinite follows, and was identified by 0.72 nm and 0.36 nm peaks. A shoulder at 1.8 nm was identified as smectite. The presence of a 0.30 nm peak in the Ckn horizon is due to the presence of calcite.

No absolute dating of the paleosol was obtained. An attempt to carbon-date the loamy sand stratigraphic layer immediately below the Ckn horizon failed due to lack of enough organic matter. It is postulated that these soils developed in a period of no net aggradation during the latest Pleistocene age which apparently was characterized at least in other parts of the Caribbean by the dryer and cooler conditions of the Younger Dryas period. The position in the landscape should be one which favored poor drainage conditions.

Summary and Conclusions

Soils in a section of the Upper-Aguán Valley bounded by two parallel faults and located on two major landscapes, alluvial-fan piedmonts and an active floodplain, were studied. Also, a paleosol identified on the wall of a fluvial scarp also was investigated. Morphological, chemical, physical, and mineralogical properties of these soils are related mainly to the type of parent materials and to the geomorphological processes that shaped these landscapes. The youthfulness of the geomorphic surfaces is the most important component in the genesis of these soils, especially in the case of the floodplain.

Soils on the floodplain are very weakly developed and, therefore, do not present diagnostic subsurface horizons. Episodic and frequent sediment depositions overlap with pedogenesis, resulted in weakly developed soils classified as Entisols, in the Mollic and Typic subgroup of the Ustifluvents.

Soils forming on the alluvial-fan piedmonts have cambic horizons. Most soils located on two of the three geomorphic surfaces separated on the alluvial-fan piedmonts also have calcic horizons. These soils were classified in the order Inceptisol and most of them pertain to the Ustropept great group.

Calcic horizons in the piedmont soils are in stage I and some in stage II in the sequence of calcic soils. These

stages are characteristic of young alluvial surfaces in arid and semiarid regions. Other morphological properties (i.e., stream pattern and incision) of these landscapes also indicate the youthfulness of these surfaces.

The Trojas Paleosol is indicative of a past period of equilibrium where the environmental conditions were different from those of the present. The properties of this paleosol support the idea of a dryer period during the latest Pleistocene, as concluded by several paleoclimatic studies in the Caribbean area.

The tectonic setting of the study site is perhaps the most influential factor in the development of the soils in the Upper-Aguán. Relatively rapid tectonic uplift of the surrounding mountain fronts, as concluded in Chapter II, explains the situation. As established by Bull (1977; 1984) when rates of uplift greatly exceed other base-level processes, the types of landscapes and associated soils described in the Upper-Aguán Valley are typical the result.

CHAPTER V
GENERAL SUMMARY AND CONCLUSIONS

North and north-central Honduras, east of the Ulua Graben, is traversed by four northeast trending faults which from south to north are, La Esperanza, Aguán, Rio Viejo, and La Ceiba Faults. The Aguán Fault is a strike-slip fault that controls the Aguán Valley and has been considered as a prolongation of other fault systems of western Honduras and eastern Guatemala (Motagua Fault System). These fault systems constitute the inland expression of the northern boundary of the Caribbean Tectonic Plate with the North America Plate that originated during late-Oligocene to early-Miocene times.

Along the Aguán Valley, no geomorphic signs of lateral motion are evident, perhaps because the resumed strike-slip faulting during Pliocene-Pleistocene does not affect the Aguán Fault (Manton, 1987). Active uplift, however, is obvious along the mountain fronts surrounding the valley and along the mountain fronts of the Caribbean coastline. Abrupt scarps, triangular facets, and hot springs along these lineaments see evidence of active tectonism.

Morphotectonics (morphological analysis of neotectonics) work was performed along the mountain-piedmont junctions on both sides of the valley and along the

Caribbean coastline with the objectives of determining and comparing the relative tectonic activity (uplifting) among these three lineaments and to assess magnitude of uplifting and trends in activity along the two margins of the valley. Two morphometric parameters, mountain front sinuosity and long stream profiles and concavity index, were used. Also, general morphology of the coalescing alluvial fans, drainage pattern, degree of channel incision in the fan surfaces, and soil development were evaluated in the investigation.

The Aguán Fault is regarded as the southern-most expression of the wide strike-slip fault system. In this study, it is estimated that the Aguán Fault controls the northern margin of the valley, whereas the more recent and active La Esperanza Fault dominates the southern margin. Morphotectonic analysis renders that the degree of tectonic activity along the north boundary of the valley (Aguán Fault) is significantly lower than that along the southern border (La Esperanza Fault) and the coastline (La Ceiba Fault). Also, that La Esperanza Fault and La Ceiba Fault present similar degree of tectonic activity.

Within the lineament of the Aguán Fault, the morphologic analysis indicates that the western part (west of the Saba Fault) is more tectonically active than the eastern part. On the western part, coalescing alluvial fans abruptly separated from the floodplain are typical whereas in the eastern part an old pediment grading to the

floodplain has developed. The tectonic activity on this part (east of the Saba Fault) is definitively lower than that of the western part of the lineament.

The trend in the south margin of the valley is opposite to that of the north margin. In the eastern part the lineament shows segments with steep escarpments without adjunct piedmonts. In some of these segments, either the escarpments are in direct contact with the floodplain or the river is impinging directly on the mountain front.

In the upper and middle parts of the valley (west of Saba Fault) the valley is narrower and both margins present coalescing alluvial fans. The alluvial-fan piedmont surfaces are smooth with gentle slopes and weakly-developed soils are forming on them. The drainage pattern is mostly distributary and shallow rivers and arroyos are incised in the surface. Rates of uplift along these mountain fronts are, undoubtedly, greater than stream downcutting and piedmont aggradation, indicating high tectonic activity. It perfectly agrees with the results of the morphologic analysis that render low sinuosity and high concavity index values in these reaches of the valley.

After its entrance into the valley, the Aguán River first flows a short distance directly beside the mountain front of the southern margin of the valley. For approximately 30 km, the river flows along the merging piedmonts. Then, the river is incised into the valley bottom where it

has built a relatively wide floodplain. No terraces are exposed between the floodplain and the incised alluvial-fan piedmonts. An abrupt scarp separates the floodplain from the alluvial-fan piedmonts. This reach of the upper valley resembles a "V" truncated in its apex. A study site in the Upper-Aguán Valley was selected to study the geomorphology and associated soils of the major landscapes, the alluvial-fan piedmonts and the floodplain.

Wetter and warmer climate conditions during early- and middle-Holocene times are considered responsible for a relatively long period of river incision and widening of the valley floor to built its floodplain. A posterior dryer period began in late-Holocene and is responsible for river aggradation, a process that continues to the present.

The floodplain stratigraphy in the Upper-Aguán Valley is dominated by vertical accretion deposition. The river regime is one of frequent (5-12 yr) moderate, and large less frequent (>50 yr) flooding events associated with tropical hurricanes. Comparisons of early (1970) to late (1987) aerial photographs and stratigraphic work indicate a regime of continuous aggradation. The river over decades acquires a slight to moderate meander pattern. Then, during a large flood or several moderate flood events, meanders are cutoff and the river attains a straight pattern. Expected changes in channel pattern due to differential uplifting along the valley were not confirmed due to the overwhelming effect of

river increasing power in the downstream direction caused by the east trending rainfall gradient. The river, accordingly, gradually increases its sinuosity downstream.

The major areas of the floodplain are covered by a floodplain basin formed by vertical accretion. A meander belt runs along the river channel and lateral accretion processes dominate this part of the floodplain. A narrow belt along the fluvial scarps forms the third floodplain landform. It consists of fine colluvium eroded from the alluvial scarp and deposited over a former floodplain basin landform.

In the floodplain, pedogenetic processes are limited to the ripening of the organic matter and the biological obliteration of the stratification. Scarcity of traceable buried A horizons within 2-2.5 m of depth, lack of structured subsurface horizons, and one carbon-date indicate an environment of continuous aggradation during the last few hundred years in the floodplain of the Upper-Aguán Valley.

The alluvial-fan piedmonts present different geomorphic surfaces that result from lateral changes of individual alluvial and coalescing fans related to changes in the source of the sediments and the size of the fans' basin. These changes are not reflected topographically in the surface but by changes in the soils. Typical soils of the fan surfaces are weakly developed with a sequence of color and textural cambic and calcic subsurface horizons.

Most calcic horizons are in stage I and some in stage II of the morphological sequence for calcic soils in arid and semiarid regions.

A paleosol identified in one wall of the alluvial scarp that separates the alluvial-fan piedmonts from the floodplain presents a well developed natric horizon. It indicates the pedogenic conditions during latest Pleistocene times in the Caribbean region inferred by paleoclimatic studies to be dryer and cooler than present (Younger Dryas). It is assumed that the equilibrium period marked by the paleosol was interrupted during an early Holocene when a significant climatic change occurred. Increase in sediment yields when the climate returned to be arid (late Holocene) is accountable for the deposition of sediments that cover the paleosol.

This research has undoubtedly contributed to a better and more detailed understanding of late-Quaternary tectonic activity along the Aguán Valley and the surrounding areas of northern Honduras, which are linked to the northern boundary of the Caribbean Plate. This study also constitutes an independent test of paleoclimatic trends during late-Pleistocene and Holocene around the Caribbean estimated elsewhere in the region.

The geomorphic evolution of the Aguán Valley was interpreted and modern tendencies of the floodplain development and the Aguán River channel morphology were

deciphered. Further detailed research in other reaches of the valley as well as in other valleys of northern Honduras and eastern Guatemala, like the Ulua, Lean, and Motagua Valleys, will improve and modificate the results and interpretations acquired in this research.

APPENDIX A
PEDON DESCRIPTIONS

Pedon CA-1 (Floodplain basin-Yaguala River)

Location: Upper-Aguán Valley between Yaguala and Aguán Rivers in Cayo "A" farm
Geomorphic position: Floodplain basin of Yaguala River
Classification: Fine-loamy, mixed (calcareous), isohyperthermic, Typic Ustifluvent
Parent material: Recent, mixed igneous and metamorphic sediments
Vegetation: Banana plantation
Elevation: Appr. 150 m

Ap--0-13 cm; dark brown (10YR 4/3) clay loam; massive with few fine stratification; friable; common mica flakes; slightly plastic and slightly sticky; many fine and medium roots; few continuous tubular pores; slightly effervescent to HCl; moderately alkaline; clear smooth boundary.

A--13-50 cm; dark brown (10YR 4/3) clay loam; massive; friable; common mica flakes; slightly plastic and slightly sticky; many fine and medium roots; many fine and medium continuous tubular pores; strongly effervescent to HCl; moderately alkaline; abrupt smooth boundary.

C1--50-70 cm; dark brown (10YR 4/3) sandy loam; single grain; loose; common mica flakes; nonplastic and nonsticky; strongly effervescent to HCl; moderately alkaline; abrupt smooth boundary.

C2--70-80 cm; dark brown (7.5YR 4/2) sandy loam; single grain; friable; common mica flakes; not plastic and not sticky; strongly effervescent to HCl; strongly alkaline; abrupt smooth boundary.

C3--80-99 cm; dark brown (7.5YR 4/2) sandy loam; single grain; loose; common mica flakes; not plastic and not sticky; strongly effervescent to HCl; strongly alkaline; abrupt smooth boundary.

C4--99-140 cm; brown (10YR 5/3) gravelly sandy loam; single grain; loose; common mica flakes; not plastic and

not sticky; slightly effervescent to HCl; strongly alkaline; abrupt smooth boundary.

Ab--140-175 cm; dark brown (7.5YR 4/2) loam; massive; friable; common mica flakes; slightly plastic and slightly sticky; strongly effervescent to HCl; moderately alkaline; abrupt smooth boundary.

C5--175-260 cm; brown (10YR 5/3) gravelly coarse loamy sand; single grain; loose; common mica flakes; not plastic and not sticky; slightly effervescent to HCl; strongly alkaline.

Diagnostic features: Ochric epipedon; O.C. decreases irregularly with depth.

Pedon CA-2 (Floodplain Aguán River)

Location: Upper-Aguán Valley between Yaguala and Aguán Rivers in Cayo "A" farm
Geomorphic position: Floodplain basin of Aguán River
Classification: Fine-silty, mixed (calcareous), isohyperthermic, Typic Ustifluvent
Vegetation: Banana plantation
Parent material: Recent, mixed-metamorphic and igneous sediments
Elevation: Appr. 150 m

Ap--0-16 cm; dark grayish brown (10YR 4/2) silty clay loam; weak coarse and very coarse subangular blocky structure; friable; common mica flakes; slightly plastic and slightly sticky; many fine and medium roots; few fine and medium continuous tubular pores; slightly effervescent to HCl; moderately alkaline; abrupt smooth boundary.

C1--16-41 cm; dark brown (10YR 4/3) silt loam; massive; friable; common mica flakes; slightly plastic and slightly sticky; few fine and medium roots; few fine and medium continuous tubular pores; strongly effervescent to HCl; moderately alkaline; gradual smooth boundary.

C2--41-72 cm; dark grayish brown (10YR 4/2) silt loam; massive; friable; common mica flakes; slightly plastic and slightly sticky; strongly effervescent to HCl; moderately alkaline; clear smooth boundary.

C3--72-112 cm; dark brown (10YR 4/3) silt loam; massive; friable; common mica flakes; slightly plastic and slightly sticky; strong to violently effervescent to HCl; moderately alkaline; clear smooth boundary.

C4--112-155 cm; brown (10YR 5/3) loamy sand; massive; very friable; common mica flakes; not plastic and not sticky; slightly effervescent to HCl; moderately alkaline.

Diagnostic features: Ochric epipedon, more than 2 g/kg O.C. down to 1.25 m.

Pedon CA-3 (Floodplain Aguan River)

Location: Upper-Aguán Valley between Yaguala and Aguán Rivers in Cayo "A" farm
Geomorphic position: Floodplain basin of Aguán River
Classification: Fine-salty, mixed (calcareous), isohyperthermic, Typic Ustifluvent
Parent material: Recent, mixed-metamorphic and igneous sediments
Vegetation: Banana plantation
Elevation: Appr. 150 m

Ap--0-20 cm; brown (10YR 4/3) silty clay loam; weak medium and coarse subangular blocky structure; firm; common mica flakes; slightly plastic and slightly sticky; many fine and medium roots; few fine and medium continuous tubular pores; slightly effervescent to HCl; moderately alkaline; clear smooth boundary.

C1--20-60 cm; dark yellowish brown (10YR 4/4) clay loam; weak medium and coarse subangular structure; firm; common mica flakes; slightly plastic and moderately sticky; many fine and medium roots; few fine and medium continuous tubular pores; slightly effervescent to HCl; moderately alkaline; clear smooth boundary.

C2--60-150 cm; dark yellowish brown (10YR 3/4) clay loam; massive; firm; common mica flakes; slightly plastic and moderately sticky; slightly effervescent to HCl; moderately alkaline; abrupt smooth boundary.

C3--150-200 cm; dark yellowish brown (10YR 3/4) sandy clay loam; massive; friable; common mica flakes; not plastic and slightly sticky; slightly effervescent to HCl; strongly alkaline; abrupt smooth boundary.

C4--200-230 cm; dark yellowish brown (10YR 4/4) sandy loam; massive; very friable; common mica flakes; not plastic and not sticky; slightly effervescent to HCl; moderately alkaline.

Diagnostic features: Ochric epipedon, more than 2.0 g/kg O.C. down to 1.25 m.

Pedon CA-4 (Floodplain Aguán River)

Location: Upper-Aguán Valley between Yaguala and Aguán Rivers in Cayo "A" farm
Geomorphic position: Floodplain basin of Aguán River
Classification: Fine-loamy over sandy, mixed (calcareous), isohyperthermic, Typic Ustifluvent
Parent material: Recent, mixed-metamorphic and igneous sediments
Vegetation: Banana plantation
Elevation: Appr. 150 m

Ap--0-20 cm; dark brown to yellowish brown (10YR 4/3, 10YR 5/4) loam; weak medium and coarse subangular blocky structure; very friable; common mica flakes; slightly plastic and slightly sticky; very slightly effervescent to HCl; few fine and medium continuous tubular pores; moderately alkaline; clear smooth boundary.

C1--20-45 cm; yellowish brown (10YR 5/4) loam; weak medium and coarse subangular blocky structure; very friable; common mica flakes; slightly plastic and slightly sticky; slightly effervescent to HCl; moderately alkaline; abrupt smooth boundary.

C2--45-80 cm; yellowish brown (10YR 5/4) loam; massive; very friable; common mica flakes; not plastic and not sticky; strongly effervescent to HCl; moderately alkaline; abrupt smooth boundary.

C3--80-100 cm; yellowish brown (10YR 5/4) cobbly coarse sand; single grain; loose; common mica flakes; not plastic not sticky; 20% by volume rounded cobbles; very slightly effervescent to HCl; strongly alkaline; abrupt smooth boundary.

C4--100-140 cm; 10-15 cm rounded cobbles.

C5--140-175 cm; yellowish brown (10YR 5/4) coarse loamy sand; single grain; loose; common mica flakes; moderately alkaline; abrupt smooth boundary.

C6--175+ cm; cobbles and boulders.

Diagnostic features: Ochric epipedon, more than 0.2 g/kg of O.C. down to 1.25 m.

Pedon CA-5 (Floodplain of Aguán River)

Location: Upper-Aguán Valley between Yaguala and Aguán Rivers in Cayo "A" farm

Geomorphic position: Floodplain basin of Aguán River
Classification: Fine-loamy, mixed (calcareous), isohyperthermic, Typic Ustifluvent
Parent material: Recent, mixed-metamorphic and igneous sediments
Vegetation: Banana plantation
Elevation: Appr. 150 m

Ap--0-7 cm; dark yellowish brown (10YR 4/4) sandy clay loam; weak medium and coarse subangular blocky structure; friable; common mica flakes; not plastic and not sticky; few fine to coarse continuous tubular pores; slightly effervescent to HCl; mildly alkaline; abrupt smooth boundary.

A--7-40 cm; dark brown (10YR 3/3); sandy clay loam; weak medium and coarse subangular blocky structure; friable; common mica flakes; not plastic and not sticky; few fine to coarse continuous tubular pores; slightly effervescent to HCl; moderately alkaline; abrupt smooth boundary.

C1--40-70 cm; dark brown (10YR 4/3) sandy clay loam; weak medium and coarse subangular blocky structure; very friable; common mica flakes; not plastic and not sticky; few fine continuous tubular pores; very slightly effervescent to HCl; mildly alkaline; abrupt smooth boundary.

C2--70-145 cm; light yellowish brown (10YR 6/4) sandy clay loam; massive; friable; common mica flakes; not plastic and not sticky; strongly effervescent to HCl; strongly alkaline; abrupt smooth boundary.

C3--145-185 cm; brownish yellow (10YR 6/6) sandy loam; single grain; loose; common mica flakes; non-plastic non-sticky; slightly effervescent to HCl; moderately alkaline; abrupt smooth boundary.

C4--185-195 cm; yellowish brown (10YR 5/4) fine sand; single grain; loose; common mica flakes; non-plastic non-sticky; slightly effervescent to HCl; moderately alkaline; abrupt smooth boundary.

C5--195-260 cm; yellowish brown (10YR 5/4) loamy sand; single grain; loose; common mica flakes; non-plastic non-sticky; strongly effervescent to HCl; moderately alkaline; abrupt smooth boundary.

C6--260 320 cm; brown (10YR 5/3) sand; single grain; loose; common mica flakes; nonplastic nonsticky; slightly effervescent to HCl; moderately alkaline.

Diagnostic features: Ochric epipedon, more than 2.0 g/kg of O.C. down to 1.25 m.

Pedon PV-1 (Floodplain of Aguán River)

Location: Upper-Aguán Valley approximately 1 km downstream the confluence of the Yaguala and Aguán Rivers in Palo Verde "B" farm
Geomorphic position: Meander belt of Aguán River
Classification: Coarse-silty, mixed (calcareous), isohyperthermic, Typic Ustifluvent
Parent material: Recent, mixed-metamorphic and igneous sediments
Elevation: Appr. 150 m

Ap--0-7 cm; very dark grayish brown (10YR 3/2) silt loam; moderate thin platy structure; friable; common mica flakes; slightly plastic and slightly sticky; many fine to medium roots; few fine and medium continuous tubular pores; slightly effervescent to HCl; neutral; abrupt smooth boundary.

A1--7-24 cm; dark grayish brown (10YR 4/2) silt loam; weak medium subangular blocky structure; friable; common mica flakes; slightly plastic and slightly sticky; many fine to medium roots; few fine and medium continuous tubular pores; strongly effervescent to HCl; mildly alkaline; clear smooth boundary.

A2--24-56 cm; dark grayish brown (10YR 4/2) silt loam; weak medium subangular blocky structure; friable; common mica flakes; slightly plastic and slightly sticky; few fine to medium roots; few fine and medium continuous tubular pores; slightly effervescent to HCl; neutral; clear smooth boundary.

C1--56-85 cm; dark brown (10YR 4/3) silt loam; massive; friable; common mica flakes; slightly plastic and slightly sticky; slightly effervescent to HCl; mildly alkaline; clear smooth boundary.

C2--85-116 cm; dark grayish brown (10YR 4/2); silt loam; massive; friable; common mica flakes; slightly plastic and slightly sticky; strongly effervescent to HCl; mildly alkaline; clear smooth boundary.

C3--116-144 cm; brown (10YR 5/3); sandy loam; massive; very friable; common mica flakes; not plastic and not sticky; slightly effervescent to HCl; mildly alkaline; abrupt smooth boundary.

C4--144-189 cm; light yellowish brown (10YR 6/4) sand; single grain; loose; common mica flakes; not plastic and not sticky; slightly effervescent to HCl; mildly alkaline; abrupt smooth boundary.

C5--189-220 cm; light yellowish brown (10YR 6/4) gravelly sandy loam; massive; very friable; common mica flakes; not plastic and not sticky; slightly effervescent to HCl; mildly alkaline.

Diagnostic features: Ochric epipedon, O.C. decreases irregularly with depth.

Pedon PV-2 (Floodplain of Aguán River)

Location: Upper-Aguán Valley approximately 1 km downstream the confluence of the Yaguala and Aguán Rivers in Palo Verde "B" farm
Geomorphic position: Floodplain basin of Aguán River
Classification: Coarse-loamy, mixed (calcareous), isohyperthermic, Mollic Ustifluvent
Parent material: Recent, mixed-metamorphic and igneous sediments
Vegetation: Banana plantation
Elevation: Appr. 155 m

Ap--0-18 cm; dark brown (10YR 3/3) clay loam; weak thick platy structure; friable; common mica flakes; slightly plastic and slightly sticky; many fine and medium roots; few fine to medium continuous tubular pores; slightly effervescent to HCl; moderately alkaline; abrupt smooth boundary.

C1--18-41 cm; brown (10YR 5/3) sandy clay loam; weak medium and coarse subangular blocky structure; friable; common mica flakes; slightly plastic and slightly sticky; few fine and medium roots; few fine continuous tubular pores; very slightly effervescent to HCl; moderately alkaline; abrupt smooth boundary.

C2--41-75 cm; dark yellowish brown (10YR 3/4) loam; weak medium subangular blocky structure; friable; common mica flakes; not plastic and not sticky; very slightly effervescent to HCl; moderately alkaline; abrupt smooth boundary.

C3--75-170 cm; yellowish brown (10YR 5/4) loamy sand; single grain; loose; common mica flakes; not plastic and not sticky; strongly effervescent to HCl; moderately alkaline; abrupt smooth boundary.

C4--170-190 cm; dark yellowish brown (10YR 4/4) loamy sand; single grain; loose; common mica flakes; not plastic and not sticky; strongly effervescent to HCl; strongly alkaline.

Diagnostic features: Ochric epipedon, O.C. decreases irregularly with depth.

Pedon PV-3 (Floodplain of Aguán River)

Location: Upper-Aguán Valley approximately 1 km downstream from the confluence of the Yaguala and Aguán Rivers in Palo Verde "B" farm
Geomorphic position: Floodplain basin of Aguán River
Classification: Coarse-silty, mixed (calcareous), isohypothermic, Typic Ustifluvent
Parent material: Mixed fine colluvium from fluvial scarp
Vegetation: Banana plantation
Elevation: Appr. 160 m

Ap--0-20 cm; dark brown (10YR 4/3) silt loam; weak coarse subangular blocky structure; firm; slightly plastic and sticky; many fine and medium roots; slightly effervescent to HCl; mildly alkaline; clear smooth boundary.

C1--20-58 cm; brown (10YR 5/3) silt loam; weak medium and coarse subangular blocky structure; firm; slightly plastic and sticky; very slightly effervescent to HCl; mildly alkaline; gradual smooth boundary.

C2--58-100 cm; yellowish brown (10YR 5/4) silt loam; massive; friable; slightly plastic and slightly sticky; strongly effervescent to HCl; moderately alkaline; gradual smooth boundary.

C3--100-235 cm; dark yellowish brown (10YR 4/4) silt loam; massive; firm; slightly plastic and sticky; strongly effervescent to HCl; strongly alkaline.

Diagnostic features: Ochric epipedon, more than 2.0 g/kg O.C. down to 1.25 m.

Pedon NA-1 (Floodplain of Aguán River)

Location: Upper-Aguán Valley approximately 7.5 km downstream the confluence of the Yaguala and Aguán Rivers in Rosario "A" farm
Geomorphic position: Floodplain basin of Aguán River
Parent material: Recent, mixed-metamorphic and igneous sediments

Classification: Coarse-silty, mixed (calcareous), isohyperthermic, Mollic Ustifluvent
Vegetation: Banana plantation
Elevation: Appr. 130 m

Ap--0-15 cm; very dark grayish brown (10YR 3/2) silt loam; weak coarse subangular blocky structure; friable; common mica flakes; slightly plastic and slightly sticky; many fine, medium, and coarse roots; many fine and medium continuous tubular pores; slightly effervescent to HCl; moderately alkaline; clear smooth boundary.

C1--15-66 cm; dark grayish brown (10YR 4/2) loam; massive; very friable; common mica flakes; not plastic and not sticky; few fine to medium roots; few fine and medium continuous tubular pores; strongly effervescent to HCl; mildly alkaline; clear smooth boundary.

C2--66-100 cm; grayish brown (10YR 5/2) silt loam; massive; friable; common mica flakes; slightly plastic and slightly sticky; strongly effervescent to HCl; moderately alkaline; clear smooth boundary.

C3--100-127 cm; dark yellowish brown (10YR 4/4) silt loam; massive; friable; common mica flakes; slightly plastic and slightly sticky; strongly effervescent to HCl; moderately alkaline; clear smooth boundary.

C4--127-166 cm; brown (10YR 5/3) silt loam; massive; friable; common mica flakes; slightly plastic and slightly sticky; strongly effervescent to HCl; mildly alkaline; abrupt smooth boundary.

C5--166-192 cm; yellowish brown (10YR 5/4) loam; massive; very friable; common mica flakes; not plastic and not sticky; strongly effervescent to HCl; moderately alkaline; abrupt smooth boundary.

C6--192-220 cm; yellowish brown (10YR 5/4) cobbly loamy sand; single grain; loose; common mica flakes; not plastic and not sticky; 10-15% cobbles 5-10 cm diameter; strongly effervescent to HCl; moderately alkaline.

Diagnostic features: Ochric epipedon, O.C. decreases irregularly with depth.

<u>Pedon NA-2 (Floodplain of Aguán River)</u>

Location: Upper-Aguán Valley approximately 7.5 km downstream from the confluence of the Yaguala and Aguán Rivers in Naranjo "A" farm

Geomorphic position: Meander belt of Aguán River
Classification: Fine-loamy, mixed (calcareous), isohyperthermic, Typic Ustifluvents
Parent material: Recent, mixed-metamorphic and igneous sediments
Vegetation: Banana plantation
Elevation: Appr. 130 m

Ap--0-6 cm; dark brown (10YR 3/3) loam; weak thick and very thick platy structure; friable; common mica flakes; not plastic and not sticky; many fine and medium roots; moderately alkaline; abrupt smooth boundary.

C--6-10 cm; brown (10YR 5/3) sandy loam; single grain; loose; common mica flakes; not plastic and not sticky; many fine and medium roots; mildly alkaline; abrupt smooth boundary.

Ab--10-20 cm; very dark grayish brown (10YR 3/2) loam; weak medium and coarse subangular blocky structure; friable; common mica flakes; not plastic and not sticky; many fine and medium roots; slightly effervescent to HCl; moderately alkaline; abrupt smooth boundary.

C1--20-70 cm; yellowish brown (10YR 5/4) sandy loam; single grain; loose; common mica flakes; not plastic and not sticky; few fine and medium roots; strongly effervescent to HCl; moderately alkaline; abrupt smooth boundary.

C2--70-130 cm; dark brown (10YR 4/3) loam; massive; friable; common mica flakes; not plastic and not sticky; slightly effervescent to HCl; moderately alkaline; abrupt smooth boundary.

C3--130-155 cm; dark brown (10YR 4/3) gravelly sandy loam; single grain; loose; common mica flakes; not plastic and not sticky; slightly effervescent to HCl; strongly alkaline.

Diagnostic features: Ochric epipedon, O.C. decreases irregularly with depth.

Pedon NA-3 (Floodplain of Aguán River)

Location: Upper-Aguán Valley approximately 7.5 km downstream from the confluence of Yaguala and Aguán Rivers in Naranjo "A" farm
Geomorphic position: Floodplain basin of Aguán River
Classification: Coarse-loamy, mixed (calcareous), isohyperthermic, Mollic Ustifluvent

Parent material: Recent, mixed-metamorphic and igneous sediments
Vegetation: Banana plantation
Elevation: Appr. 130 m

Ap--0-19 cm; dark brown (10YR 3/3) silt loam; weak fine and medium subangular blocky structure; friable; common mica flakes; slightly plastic and slightly sticky; many fine and medium roots; few fine to medium continuous tubular pores; slightly effervescent to HCl; mildly alkaline; clear smooth boundary.

C1--19-63 cm; dark brown (10YR 4/3) silt loam; massive; firm; common mica flakes; slightly plastic and slightly sticky; few fine and medium roots; strongly effervescent to HCl; mildly alkaline; abrupt smooth boundary.

C2--63-95 cm; yellowish brown (10YR 5/4) sandy loam; massive; very friable; common mica flakes; not plastic and not sticky; slightly effervescent to HCl; mildly alkaline; abrupt smooth boundary.

C3--95-120 cm; dark yellowish brown (10YR 4/4) sand; single grain; loose; common mica flakes; not plastic and not sticky; slightly effervescent to HCl; mildly alkaline; abrupt smooth boundary.

C4--120-210 cm; yellowish brown (10YR 5/4) sandy loam; massive; very friable; common mica flakes; not plastic and not sticky; slightly effervescent to HCl; mildly alkaline.

Diagnostic features: Ochric epipedon; more than 2.0 g/kg O.C. down to 1.25 m.

Pedon RC-1 (Floodplain of Aguán River)

Location: Upper-Aguán Valley approximately 12.5 km downstream from the confluence of the Yaguala and Aguán Rivers in Rosario "C" farm.
Geomorphic position: Floodplain basin of Aguán River
Classification: Fine-silty, mixed (calcareous), isohyperthermic, Mollic Ustifluvent
Parent material: Fine colluvium from fluvial scarp
Vegetation: Banana plantation
Elevation: Appr. 120 m

Ap--0-15 cm; dark brown (10YR 3/3) clay loam; weak medium and coarse subangular blocky structure; firm; moderately plastic and moderately sticky; common fine and medium roots; few fine to medium continuous tubular pores;

slightly effervescent to HCl; mildly alkaline; gradual smooth boundary.

C1--15-60 cm; dark brown (10YR 4/3) silty clay loam; massive; firm; moderately plastic and moderately sticky; few fine and medium roots; few fine to medium continuous tubular pores; slightly effervescent to HCl; moderately alkaline; clear smooth boundary.

C2--60-100 cm; dark yellowish brown (10YR 4/4) clay loam; massive; friable; slightly plastic and slightly sticky; strongly effervescent to HCl; moderately alkaline; abrupt smooth boundary.

C3--100-130 cm; yellowish brown (10YR 5/4) loamy sand; single grain; loose; rare mica flakes; not plastic and not sticky; slightly effervescent to HCl; strongly alkaline; abrupt smooth boundary.

C4--130-180 cm; dark yellowish brown (10YR 4/4) sandy clay loam; massive; friable; slightly plastic and slightly sticky; strongly effervescent to HCl; moderately alkaline; abrupt smooth boundary.

C5--180-200 cm; dark yellowish brown (10YR 4/4) sandy loam; massive; very friable; not plastic and not sticky; slightly effervescent to HCl; moderately alkaline.

Diagnostic features: Ochric epipedon; more than 2.0 g/kg of O.C. down to 1.25 m.

Pedon RC-2 (Floodplain of Aguán River)

Location: Upper-Aguán Valley approximately 12.5 km downstream from the confluence of the Yaguala and Aguán Rivers in Rosario "C" farm
Geomorphic position: Floodplain basin of Aguán River
Classification: Fine-silty, mixed (calcareous), isohyperthermic, Typic Ustifluvent
Parent material: Recent, mixed-metamorphic and igneous sediments
Vegetation: New established banana plantation
Elevation: Appr. 120 m

Ap--0-23 cm; yellowish brown (10YR 5/4) sandy loam; weak thick platy structure; very friable; common mica flakes; not plastic and not sticky; many fine and medium roots; few fine to medium continuous tubular pores; slightly effervescent to HCl; mildly alkaline; abrupt smooth boundary.

Ab--23-60 cm; dark grayish brown (10YR 4/2) silty clay loam; weak coarse subangular blocky structure; firm; moderately plastic and moderately sticky; few fine and medium roots; few fine to medium continuous tubular pores; slightly effervescent to HCl; moderately alkaline; clear smooth boundary.

C1--60-100 cm; dark brown (10YR 4/3) silty clay loam; massive; firm; moderately plastic and moderately sticky; strongly effervescent to HCl; moderately alkaline; clear smooth boundary.

C2--100-125 cm; dark yellowish brown (10YR 4/4) sandy clay loam; massive; friable; rare mica flakes; slightly plastic and slightly sticky; strongly effervescent to HCl; moderately alkaline; abrupt smooth boundary.

C3--125-190 cm; light yellowish brown (10YR 6/4) loamy sand; single grain; loose; common mica flakes; not plastic and not sticky; slightly effervescent to HCl; moderately alkaline; abrupt smooth boundary.

C4--190-225 cm; light yellowish brown (10YR 6/4) loamy sand; few fine and medium faint yellowish red mottles (5YR 5/6); single grain; loose; common mica flakes; not plastic and not sticky; slightly effervescent to HCl; strongly alkaline; abrupt smooth boundary.

C5--225+ cm; cobbles and stones.

Diagnostic features: Ochric epipedon; O.C. decreases irregularly with depth.

Pedon RC-3 (Floodplain of Aguán River)

Location: Upper-Aguán Valley approximately 12.5 km downstream the confluence of the Yaguala and Aguán Rivers in Rosario "C" farm
Geomorphic position: Meander belt of Aguán River
Classification: Fine-silty, mixed (calcareous), isohyperthermic, Typic Ustifluvent
Parent material: Recent, mixed-metamorphic and igneous sediments
Vegetation: New established banana plantation
Elevation: Appr. 120 m

Ap--0-18 cm; dark grayish brown (10YR 4/2) silty clay loam; weak fine and medium granular structure; friable; slightly plastic and slightly sticky; few fine and medium roots; few fine to medium continuous tubular pores;

slightly effervescent to HCl; mildly alkaline; clear smooth boundary.

C1--18-40 cm; dark brown (10YR 4/3) clay loam; weak fine and medium granular structure; friable slightly plastic and slightly sticky; few fine and medium roots; slightly effervescent to HCl; moderately alkaline; clear smooth boundary.

C2--40-130 cm; dark yellowish brown (10YR 4/4) silty clay loam; massive; friable; rare mica flakes; slightly plastic and slightly sticky; strongly effervescent to HCl; moderately alkaline; abrupt smooth boundary.

C3--130-150 cm; yellowish brown (10YR 5/4) loam; massive; very friable; common mica flakes; not plastic and not sticky; slightly effervescent to HCl; moderately alkaline; abrupt smooth boundary.

C4--150-200 cm; dark yellowish brown (10YR 4/4) sand; single grain; loose; common mica flakes; not plastic and not sticky; strongly effervescent to HCl; strongly alkaline; abrupt smooth boundary.

C5--200+ cm; pebbles, cobbles, and stones.

Diagnostic features: Ochric epipedon, more than 2.0 g/kg O.C. down to 1.25 m.

Pedon LA-1 (Alluvial-fan piedmont)

Location: South margin Upper-Aguán Valley in Limones "A" farm
Geomorphic position: Medium part of alluvial fan piedmont
Classification: Fine-silty, micaceous (calcareous), isohyperthermic, Typic Haplustoll
Parent material: Recent sediments from Cacaguapa Schist Formation
Vegetation: Banana plantation
Elevation: Appr. 180 m

A1--0-33 cm; very dark gray (5YR 3/1) silt loam; weak medium subangular blocky structure; friable; smeary; few fine and medium roots; slightly effervescent to HCl; mildly alkaline; abrupt smooth boundary.

A2--33-56 cm; dark brown (7.5YR 3/2) silt loam; weak medium subangular structure; friable; smeary; slightly effervescent to HCl; mildly alkaline; clear smooth boundary.

2C1--56-70 cm; very dark gray (10YR 3/1) gravelly loam; massive; very friable; weakly smeary; slightly effervescent to HCl; mildly alkaline; abrupt smooth boundary.

3C2--70-95 cm; dark brown (7.5YR 3/2) silt loam; massive; friable; slightly effervescent to HCl; moderately alkaline; abrupt smooth boundary.

4C3--95-140 cm; very dark gray (7.5YR 3/0) sandy loam; massive; very friable; weakly smeary; slightly effervescent to HCl; moderately alkaline.

Diagnostic features: Mollic epipedon, no diagnostic subsurface horizon.

Pedon LA-2 (Alluvial-fan piedmont)

Location: South margin Upper-Aguán Valley in Trojas "B" farm
Geomorphic position: Distal part of alluvial fan piedmont
Classification: Very fine, micaceous (calcareous), isohyperthermic, Typic Ustropept
Parent material: Sediments from Cacaguapa Schists Formation
Vegetation: Banana plantation
Elevation: Appr. 160 m

Ap--0-19 cm; very dark grayish brown (10YR 3/2) clay; weak coarse subangular blocky structure; very firm; smeary moderately plastic and moderately sticky; many fine and medium roots; few fine to medium continuous tubular pores; very slightly effervescent to HCl; mildly alkaline; gradual smooth boundary.

A--19-70 cm; very dark gray (10YR 3/1) clay; massive; very firm; smeary moderately plastic and moderately sticky; few fine and medium roots; slightly effervescent to HCl; moderately alkaline; clear smooth boundary.

Bw--70-90 cm; dark yellowish brown (10YR 4/4) clay; moderate medium to coarse subangular blocky structure; very firm; smeary moderately plastic and moderately sticky; slightly effervescent to HCl; moderately alkaline; clear smooth boundary.

2C1--90-150 cm; brown (10YR 5/3) silt loam; massive; friable; smeary slightly plastic and slightly sticky; strongly effervescent to HCl; moderately alkaline; clear smooth boundary.

2C2--150-230 cm; yellowish brown (10YR 5/4) silt loam; friable; smeary slightly plastic and slightly sticky; strongly effervescent to HCl; moderately alkaline.

Diagnostic features: Ochric epipedon, cambic subsurface horizon.

Pedon TB-1 (Alluvial-fan piedmont)

Location: South margin Upper-Aguán Valley in Trojas "B" farm
Geomorphic position: Distal part of alluvial-fan piedmont
Classification: Fine-loamy, mixed (calcareous), isohyperthermic, Typic Ustropept
Parent material: Andesitic sediments from Tva formation
Vegetation: Banana plantation
Elevation: Appr. 160 m

Ap--0-12 cm; dark brown (7.5YR 4/4) clay loam; massive; firm; moderately plastic and moderately sticky; many fine and medium roots; slightly effervescent to HCl; neutral; clear smooth boundary.

Bw--12-42 cm; brown (7.5YR 5/4) silty clay loam; massive; firm moderately plastic and moderately sticky; few fine and medium roots; slightly effervescent to HCl; neutral; clear smooth boundary.

Btk--42-80 cm; yellowish brown (10 YR5/4) silt loam; weak medium and coarse subangular blocky structure; slightly plastic and slightly sticky; few faint clay films on peds faces; soft masses of secondary carbonate; violently effervescent to HCl; mildly alkaline; gradual smooth boundary.

Ck--80-120 cm; light yellowish brown (10YR 6/4) loam; weak medium and coarse subangular blocky structure; not plastic and not sticky; soft masses of secondary carbonate; violently effervescent to HCl; moderately alkaline; abrupt smooth boundary.

2C1--120-152 cm; light olive brown (2.5Y 5/4) sand; single grain; loose; not plastic and not sticky; very slightly effervescent to HCl; moderately alkaline; abrupt smooth boundary.

2C2--152-180 cm; light olive brown (2.5Y 5/4) loamy fine sand; single grain; loose; not plastic and not sticky; slightly effervescent to HCl; moderately alkaline; clear smooth boundary.

3C3--180-225 cm; yellowish brown (10YR 5/4) silty clay loam; slightly effervescent to HCl; moderately alkaline; abrupt smooth boundary.

4C4--225-245 cm; angular gravel

5C5--245-280 cm; olive brown (2.5Y 4/4) coarse sand; not plastic and not sticky; slightly effervescent to HCl; moderately alkaline; abrupt smooth boundary.

6C6--280-295 cm; angular gravel

7Ck--295-340 cm; light olive brown (2.5Y 5/4) silty clay loam; slightly plastic and slightly sticky; soft masses of carbonate strongly effervescent to HCl; moderately alkaline.

Diagnostic features: Ochric epipedon, cambic and calcic subsurface horizons.

<u>Pedon TB-2 (Alluvial-fan piedmont)</u>

Location: South margin Upper-Aguán Valley in Rosario "A" farm
Geomorphic position: Distal part of alluvial-fan piedmont
Classification: Fine-loamy, mixed (calcareous), isohyperthermic, Typic Ustropept
Parent material: Andesitic sediments from Tva formation
Vegetation: Banana plantation
Elevation: Appr. 160 m

Ap--0-20 cm; dark brown (10YR 4/3) loam; weak coarse subangular blocky structure; friable; not plastic and not sticky; many fine and medium roots; few fine to medium continuous tubular pores; mildly alkaline; clear smooth boundary.

Bt--20-52 cm; brown (7.5YR 4/4) loam; weak coarse subangular blocky structure; friable; slightly plastic and slightly sticky; few fine and medium roots; few faint clay films on peds faces; very slightly effervescent to HCl; mildly alkaline; gradual smooth boundary.

Bk1--52-73 cm; dark yellowish brown (10YR 4/4) sandy loam; massive; very friable; not plastic and not sticky; few medium roots; soft masses of secondary carbonate; strongly effervescent to HCl; moderately alkaline; gradual smooth boundary.

Bk2--73-122 cm; dark yellowish brown (10YR 4/4) silt loam; massive; friable; not plastic and not sticky; soft masses

of secondary carbonate; strongly effervescent to HCl; moderately alkaline; clear smooth boundary.

2Ck1--122-144 cm; dark yellowish brown (10YR 4/4); loamy sand; single grain; loose; not plastic and not sticky; soft masses of secondary carbonate; strongly effervescent to HCl; moderately alkaline; clear smooth boundary.

3Ck2--144-190 cm; yellowish brown (10YR 5/4) silt loam; massive; friable; not plastic and not sticky; soft masses of secondary carbonate; strongly effervescent to HCl; moderately alkaline.

Diagnostic features: Ochric epipedon; cambic and calcic subsurface horizons.

Pedon MA-1 (Alluvial-fan piedmont)

Location: North margin of Upper-Aguán Valley in Mangos Farm
Geomorphic position: Alluvial-fan piedmont
Classification: Fine-silty, mixed (calcareous), isohyperthermic, Typic Ustropepts
Parent material: Andesitic sediments of Tva formation
Vegetation: Banana plantation
Elevation: Appr. 170 m

Ap--0-22 cm; dark brown (7.5YR 3/2) silt loam; moderate medium subangular blocky structure; firm; slightly plastic and slightly sticky; many fine and medium roots; moderately alkaline; gradual smooth boundary.

Bt--22-57 cm; reddish brown (5YR 4/4) silt loam; moderate medium subangular structure; firm; moderately plastic and moderately sticky; many fine and medium roots; few faint clay films on peds faces; very slightly effervescent to HCl; moderately alkaline; clear smooth boundary.

Bk--57-90 cm; yellowish brown (10YR 5/4) silt loam; moderate and strong medium and coarse subangular blocky structure; very firm; slightly plastic and slightly sticky; few fine and medium roots; soft masses of secondary carbonate; violently effervescent to HCl; moderately alkaline; clear smooth boundary.

Ck1--90-142 cm; yellowish brown (10YR 5/6) silt loam; weak medium and coarse subangular blocky structure; very firm; not plastic and not sticky; soft masses of secondary carbonate; strongly effervescent to HCl; moderately alkaline; clear smooth boundary.

Ck2--142-200 cm; yellowish brown (10YR 5/8) silt loam; massive; firm; not plastic and not sticky; soft masses of secondary carbonate; strongly effervescent to HCl; moderately alkaline.

Diagnostic features: Ochric epipedon; cambic and calcic subsurface horizons.

Pedon MA-2 (Alluvial-fan piedmont)

Location: North margin Upper-Aguán Valley in Naranjo "B" Farm
Geomorphic position: Medium part of alluvial-fan piedmont
Classification: Fine-silty, mixed (calcareous), isohyperthermic, Typic Ustropepts
Parent material: Andesitic sediments from the Tva formation.
Vegetation: Banana plantation
Elevation: Appr. 160 m

Ap--0-23 cm; dark reddish brown (5YR 3/2) silt loam; moderate medium and coarse subangular blocky structure; firm; moderately plastic and moderately sticky; many fine and medium roots; neutral; gradual smooth boundary.

Bt--23-70 cm; brown (10YR 4/3) silt loam; moderate medium and coarse subangular blocky structure; firm; moderately plastic and moderately sticky; few fine and medium roots; few faint clay films on peds faces; mildly alkaline; gradual smooth boundary.

Bk--70-130 cm; reddish brown (5YR 4/4) silt loam; moderate fine and medium subangular blocky structure; friable; slightly plastic and slightly sticky; soft masses of secondary carbonate; strongly effervescent to HCl; mildly alkaline; gradual smooth boundary.

Ckm--130-200 cm; brown (7.5YR 4/4) silt loam; massive; very hard and very firm; not plastic and not sticky; strongly effervescent to HCl; mildly alkaline.

Diagnostic features: Ochric epipedon, cambic and calcic subsurface horizons.

Pedon MA-3 (Alluvial-fan piedmont)

Location: North margin Upper-Aguán Valley in Naranjo "C" Farm
Geomorphic position: Medium part of alluvial-fan piedmont
Classification: Coarse-loamy, mixed, Typic Ustropepts
Parent material: Sediments from the Tva Formation
Vegetation: Banana plantation
Elevation: Appr. 160 m

Ap--0-19 cm; dark reddish brown (5YR 3/3) loam; weak fine and medium subangular blocky structure; friable; not plastic and not sticky; few fine and medium roots; neutral; gradual smooth boundary.

Bt--19-46 cm; reddish brown (5YR 4/3) loam; moderate fine and medium subangular blocky structure; friable; not plastic and not sticky; few medium roots; few faint clay films on peds faces; neutral; clear smooth boundary.

C1--46-65 cm; brown (7.5YR 4/2) sandy loam; massive; very friable; not plastic and not sticky; mildly alkaline; abrupt smooth boundary.

C2--65-170 cm; brown (7.5YR 4/4) coarse gravelly sand; single grain; loose; not plastic and not sticky; mildly alkaline.

Diagnostic horizons and characteristics: Ochric epipedon, cambic subsurface horizon.

APPENDIX B
PARTICLE-SIZE DATA FOR THE SOILS STUDIED IN THE UPPER-AGUÁN VALLEY

Appendix B. Particle-size data for the soils studied in the Upper-Aguán Valley

Horizon[a]	Depth	VCS	CS	MS	FS	VFS	TS	CSi	MSi	FSi	TSi	Clay
Pedon CA-1												
Ap	0-13	0.8	1.1	12.3	10.5	9.8	34.5	14.3	12.8	11.1	38.2	27.3
A1	13-50	0.7	1.6	7.4	7.9	14.1	31.7	15.1	13.2	11.2	39.5	28.8
C1	50-70	3.6	5.4	30.1	18.3	13.5	70.9	6.2	3.1	2.0	11.3	17.8
C2	70-80	3.0	4.6	14.6	20.2	17.1	59.5	5.8	7.1	8.2	21.1	19.4
C3	80-99	4.9	6.1	25.8	15.7	24.3	76.8	6.3	3.7	2.4	12.4	10.8
C4	99-140	10.1	13.2	20.4	18.3	18.1	80.1	2.1	2.5	3.0	7.6	12.3
Ab	140-175	2.2	4.1	15.4	12.8	10.3	44.8	11.3	9.8	8.3	29.4	25.8
C5	175-260	17.1	20.1	26.7	12.6	10.0	86.5	1.8	1.4	1.3	4.5	9.0
Pedon CA-2												
Ap	0-16	0.1	0.1	0.2	3.4	12.3	16.1	31.0	19.8	5.0	55.8	28.1
C1	16-41	0.0	0.1	0.3	1.6	8.7	10.8	37.4	24.1	7.5	69.0	20.2
C2	41-72	0.1	0.1	0.4	4.3	25.3	30.2	35.5	13.8	5.7	55.1	14.7
C3	72-112	0.0	0.1	0.9	18.4	18.3	37.8	34.3	9.5	9.6	53.5	8.7
C4	112-155	0.1	0.2	5.7	47.1	21.1	74.2	15.1	5.2	2.5	22.8	3.0
Pedon CA-3												
Ap	0-20	0.9	1.2	3.2	3.7	5.1	14.1	23.7	19.2	14.4	57.3	28.6
C1	20-60	2.0	2.1	3.3	6.9	8.6	22.9	13.9	16.2	18.3	48.4	28.7
C2	60-150	2.4	4.6	8.8	9.2	9.4	34.4	11.7	12.6	13.7	38.0	27.6
C3	150-200	6.7	8.9	15.8	13.3	12.7	57.4	8.3	7.4	6.5	22.2	20.4
C4	200-230	5.2	6.2	17.3	19.3	16.5	64.5	7.6	6.5	5.5	19.5	16.0
Pedon CA-4												
Ap	0-20	1.5	4.3	12.1	10.4	10.3	38.6	16.1	14.2	10.1	40.4	21.0
C1	20-45	2.1	6.4	13.3	10.2	10.1	43.1	14.3	12.3	10.2	36.8	20.1
C2	45-80	3.8	7.5	20.4	10.6	8.4	50.7	13.7	10.2	6.7	30.6	18.7
C3	80-100	9.7	30.2	25.3	17.3	7.3	89.8	1.8	1.0	0.2	3.0	7.2
C4	100-140	nd[b]	nd	nd	nd	nd	nd	nd	nd	nd	nd	nd
C5	140-175	8.3	28.1	21.4	16.0	11.4	85.2	4.6	2.0	0.8	7.4	7.4

Appendix B.--Continued

Horizon[a]	Depth	VCS	CS	MS	FS	VFS	TS	CSi	MSi	FSi	TSi	Clay
Pedon CA-5												
A1	0-7	1.1	2.4	19.4	23.5	15.2	61.6	8.2	5.8	3.1	17.5	20.9
A2	7-40	0.5	1.2	15.3	4.0	26.7	47.7	11.7	8.7	5.2	25.3	21.0
C1	40-70	3.4	4.5	9.0	24.1	16.5	57.5	7.9	5.4	3.0	16.3	26.1
C2	70-145	0.3	0.9	15.0	21.4	18.2	55.8	10.2	7.6	5.1	22.9	21.3
C3	145-185	3.2	4.2	11.1	29.8	23.2	71.5	5.6	3.7	1.8	11.1	13.4
C4	185-195	nd	nd	nd	nd	nd	nd	nd	nd	nd	nd	nd
C5	195-260	nd	nd	nd	nd	nd	nd	nd	nd	nd	nd	nd
C6	260-320	nd	nd	nd	nd	nd	nd	nd	nd	nd	nd	nd
Pedon PV-1												
Ap	0-7	0.7	0.2	1.1	7.3	19.9	29.2	46.9	12.2	6.8	65.9	4.9
A1	7-24	0.0	0.3	0.4	4.7	14.0	19.4	53.7	15.3	5.8	74.8	5.8
A2	24-56	0.1	0.2	0.5	3.4	18.9	23.1	41.1	16.1	5.7	62.9	14.0
C1	56-85	0.1	0.2	0.4	2.6	5.8	9.1	27.3	33.9	9.1	70.3	20.6
C2	85-116	0.1	0.1	0.3	6.6	21.0	28.1	10.4	14.3	3.7	58.4	13.5
C3	116-144	0.1	0.2	3.1	15.0	27.3	45.7	41.7	4.3	2.1	48.1	6.2
C4	144-189	0.0	2.8	41.5	44.4	5.3	94.0	1.1	1.3	1.0	3.4	2.6
C5	189-220	0.1	0.3	25.2	25.2	34.4	62.4	21.6	6.4	1.8	29.8	7.8
Pedon PV-2												
Ap	0-18	0.1	0.4	1.4	12.3	19.4	33.6	19.2	12.5	5.9	37.7	28.7
C1	18-30	0.0	0.1	3.8	29.0	20.4	53.4	8.2	9.2	5.3	22.7	23.9
C1	30-41	0.0	0.3	1.2	10.1	20.1	31.7	32.4	15.3	5.7	53.3	15.0
C2	41-50	0.0	0.3	1.4	14.2	23.6	40.0	33.8	11.2	3.8	48.9	11.1
C2	50-60	0.0	0.2	5.9	48.8	16.4	65.3	15.2	6.7	4.2	26.1	8.6
C2	60-75	0.0	0.1	0.8	23.6	37.8	62.3	21.0	5.4	4.4	30.7	7.0
C3	75-170	0.0	0.1	7.6	57.6	17.0	82.3	9.9	3.2	3.5	16.6	1.1
C3	170-190	0.1	0.3	0.6	16.9	33.5	51.5	28.5	8.9	3.6	41.0	7.5

Appendix B.--Continued

Horizon[a]	Depth	VCS	CS	MS	FS	VFS	TS	CSi	MSi	FSi	TSi	Clay
Pedon PV-3												
Ap	0-10	1.9	0.9	1.1	7.1	11.6	22.6	30.0	23.7	15.1	68.8	8.6
Ap	10-20	0.0	1.1	2.2	10.2	12.3	25.8	29.8	17.4	8.1	55.3	18.9
C1	20-30	nd	nd	nd	nd	nd	nd	nd	nd	nd	nd	nd
C1	30-58	0.0	0.3	1.3	10.0	14.1	25.7	29.2	17.2	13.3	59.7	14.6
C2	58-100	0.1	0.2	1.6	12.0	15.7	29.7	28.7	17.2	5.0	50.9	19.4
C3	100-120	0.0	0.1	1.4	12.0	12.2	25.7	28.3	17.1	9.6	55.1	19.2
C3	120-140	0.0	0.2	1.3	10.0	14.1	25.6	21.3	14.7	11.1	53.1	21.3
C3	140-150	0.6	1.3	2.1	7.2	12.2	23.4	30.7	19.5	9.2	59.4	17.1
C3	150-190	0.0	0.4	0.9	4.5	10.0	15.9	32.17	23.2	9.4	64.8	19.3
Pedon NA-1												
Ap	0-15	0.1	0.3	0.6	4.2	16.3	21.5	52.0	16.6	4.7	73.3	5.2
C1	15-66	0.0	0.2	0.5	13.9	22.7	37.3	31.3	12.4	5.2	48.9	13.8
C2	66-100	0.0	0.1	0.2	5.5	19.3	25.1	38.3	16.1	5.1	59.5	15.4
C3	100-127	0.0	0.1	0.1	0.2	10.7	11.1	40.1	22.5	6.8	70.2	18.7
C4	127-166	0.1	0.1	0.4	4.7	26.4	31.7	38.2	12.7	4.3	55.2	13.1
C5	166-192	0.5	0.5	1.0	14.5	27.9	44.4	29.5	10.9	4.1	44.5	11.1
C6	192-220	12.6	13.7	17.4	21.3	10.7	75.8	13.5	4.8	1.6	19.8	4.4
Pedon NA-2												
Ap	0-6	0.5	0.6	4.8	7.4	24.2	37.5	21.2	12.8	7.5	41.5	21.0
C1	6-10	2.2	5.6	11.1	24.1	26.1	69.1	9.0	6.2	3.3	18.5	12.4
Ab	10-20	0.8	1.1	6.7	6.9	25.1	40.6	20.6	13.4	5.0	39.0	20.4
C2	20-40	0.2	0.3	5.2	10.2	26.1	42.0	21.6	13.8	4.6	40.0	18.0
C2	40-70	0.4	1.3	5.1	17.5	27.9	52.2	24.2	6.7	5.8	33.8	14.0
C3	70-130	0.2	0.4	4.1	17.4	23.2	45.3	19.2	17.5	5.0	36.7	18.0
C4	130-155	12.4	15.2	18.1	19.3	12.0	77.0	6.1	2.2	1.9	10.2	12.8

Appendix B.--Continued

Horizon[a]	Depth	VCS	CS	MS	FS	VFS	TS	CSi	MSi	FSi	TSi	Clay
Pedon NA-3												
Ap	0-19	0.5	1.2	2.4	3.6	9.4	17.1	47.7	16.6	6.4	70.7	12.2
C1	19-63	0.4	1.1	2.0	4.0	8.1	15.6	44.0	18.2	7.0	69.1	15.3
C2	63-95	0.1	1.1	5.5	17.4	27.8	51.9	27.8	8.7	2.8	39.3	8.8
C3	95-120	0.3	6.0	32.0	43.0	10.3	91.6	5.0	1.4	1.7	8.1	0.3
C4	120-210	1.6	5.8	13.0	23.8	25.1	69.3	22.0	3.8	4.6	30.4	0.3
Pedon RC-1												
Ap	0-15	0.0	0.1	2.4	5.8	13.1	21.4	17.5	13.2	8.8	39.5	39.1
C1	15-60	0.0	0.0	1.1	2.2	3.6	6.9	24.1	12.6	17.3	54.0	39.1
C2	60-100	0.0	1.0	4.9	16.1	10.3	32.3	16.9	11.4	9.8	38.1	29.7
C3	100-130	2.8	3.5	37.8	20.1	17.2	81.4	3.2	2.8	2.6	8.6	10.0
C4	130-180	0.8	2.6	14.8	15.6	12.5	46.3	12.1	8.5	6.4	27.0	26.7
C5	180-220	2.6	4.3	31.2	24.2	7.3	69.6	6.2	3.1	4.2	13.5	16.9
Pedon RC-2												
C1	0-23	1.1	2.5	8.3	24.2	27.1	63.2	8.3	6.8	5.3	20.4	16.4
A	23-60	0.0	0.1	1.1	1.5	4.1	6.8	23.2	19.5	15.8	58.5	34.7
C2	60-100	0.0	0.0	0.2	0.8	2.2	3.2	20.3	21.4	17.0	58.7	38.1
C3	100-125	1.0	2.5	10.5	14.7	18.3	48.0	9.4	8.7	8.1	26.2	25.8
C4	125-190	1.2	3.1	28.2	31.8	19.1	83.4	2.1	1.7	1.3	5.1	11.5
C5	190-225	1.0	1.6	29.1	33.0	18.3	83.0	2.6	1.4	1.2	5.2	11.8
Pedon RC-3												
Ap	0-18	0.0	0.0	0.0	0.0	0.2	0.2	27.3	21.9	16.5	65.7	34.1
C1	18-40	0.2	0.4	0.7	8.5	18.7	28.5	18.1	14.6	10.5	43.2	28.3
C2	40-60	0.0	0.0	0.2	2.0	3.5	5.7	25.1	23.1	17.0	65.2	29.1
C3	60-130	0.0	0.1	1.5	7.8	21.0	30.4	18.3	15.1	10.6	44.0	25.6
C4	130-150	4.8	5.1	43.1	32.5	4.5	90.0	2.1	2.9	3.5	8.5	1.5
C5	150-200	0.3	1.0	8.3	21.3	18.2	49.1	7.0	9.5	11.1	27.6	23.3

Appendix B.--Continued

Horizon[a]	Depth	VCS	CS	MS	FS	VFS	TS	CSi	MSi	FSi	TSi	Clay
Pedon LA-1												
A1	0-33	0.7	1.5	1.8	3.2	6.0	13.2	30.5	23.7	11.0	64.7	22.0
A2	33-56	0.5	1.3	1.5	3.2	8.3	14.8	25.0	25.0	10.7	60.8	24.4
2C1	56-70	5.9	9.3	4.7	5.5	7.8	33.3	18.6	20.6	7.6	46.8	19.9
3C2	70-95	0.3	1.0	1.4	4.4	6.8	13.9	22.8	26.0	11.1	59.9	26.2
4C3	95-136	0.0	0.1	0.9	15.4	28.4	44.7	43.6	3.9	1.6	49.1	6.2
Pedon LA-2												
Ap	0-19	0.4	1.5	2.0	1.9	1.5	7.3	5.2	27.0	6.0	38.2	54.5
A	19-70	0.4	1.4	1.9	1.7	1.3	6.7	11.5	13.2	5.9	30.6	62.7
Bw	70-90	0.1	0.3	0.4	0.3	0.2	1.2	14.6	16.7	7.5	38.8	60.7
2C1	90-150	1.4	5.7	8.6	14.3	11.2	41.2	27.2	18.0	6.6	51.7	7.0
2C2	150-230	0.7	3.4	6.0	11.9	11.7	33.7	27.2	21.4	9.0	57.6	8.7
Pedon TB-1												
Ap	0-12	1.5	4.6	5.6	5.3	4.2	21.2	22.5	15.1	7.8	45.3	33.5
Bt	12-42	1.1	4.0	3.9	4.3	3.6	16.8	20.2	15.2	12.0	47.4	35.7
Bk	42-80	1.5	3.7	4.7	6.2	5.1	21.1	23.2	19.1	14.3	56.7	22.3
Ck	80-120	3.1	5.7	12.3	15.9	10.6	47.6	18.3	14.6	3.8	36.7	17.7
2C1	120-152	10.6	20.1	29.8	21.1	3.8	85.3	2.3	2.3	0.6	5.1	9.6
3C2	152-180	1.2	3.9	12.6	36.2	18.7	72.4	8.2	5.3	1.4	14.9	12.7
3C3	180-225	3.1	7.2	11.7	18.0	9.6	39.6	9.8	13.6	4.7	28.2	22.2
4C4	225-245	nd	nd	nd	nd	nd	nd	nd	nd	nd	nd	nd
5C5	245-280	17.8	29.6	23.3	13.5	3.9	88.2	4.2	2.9	0.2	7.3	4.5
6C6	280-295	nd	nd	nd	nd	nd	nd	nd	nd	nd	nd	nd
7Ck	295-340	0.7	1.9	1.9	1.7	2.7	8.9	17.4	38.3	10.2	65.9	25.2
Pedon TB-2												
Ap	0-20	0.1	0.4	1.4	11.6	26.5	40.0	31.3	9.4	7.3	48.1	11.9
Bt	20-52	0.2	0.3	0.9	9.5	23.5	34.3	25.9	9.5	4.8	40.3	25.4
Bk1	52-73	0.0	0.5	3.6	24.3	36.6	65.1	4.5	5.4	6.6	16.5	18.4
Bk2	73-122	0.0	0.0	0.4	2.7	7.4	10.5	58.4	15.7	5.3	79.3	10.2
2Ck1	122-144	0.1	0.4	10.2	47.6	20.0	78.2	13.0	4.1	2.1	19.1	2.7
3Ck2	144-190	0.0	0.1	0.5	6.3	17.0	23.9	42.3	18.2	7.0	67.5	8.6

Pedon MA-1												
Ap	0-22	0.0	0.5	0.8	6.5	16.9	24.7	36.1	12.6	8.6	57.3	18.0
Bt	22-57	0.1	0.2	0.2	5.2	18.1	23.9	29.8	14.3	6.9	51.0	25.1
Bk	57-90	0.0	0.1	0.3	4.7	10.6	15.7	31.3	23.3	9.4	64.1	20.2
Ck1	90-142	0.5	4.9	7.2	9.6	12.0	34.3	39.0	18.4	4.5	61.9	3.8
Ck2	142-200	0.1	0.1	0.2	2.4	14.7	17.5	42.1	19.6	7.4	69.2	13.3
Pedon MA-2												
Ap	0-23	0.5	1.3	3.4	7.5	7.4	20.1	33.6	14.1	10.7	58.5	21.5
Bt	23-70	0.4	1.2	3.0	7.0	7.1	18.8	29.7	14.8	11.2	55.3	25.4
Bk	70-130	0.9	3.1	5.9	12.5	11.8	34.2	28.1	18.0	8.8	54.9	10.8
Cmk	130-200	4.5	6.1	9.0	22.7	16.7	59.1	21.8	9.1	4.0	35.0	5.9
Pedon MA-3												
Ap	0-19	4.4	10.6	9.9	10.3	6.9	42.2	23.8	10.0	9.4	43.2	14.5
Bt	19-46	2.8	8.5	9.8	11.6	8.3	41.2	20.0	11.8	5.4	37.2	21.5
C1	46-65	6.3	15.5	16.9	11.9	6.0	56.6	16.0	8.8	3.8	28.7	14.7
C2	65-170	31.7	39.6	16.0	4.2	1.5	92.0	0.0	0.2	1.5	1.7	6.3

NOTE: VCS = very coarse sand, CS = coarse sand, MS = medium sand, FS = fine sand, VFS = very fine sand, TS = total sand, CSi = coarse silt, MSi = medium silt, FSi = fine silt, TSi = total silt.

[a]Horizons with the same designation were subsampled.

[b]Not determined.

REFERENCES

Adams, J. 1980. Active tilting of the United States midcontinent: Geodetic and geomorphic evidence. Geology 2:442-446.

Arkley, R.J. 1963. Calculations of carbonate and water movement in soil from climatic data. Soil Science 96:239-248.

Arnold, R.W., and F.L. Gilbert. 1979. Cartography and soil survey procedures. Part I. Report to committee 5 of the National Cooperative Soil Survey: Confidence limits for soil survey information. Soil Conservation Service, New York.

Bachman, G.O., and M.N. Machette. 1977. Calcic soils and calcretes in the southeastern United States. U.S. Geol. Surv. Open-File Report 77-794. 163p.

Bender, M.L., R.G. Fairbanks, F.W. Taylor, R.K. Matthews, J.G, Goodard, and W.S. Broecker. 1979. Uranium-series dating of Pleistocene reefs tracts of Barbados, West Indies. Geol. Soc. Am. Bull. 90:577-594.

Bindford, M.W. 1982. Ecological History of Lake Valencia, Venezuela: Interpretation of animal microfossils and some chemical, physical, and geological features. Ecological Monographs 52:307-333.

Birkeland, P.W. 1984. Soils and geomorphology. Oxford University Press. New York. 372p.

Bonis, S.B., O.H. Bohnenberger, and G. Dengo. 1970. Mapa geologico de la Republica de Guatemala, scale 1:500,000. Inst. Geogr. Nac. de Guatemala, Guatemala City.

Bradbury, J.P., B.W. Leyden, M. Salgado-Labouriau, W.M. Lewis Jr., C. Schubert, M.W. Bindford, D.G. Frey, D.R. Whitehead, and F.H. Weibezahn. 1981. Late Quaternary environmental history of Lake Valencia, Venezuela. Science 214:1299-1305.

Brakenridge, G.R. 1980. Widespread episodes of stream erosion during the Holocene and their climatic cause. Nature 283:655-656.

Brakenridge, G.R. 1983. Late Quaternary floodplain sedimentation along the Pomme de Terre River, southern Missouri. Part II. Notes on sedimentology and pedogenesis. Geologisches Jarribuch, Series A 71:265-283.

Brakenridge, G.R. 1984. Alluvial stratigraphy and radiocarbon dating along the Duck River, Tennessee: Implications regarding floodplain origin. Geol. Soc. Am. Bull. 95:9-25.

Brakenridge, G.R. 1985. Rate estimates for lateral bedrock erosion based on radiocarbon ages, Duck River, Tennessee. Geology 13:111-114.

Brakenridge, G.R. 1988. Flood regime and floodplain stratigraphy. pp. 139-156. In: V.R. Baker, C. Kochel, and P. Patton (ed.) Flood geomorphology. John Wiley & Sons, Inc., New York.

Bull, W.B. 1977. Tectonic geomorphology of the Mojave Desert. U.S. Geol. Surv. Contract Report 14-08-001-G-394. Office of Earthquakes, Volcanos, and Engineering, Menlo Park, CA. 188p.

Bull, W.B. 1978. Geomorphic tectonic activity classes of the south front of the San Gabriel Mountains, California. U.S. Geol. Surv. Contract Report 14-08-001-G394. Office of Earthquakes, Volcanos, and Engineering, Menlo Park, CA. 59p.

Bull, W.B. 1984. Tectonic geomorphology. Journal of Geological Education 32:310-324.

Bull, W.B. 1991. Geomorphic responses to climatic changes. Oxford University Press., New York. 326p.

Bull, W.B., and L.D. McFadden. 1977. Tectonic geomorphology north and south of the Garlock Fault, California. pp. 115-138. In: D.O. Doehring (ed.) Proceedings Vol. of 8th Annual Geomorph. Symp., New York State University at Binghamton, NY.

Catt, J.A. 1988. Quaternary geology for scientists and engineers. John Wiley & Sons, New York. 340p.

Christenson, G.E., and C. Purcell. 1985. Correlation and age of Quaternary alluvial-fan sequences, Basin and

geology of the southwestern United States. Geol. Soc. Am. Special Paper 203.

Curtis, J.H. 1992. Natural variability of late Pleistocene -Holocene climates in the Caribbean from isotopic and trace element analysis of lake sediments (10,500 years BP to present). MS thesis, University of Florida.

Deevey, E.S., M. Brenner, and M.W. Bindford. 1983. Paleolymnology of the Peten lake district, Guatemala III. Late Pleistocene and Gamblian environments of the Maya area. Hidrobiologia 103:211-216.

Dengo, G., and Bohnenberger. 1969. Structural development of northern Central America. Memoir Am. Assoc. Pet. Geol. 11:203-220.

Dodge, R.E., R.G. Fairbanks, L.K. Benninger, and F. Maunasse. 1983. Pleistocene sea level from raise coral reefs of Haiti. Science 219:1423-1425.

Doornkamp, J.C. 1986. Geomorphological approaches to neotectonics. J. Geol. Soc. London 143:335-342.

Erskine, W.D., and R.F. Warner. 1988. Geomorphic effects of alternating flood- and drought-dominated regimes on NSW coastal rivers. pp. 223-244. In: R,F Warmer (ed.) Fluvial geomorphology in Australia. Academic Press, Sidney.

Fakundiny, R.H. 1970. Geology of El Rosario and Comayagua quadrangles, Honduras, Central America. Ph.D. dissertation. University of Texas, Austin.

Finch, R.C. 1981. Mezosoic stratigraphic of central Honduras. Am. Assoc. Pet. Geol. Bull. 65:1320-1333.

Frye, J.C., and A.R. Leonard. 1954. Some problems of alluvial terrace mapping. Am. J. Sci. 252:242-251.

Gardner, T.W. 1987. Overview of Caribbean geomorphology. pp. 343-347. In: Graf, W.L. (ed) Geomorphic systems of North America. Geological Society of America Centennial Special Volume 2. Boulder, CO.

Garner, H.F. 1959. Stratigraphic-sedimentary significance of contemporary climate and relief in four regions of the Andes mountains. Geol. Soc. Am. Bull. 70:1327-1368.

Gates, W.I. 1976. Modelling the Ice-Age climate. Science 191:1138-1144.

Gile, L.H. 1975. Holocene soils and soil-geomorphic relations in an arid region of southern New Mexico. Quaternary Research 5:321-360.

Gile, L.H. 1977. Holocene soils and soil-geomorphic relations in an arid region of southern New Mexico. Quaternary Research 7:112-132.

Gile, L.H., F.F. Peterson, and R.B. Grossman. 1966. Morphological and genetic sequences of carbonate accumulation in desert soils. The Desert Project Soil Monograph: U.S. Department of Agriculture, Washington, D.C., U.S. Soil Conservation Service. 984p.

Gose, W.A. 1985. Paleomagnetic results from Honduras and their bearing on Caribbean tectonics. Tectonics 4:565-585.

Harden, J.W. 1982. A quantitative index of soil development from field descriptions: Examples from a chronosequence in Central California. Geoderma 28:1-28.

Harden, J.W., E.M. Taylor, L.D. McFadden, and M.C. Reheis. 1991. Calcic, gypsic, and siliceous soil chrono-sequences in arid and semiarid environments. In: Nettleton, W. E. (ed.) Ocurrence, characteristics, and genesis of carbonate, gypsum, and silica accumulation in soils. Soil Science Society of America, Special Publication 26. Madison, WI.

Hastenrath, S. 1976. Variations in the low-latitude circulation and extreme climatic events in the tropical Americas. J. Atmos. Sci. 33:202-215.

Hayden, B.P. 1989. Flood climates. pp. 13-26. In: V.R. Baker, R.C. Kochel, and P.C. Patton (ed.) Flood geomorphology. John Wiley & Sons, New York.

Hereford, R. 1984. Climate and ephemeral-stream processes: Twentieth-century geomorphology and alluvial stratigraphy of the Little Colorado River, Arizona. Geol. Soc. of Am. Bull. 95:654-668.

Hickin, D.J. 1974. The development of meanders in natural river-channels. Am. J. Sci. 274:414-442.

Higuera-Gundy, A. 1991. Antillean vegetational history and paleoclimate reconstructed from the paleolimnological record of lake Miragoane, Haiti. Ph.D. dissertation University of Florida, Gainesville.

Hodell, D.A., J.H. Curtis, G.A. Jones, A. Higuera-Gundy, M. Brenner. M.W. Bindford, K.T. Dorsey. 1991. Reconstruction of Caribbean climate change over the past 10,500 years. Nature 352:790-793.

Hoeksema, K.J. 1953. The natural homogenization of the soil profile in the Netherlands. Boor en Spade 6:24-30.

Horne, G.S., G.S. Clark, and P. Pushkar. 1976, Pre-Cretaceous rocks of northwestern Honduras: Basement terrane in Sierra de Omoa. Am. Assoc. Pet. Geol. Bull. 60:566-583.

Jordan, T.H. 1975. The present-day motions of the Caribbean Plate. J. of Geophys. Res. 80:4433-4439.

Keller, E.A., and T.K. Rockwell. 1984. Tectonic geomorphology, Quaternary chronology, and paleoseismicity. pp.203-239. In: J.E. Costa, and P.J. Fleisher (ed.) Developments and applications of geomorphology. Springer-Verlag, New York.

Kelson, K. 1986. Long-term tributary adjustments to base-level lowering, northern Rio Grande rift, New Mexico. M.S. thesis. University of New Mexico, Albuquerque.

Kesel, H.K., K.C. Dunne, R.C. McDonald, K.R. Allison. 1974. Lateral erosion and overbank deposition on the Mississippi River in Louisiana caused by 1973 flooding. Geology 2:461-464.

Kesel, R.H. 1985. Alluvial fan systems in a wet-tropical environment, Costa Rica. National Geographic Research 1:450-469.

Kesel, R.H., and B.E. Spicer. 1985. Geomorphological relationships and ages of soils on alluvial fans in the Rio General Valley, Costa Rica. Catena 12:149-166.

Knox, J.C. 1983. Responses of river systems to Holocene climates. pp. 26-41. In: H.E. Wright, Jr. (ed.) Late Quaternary environments of the United States. University of Minnesota Press, Minneapolis.

Knox, J.C. 1984. Fluvial responses to small scale climate changes. pp. 318-342. In: J.E. Costa and P.J. Fleischer (ed.) Developments and applications in geomorphology. Springer Verlag, Berlin.

Knox, J.C. 1985. Responses of floods to Holocene climatic change in the upper Mississippi Valley. Quaternary Research 23:287-300.

Knuepfer, P.L.K. 1988. Estimating ages of late Quaternary terraces from analysis of weathering rinds and soils. Geol. Soc. Am. Bull. 100:1224-1236.

Kozarski, S., and K. Rotnicki. 1977. Valley floors and changes of river channel patterns in the north Polish Plain during the late Wurm and Holocene. Quaestiones Geographicae 4:51-93.

Kozuch, M.J. 1991. Mapa geologico de Honduras. Scale: 1:500,000. Secretaria de Comunicaciones Obras Publicas y Transporte. Instituto Geografico Nacional. Teguagalpa, Honduras.

Kutzbach, J.E., and F.A. Street-Perot. 1985. Milankovitch forcing of fluctuations in the level of tropical lakes from 18 to 0 kyr bp. Nature 317:130-134.

Leyden, B.W. 1984. Guatemalan forest synthesis after Pleistocene aridity. Proceedings of the National Academy of Sciences, USA 81:4856-4859.

Leyden, B.W. 1985. Late Quaternary aridity and Holocene moisture fluctuations in the Lake Valencia Basin, Venezuela. Ecology 66:1279-1295.

Machette, M.N. 1985. Calcic soils of the southwestern United States. pp. 1-21. In: D.L. Weide, and M.L. Faber (ed.) Quaternary soils and geomorphology in the southwest, Boulder, CO. Geological Society of America, Special Paper 203.

Malfait, B.T., and M.G. Dinkelman. 1972. Circum-Caribbean tectonic and igneous activity and the evolution of the Caribbean Plate. Geo. Soc. Am. Bull. 83:251-272.

Manabe, S., and D.G. Hahn. 1977. Simulation of tropical climate of an ice age. J. Geophys. Res. 82:3889-3911.

Manton, W.I. 1985. An outline of the tectonics of northern and central Honduras. Eos Trans. AGU 66:1087.

Manton, W.I. 1987. Tectonic interpretation of the morphology of Honduras. Tectonics 6:633-651.

Markgraf, V. 1989. Paleoclimates in Central and South America since 18,000 BP based on pollen and lake-level records. Quaternary Science Reviews 8:1-24.

McDowell, P.F. 1983. Evidence of stream response to Holocene climatic change in a small Wisconsin watershed. Quaternary Research 19:100-116.

Menges, C.M., S.G. Wells, and T.F. Bullard. 1987. Morphometric of tectonic landscapes along a convergent plate boundary, Pacific Coast of Costa Rica. pp. 373-385. In: Graf, W.L. (ed), Geomorphic systems of North America, Boulder, CO. Geological Society of America, Centennial Special Volume 2.

Mills, R.A., K.E. Hugh, D.E. Feray, and H.C. Swolfs. 1967. Mezosoic stratigraphy of Honduras. Am. Soc. Pet. Geol. Bull. 51:1711-1786.

Minster, J.B., T.H. Jordan, P. Molnar, and E. Haines. 1974. Numerical modelling of instantaneous plate tectonics. Geophys. J. Roy. Astron. Soc. 36:541-575.

Molnar, P., and L.R. Sykes. 1969. Tectonic of the Caribbean and middle America regions from focal mechanisms and seismicity. Geol. Soc. Am. Bull. 80:1639-1684.

Nanson, G.C. 1986. Episodes of vertical accretion and catastrophic stripping: A model of disequilibrium flood-plain development. Geol. Soc. Am. Bull. 97:1467-1475.

Ouchi, S. 1985. Reponse of alluvial rivers to slow active tectonic movement. Geol. Soc. Am. Bull. 96:504-515.

Pinet, P.R. 1972. Diapirlike features offshore Honduras: Implications regarding tectonic evolution of Cayman Trough and Central America. Geol. Soc. Am. Bull. 83:1911-1922.

Pinet, P.R. 1975. Structural evolution of the Honduras continental marging and the sea floor south of the western Cayman Trough. Geol. Soc. Am. Bull. 86:830-836.

Piperno, D.R., M.B. Busch, and P.A. Colinvaux. 1990. Paleoenvironments and human occupation in late-glacial Panama. Quaternary Research 33:108-116.

Portig, W.H. 1976. The climate of Central America. pp. 405-45. In: W. Schwerdtfeger (ed.) Climates of Central and South America. Elsevier Scientific Publishing Co., Amsterdam-Oxford-New York.

Ramsay, J.G., and M.I. Huber. 1987. The techniques of modern structural geology. Vol. 2. Academic Press, Inc. Orlando, FL.

Reading, H.G. 1980. Characteristics and recognition of strike-slip fault systems. pp. 7-26. In: P.F. Ballance, and H.G. Reading (ed.) Sedimentation on oblique-slip mobile zones. Blackwell Scientific Publications, Boston.

Retallack, G.J. 1988. Field recognition of paleosols. pp. 1-20. In: J. Reinhardt, and W.R. Sigleo (ed.) Paleosols and weathering through geologic time: Principles and applications. Boulder, CO. Geological Society of America Special Paper 216.

Rhoades, J.D. 1986. Cation exchange capacity. pp. 149-157. In: A. Klute (ed.) Methods of soil analysis Part II. 2nd ed. Agronomy 9:149-157. SSSA, Madison, WI.

Riley, S.J. 1988. Secular change in the annual flows of streams in the NSW section of the Murray-Darling basin. pp. 245-266. In: R.F. Warner (ed.) Fluvial geomorphology of Australia. Academic Press, Inc., London.

Rockwell, T.K., E.A. Keller, and D.L. Johnson. 1991. Tectonic geomorphology of alluvial fans and mountain fronts near Ventura, California. pp. 183-207. In: M. Mousaica and J. T. Hack (ed.) Tectonic geomorphology. The Binghamton Symposium in Geomorphology. No. 15. Allen and Unwin, Inc., Manchester, NY.

Rosencrantz, E., and J.G. Sclater. 1986. Depth and age in the Cayman Trough. Earth and Planetary Science Letters. 79:133-144.

Ross, M.I., and C.R. Scotese. 1988. A hierarchical tectonic model of the Gulf of Mexico and Caribbean region. Tectonophysics 155:139-168.

Scholer, H.A. 1974. Geomorphology of New South Wales coastal rivers. Univ. NSW Wat. Res. Lab. Rep. No. 139.

Schramm, W.E. 1981. Humid tropical alluvial fans northwest Honduras. MS thesis, Louisiana State University.

Schumm, S.A. 1977. The fluvial system. John Wiley & Sons, Inc., New York. 338p.

Schumm, S.A. 1985. Patterns of alluvial rivers. Ann. Rev. Earth Planet. Sci. 13:5-27.

Schumm, S.A. 1986. Alluvial river response to active tectonics. pp. 80-94. In: Active tectonics. National Academy Press. Washington, DC.

Schumm, S.A. 1991. To interpret the earth: Ten ways to be wrong. Cambridge University Press, New York. 133p.

Schumm, S.A., and R.W. Litchy. 1963. Channel widening and floodplain construction along Cimarron River in southwestern Kansas. pp. 71-88. U.S. Geol. Surv. Professional Paper 352-D.

Schumm, S.A., and R.S. Parker. 1973. Implications of complex response of drainage systems for Quaternary alluvial stratigraphy. Nature 243:99-100.

Schwartz, D.P. 1976. The Montagua Fault zone, Guatemala: Tertiary and Quaternary tectonics. Geol. Soc. Am. Abstr. 8:1092-1093.

Schwartz, S.A., L.S. Cluff, and T.W. Donnelly. 1979. Quaternary faulting along the Caribbean-North American Plate boundary in Central America. Tectonophysics 52:431-445.

Shepherd, R.G. 1979. River channel and sediment responses to bedrock lithology and stream capture, sandy creek drainage, central Texas. pp. 255-275. In: D.D. Rhodes, and G.P. Williams (ed.) Adjustments of the fluvial system. Kendall Hunt Publishing Co, IA.

Soil Survey Staff. 1975. Soil taxonomy: A basic system of soil classification for making and interpreting soil survey. SCS-USDA, Handbook 436, U.S. Government Printing Office, Washington, DC.

Soil Survey Staff. 1981. Soil survey manual. Chap. 4. SCS-USDA, U.S. Government Printing Office, Washington, DC.

Soil Survey Staff. 1991. Soil survey laboratory methods manual. Soil Surv. Investig. Rep. No. 42. Version 1.0. SCS-USDA, U.S. Government Printing Office, Washington, DC.

Soil Survey Staff. 1992. Keys to soil taxonomy, 5th edition, Soil Management Support Services technical monograph No. 19. Pocahontas Press, Inc., Blacksburg, VA, 556pp.

Stevens, P.R., and T.W. Walker. 1970. The chronosequence concept and soil formation. The Quarterly Review of Biology 45:333-347.

Strahler, A.N. 1952. Hypsometric (area-altitude) analysis of erosional topography. Geol. Soc. Am. Bull. 69:279-300.

Wadge, G., and K. Burke. 1983. Neogene Caribbean plate rotation and associated Central American tectonic evaluation. Tectonics 2:633-643.

Walker, P.H., and R.J Coventry. 1976. Soil profile in some alluvial deposits of eastern New South Wales. Australian Jour. Soil Res. 14:305-317.

Weyl, R. 1980. Geology of Central America. Berlin-Stuttgart, Gerbruder Borntraeger. 371p.

Winslow, M.A., and W.R. McCann. 1985. Neotectonics of a subduction/strike-slip transition zone; the northeastern Dominican Republic. Geol. Soc. Am. Abstr. with Programs 17:753.

Whittig, L.D., and W.R. Allardice. 1986. X-ray diffraction techniques. pp. 331-362. In: A. Klute (ed.) Methods of soil analysis Part I. 2nd ed., Soil Science Society of America, Madison, WI.

Wolman, M.G., and L.B. Leopold. 1957. River flood plains: some observations on their formation. pp. 87-100. U.S. Geol. Surv. Professional Paper 282-C.

BIOGRAPHICAL SKETCH

Fernando de Jesus Cabrera Martinez was born September 23, 1950 in Pepillo Salcedo, province of Montecristi, The Dominican Republic. He grew up in Villa Vasquez, Montecristi, where he attended public school. He graduated from Loyola High School, Santo Domingo, in 1966, and entered Universidad Autonoma de Santo Domingo in 1967, where he completed the general preparatory year. In 1968, he attended a one year course of social catholic doctrine in Bogota, Colombia. He reentered Universidad Autonoma de Santo Domingo in 1969, and received a bachelor degree in agronomy in 1975.

During the period 1975 to 1985, he was employed by three government agencies, first as agronomist and later as a soil surveyor. During this time he attended two training courses in Egypt and Spain.

In January 1986, he began graduate studies at the University of Florida under the direction of Willie G. Harris in the Soil Science Department and received a Master of Science degree in soil science in 1988. He continued graduate studies in the same department and university, under the direction of Mary E. Collins. He was employed as

a graduate research assistant from July 1988 through December 1992.

I certify that I have read this study and that in my opinion it conforms to acceptable standards of scholarly presentation and is fully adequate, in scope and quality, as a dissertation for the degree of Doctor of Philosophy.

Mary E. Collins

Mary E. Collins, Chair
Professor of Soil and Water Science

I certify that I have read this study and that in my opinion it conforms to acceptable standards of scholarly presentation and is fully adequate, in scope and quality, as a dissertation for the degree of Doctor of Philosophy.

Willie G. Harris

Willie G. Harris
Associate Professor of Soil and Water Science

I certify that I have read this study and that in my opinion it conforms to acceptable standards of scholarly presentation and is fully adequate, in scope and quality, as a dissertation for the degree of Doctor of Philosophy.

Randall B. Brown

Randall B. Brown
Professor of Soil and Water Science

I certify that I have read this study and that in my opinion it conforms to acceptable standards of scholarly presentation and is fully adequate, in scope and quality, as a dissertation for the degree of Doctor of Philosophy.

G. H. McClellan

Guerry H. McClellan
Professor of Geology

I certify that I have read this study and that in my opinion it conforms to acceptable standards of scholarly presentation and is fully adequate, in scope and quality, as a dissertation for the degree of Doctor of Philosophy.

Joann Mossa
Assistant Professor of Geography

This dissertation was submitted to the Graduate Faculty of the College of Agriculture and to the Graduate School and was accepted as partial fulfillment ofthe requirements for the degree of Doctor of Philosophy.

August 1993

Jack L. Fry
Dean, College of Agriculture

Dean, Graduate School